

DELFT UNIVERSITY OF TECHNOLOGY

MASTER OF SCIENCE THESIS

**Diaphragm Wall Panels: Non-Linear
FEM Analysis Of Forces In
Construction Joints**

Author:
Volkan Erdem GOKCEK

Supervisor:
Prof.dr.ir. D.A. Hordijk
Dr.ir. C.R. Braam
Dr.ir. M.A.N. Hendriks
Dr.ir.R.A.Vonk
Ir.C.M.P.'t Hart

*A thesis submitted in fulfillment of the requirements
for the degree of Master of Science*

in the

Structural Engineering
Concrete Structures

July 13, 2017

Declaration of Authorship

I, Volkan Erdem GOKCEK, declare that this thesis titled, "Diaphragm Wall Panels: Non-Linear FEM Analysis Of Forces In Construction Joints" and the work presented in it are my own. I confirm that:

- This work was done wholly or mainly while in candidature for a master of science degree at this University.
- Where any part of this thesis has previously been submitted for a degree or any other qualification at this University or any other institution, this has been clearly stated.
- Where I have consulted the published work of others, this is always clearly attributed.
- Where I have quoted from the work of others, the source is always given. With the exception of such quotations, this thesis is entirely my own work.
- I have acknowledged all main sources of help.

Signed:

Date:

DELFT UNIVERSITY OF TECHNOLOGY

Abstract

Civil Engineering Faculty
Structural Engineering
Concrete Structures

Master of Science

Diaphragm Wall Panels: Non-Linear FEM Analysis Of Forces In Construction Joints

by Volkan Erdem GOKCEK

The aim of this thesis is to investigate the behavioral differences of walls that have different load transfer mechanisms and identify a simple engineering model for a construction joint that connects these two different wall types.

Within the text; First, the problem description is provided among with a simple yet reliable soil modeling for finite element method, to illustrate the excavation work. Then, six engineering models have been constructed and analyzed and results are compared. Phased excavation in layered soil is performed by shell and interface elements provided by the FEM package Diana 10.1. In addition, the section forces are estimated for an upper and lower bound given for different wall mechanisms. To conclude, the critical construction stage and the critical depths are reached. Expected section forces are computed and compared with the capacity of the critical construction joint.

This thesis highlights the reliable and simple modeling of a laterally supported phased excavation analysis. Furthermore, it outlines the factors effecting the resulting forces from different load transfer mechanisms and concludes that the critical section subject to this thesis is safe with the given conditions. ...

Acknowledgements

My special thanks to my family for allowing me to follow my dream.

And to Dr.ir. C.R. Braam who accepted to work with me for my master thesis and his supervision, to Prof.dr.ir. D.A. Hordijk that accepted to be in my thesis committee although his busy schedule. To Dr.ir. M.A.N. Hendriks for his supervision. And Dr.ir.R.A.Vonk who helped me with D-Sheet analysis and to Ir.C.M.P.'t Hart that supervised me through the process and thought me to use Diana Finite Element Method and showed compassion and understanding in though times. To Royal Haskoning DHV that allowed me the chance to complete my thesis within their environment. And i would like to add my thanks to K.J. Bakker who helped me to understand the soil behavior in such short time and directed me to correct literature on the subject which is out of the limits of my master thesis.

Contents

Declaration of Authorship	iii
Abstract	v
Acknowledgements	vii
1 Introduction	1
1.1 Introduction	1
1.1.1 Problem Description	2
1.1.2 Problem Background	2
1.1.3 Target of Thesis	4
1.1.4 Approach	4
2 Theoretical Background	7
2.1 General Background	7
2.2 Requirements and criteria	8
2.3 Construction Method and Sequencing	10
2.3.1 Excavation of Trench	10
2.3.2 Supporting Of Trench With Slurry	12
2.3.3 Placement of Reinforcement Cage	14
2.3.4 Filling Of Trench with Structural Concrete	14
Attainable Concrete Strength	16
Recommended Concrete Strength	16
Bond Stress And Strength: Deformed Bars	17
2.3.5 Sequencing And Construction Joints	17
2.4 Design, Execution, Quality Control And Monitoring	21
2.4.1 Design and Execution	21
2.4.2 Quality Control	22
The need for continuous construction	22
Panel instability	22
Inclusions	22
Tolerances	23
Concrete quality	23
Water resistant construction	24
2.4.3 Monitoring	25
(i) First Group Of Monitoring Work	25
(ii) Second Group Of Monitoring Work	25
(iii) Third Group: Performance Monitoring	25
3 Problem Description And Method Of Simulation	27
3.1 Construction Properties	27
3.1.1 Soil Properties	27
3.1.2 Construction Method	28
3.1.3 Structural Data	29

	Reference Period and Durability	29
	Structural Geometry	30
	Diaphragm Walls	31
	Struts	32
	Floors	33
	Under Water Concrete	33
	Construction Joints	35
3.2	Decision For Soil Model	36
3.2.1	Beam On Elastic Foundation Method	37
3.2.2	Finite Element Method	39
3.2.3	Modeling Method Of This Thesis	39
3.2.4	Geotechnical Design Approaches	40
	Decision	42
3.3	Assumptions on the Soil and Structure Behavior	43
3.3.1	Executorial Assumptions	43
3.3.2	Assumptions On Behavior Of Soil	44
3.3.3	Assumptions On Wall Structure	45
4	Preliminary D-Sheet and K₀ Analyses	47
4.1	D-Sheet Analysis	47
4.1.1	Applied Soil Properties	47
4.1.2	Applied Structural Properties	49
4.1.3	Analysis Results	53
4.1.4	Analysis Results: Points To Take For Diana Analysis	59
4.2	K ₀ Analysis: Cylinder Under Pressure	60
4.2.1	Results of K ₀ Analysis	63
5	Description of Diana Models: Plane Strain, Axi-symmetric Condi- tions	65
5.1	Modeling Strategy	65
5.1.1	Definition:Plane Strain Conditions and Axi-symmetric Conditions, Phased Analysis	66
5.1.2	Chosen Elements And Properties	67
5.2	Model, Supports, Loads, Mesh	73
5.3	Results	80
6	Introduction Of The Engineering Model For Critical Joint	91
6.1	Critical Construction Joint's Deflection Estimation	91
6.2	Estimation Of Resulting Section Forces (M, V)	96
6.3	Determining The Effect Of Eccentricity At Critical Joint	101
6.4	Determination Of The Axial Hoop Forces (N) That Acts On Eccentric Connection	102
6.5	Superposition Of Results	107
6.6	Failure Mechanisms	109
6.6.1	Tension Failure Mechanism	109
6.6.2	Shear Failure Mechanism	111
7	Conclusions and Recommendations	113
7.1	Results Taken From This Thesis	113
7.2	Analysis Methodology Limitations	114
7.3	Suggestions For Future Researches	114

Bibliography

List of Figures

1.1	Top View of Construction Pit: Green Panels Straight; Blue Panels Circular; Critical Connections Marked By Red	2
1.2	Tangential Forces Due To Inwards Pressure	3
1.3	Eccentricity at the Particular Joint	3
1.4	Expected Deformations Due To Ovalisation: Red shows the deformed wall[Top View]	4
2.1	A Circular Diaphragm Wall Application	8
2.2	Difference of Ranking Between Requirements	9
2.3	General Requirements: Red, Functional Requirements: Purple, Functional Criteria: Yellow	10
2.4	Execution Of One Panel	11
2.5	Two Parallel Rectangular Guide Walls Separated By Timber struts	11
2.6	Two Parallel Rectangular Guide Walls Separated By Timber struts	11
2.7	Filter Cake Effect Due To Displacement Of Soil Particles. Caused By Slurry Flow Reversing While Clam Shell Excavator Pulls Up	13
2.8	Bauer Catalog: Slurry Circulation System With Trench Cutter Method	13
2.9	Sequencing of Cage Installment, End Tube Installation, Concreting	14
2.10	Tracing Of Concrete Batches In The Panel	15
2.11	Rising Concrete Strength Along Depth	17
2.12	Successive Sequencing	18
2.13	Execution Of Primary Panels	18
2.14	Execution Of Secondary Panels	18
2.15	Different Types of Vertical End Stops	19
2.16	Cost Analysis For Different Aspects Of Different Stop Ends According to Brinckerhoff, 2008: 1-low cost, 2- below average cost, 3-average cost, 4-above average cost, 5-high cost	20
2.17	Water Stop Methods: 1CWS or 2 CWSs	20
3.1	Soil Stratification According To CPT Measurement 15	28
3.2	Top View And Dimensions Of Excavation Pit, Including Panel Lengths	30
3.3	Side View Of the Construction and Levels of Floors [mNAP]	31
3.4	Top View Of Two Different Panels	32
3.5	Two Rows Of Hollow Core Struts	32
3.6	Effect Of Vibration And Slump For Strength Of UWC	34
3.7	Basal Heave Balanced With UWC and Piles(Yellow)	35

3.8	Requirements For Spacing Between Joint Tape And Cage And Two Cages	35
3.9	Straight Panels [m]	36
3.10	Curved Panels [m]	36
3.11	Wall Modeled With Soil as Winkler Springs	37
3.12	$p-\Delta u$ Curve of Soil: CUR166	38
3.13	Required Vastness Of Soil For A Reliable Continuum Model	39
3.14	CUR Step 6.1	42
3.15	CUR Step 6.2	42
3.16	CUR Step 6.3	42
3.17	CUR Step 6.4	42
3.18	CUR Step 6.5	43
3.19	Straight Slip Surface Assumption	45
4.1	Soil Stratification Representation	48
4.2	Position of Struts in Excavation	50
4.3	Floors Modeled as Springs	51
4.4	Stage 1 Verification Step 6.5: Unit [$mNAP$]	52
4.5	Stage 1 Verification Step 6.5	53
4.6	Stage 2 Verification Step 6.5	53
4.7	Stage 3 Verification Step 6.5	54
4.8	Stage 4 Verification Step 6.5	54
4.9	Stage 5 Verification Step 6.5	55
4.10	Stage 6 Verification Step 6.5	55
4.11	Comparison Of Deflections For Different Stages	56
4.12	Comparison Of Bending Moments For Different Stages	57
4.13	Comparison Of Shear Forces For Different Stages	58
4.14	Top View Cylindrical Wall	60
4.15	Side View Cylindrical Wall	60
4.16	Geometrical and Material Properties that are used in the Ko Analysis	61
4.17	Inner and Outer pressures subjected to a diaphragm wall supporting an excavation	62
4.18	3-Pinned Arch Graphical Representation	63
4.19	Analyses Results: Displacement Results From Ko Analysis; Hoop Force Results From 3-Pinned Arch and Ko Analyses	64
5.1	A Simple Plot Showing The Diaphragm Wall	65
5.2	Plane Strain Element	66
5.3	Axisymmetric Element	66
5.4	Nodes and Local Axes of CL9PE Infinite Shell Element	68
5.5	CL9PE Deformations and Rotation Definition	68
5.6	Nodes and Local Axes of CL9AX Shells of Revolution (SOR) Element	68
5.7	CL9AX Deformations and Rotation Definition	68
5.8	Line Interface Element CL12I	69
5.9	CL12I Element Variables	69
5.10	$p-\Delta u$ Graph of CUR transformed to Diana Input	70
5.11	$p-\Delta u$ Graph Of An Exemplary Soil Layer On Excavated Side	70
5.12	Local Axes Of Interface CL12I On Both Sides Of the Wall: Green local y, Red local x	72

5.13	Topology and Variables of Discrete Spring Element SP2TR	73
5.14	D-Sheet Results of Strut Forces and Displacements: Top Strut 1st chart, Bottom Strut 2nd chart	73
5.15	Element lengths and real life positions of shell elements [$mNAP$] and interface elements attached to them. Length [m], differ- ent Soil Layers Colored Separately	74
5.16	Graphical representation of Geometry	75
5.17	Bottom support defined at the bottom of the wall, Side sup- ports defined at the end of interface elements	76
5.18	Different Phases and Applied P_{out} P_{in} and Resulting Load	77
5.19	Different Phases and Applied Resulting Load	78
5.20	Graphical Representation Of Phased Excavation: Water Level Represented Blue, Soil Level Represented Brown, Struts Rep- resented Red, Concrete Represented Grey	79
5.21	Different Phases: Mesh Transformation	79
5.22	Phase 1 Results	81
5.23	Phase 2 Results	81
5.24	Phase 3 Results	82
5.25	Phase 4 Results	82
5.26	Phase 1 Results	84
5.27	Phase 2 Results	84
5.28	Phase 3 Results	85
5.29	Phase 4 Results	85
5.30	Plane Strain Model for 1.2 Meter Thick Straight Wall	86
5.31	Idealized Axisymmetric Model for 0.8 Meter Thick Cylindri- cal Wall	86
5.32	Phase 1 Comparative Results	88
5.33	Phase 2 Comparative Results	88
5.34	Phase 3 Comparative Results	89
5.35	Phase 4 Comparative Results	89
6.1	Critical Joint Top View: Deformation Of Idealized Condi- tions Meeting At Joint, Searching For A Deformation Line	92
6.2	Line Searches For Phase 1	93
6.3	Line Searches For Phase 2	93
6.4	Line Searches For Phase 3	94
6.5	Line Searches For Phase 4	94
6.6	Top View: Deformation w , Curvature κ and Subgrade Reac- tion Coefficient k_{hi} and Displacement w Differences At Dif- ferent Positions	96
6.7	Phase 1: Out Of Plane Moments And Shear Forces Redistri- bution	98
6.8	Phase 2: Out Of Plane Moments And Shear Forces Redistri- bution	99
6.9	Phase 3: Out Of Plane Moments And Shear Forces Redistri- bution	99
6.10	Phase 4: Out Of Plane Moments And Shear Forces Redistri- bution	100
6.11	Top View: Eccentric Connection And Acting Section Forces (Axes are not related to Diana Global reference system)	101

6.12 (a)Side View: Diaphragm Wall Subject To Out Of Plane Bending M_b (b)Top View: Diaphragm Wall Subject To In-Plane (Rotational) Bending M_r	101
6.13 Arch with radius r Subjected to Outer Uniform Pressure P , resulting in support reaction N	102
6.14 Axi-symmetrical Mesh With Applied Imposed Deformation on 0.8 m thick cylindrical Wall	103
6.15 Axial Forces Obtained From Arch Method	104
6.16 Axial Forces Obtained From Imposed Deformations	104
6.17 Resulting Eccentricity Moment M_N concluded From Arch Method	105
6.18 Resulting Eccentricity Moment M_N concluded From FEM Analysis With Imposed Deformations	106
6.19 Uneven Displacements Resulting In Rotational Deformations, Thus Tension (t) In Unarmed Joint	108
6.20 Eccentric Load And The Resulting Distributed Stress	108
6.21 Shear Failure At Critical 0.8 m Thick Section	108
6.22 σ_1 and σ_2 Calculated By Lower Bound N Value OF Arch Method: Construction Phase 4	110
6.23 σ_1 and σ_2 Calculated By Upper Bound N Value Of FEM Analysis With Imposed Deformations: Construction Phase 4	110
6.24 Shear Capacity Compared With Absolute Shear Values: Phase 4	112

List of Tables

3.1	Soil Properties	28
3.2	Material Properties Of Concrete Strength Class C28/35	32
3.3	Geometrical Data On Panels	32
3.4	Floor Geometrical Properties	33
3.5	Soil Properties	34
3.6	Moduli Of Subgrade Reaction k_h [kN/m^3]	38
3.7	Partial Factors And Geometrical Deviations For EN7 RC3	41
3.8	Partial Factors And Geometrical Deviations For CUR166 Method:III-A	41
3.9	Design Values For Soil And Geometry Properties In CUR Steps ($k_{high,rep} = 2.25 * k_{low,rep}$)	43
4.1	Soil properties CPT15	47
4.2	Lateral Displacement Stiffness Parameters	48
4.3	Struts Structural Properties	50
4.4	Properties of Floors	51
4.5	Spring Constants of Floors	51
4.6	Diaphragm Wall Properties	52
5.1	Wall Elements Applied Properties	69

Chapter 1

Introduction

1.1 Introduction

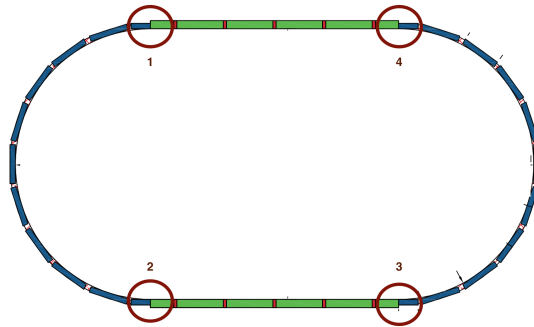
After the heavy industrialization and increasing need for developed areas with modern regulations for city urban development requirements, underground structures has increased remarkably in the practice. These types of structures are standing in need of big excavation works which need to be laterally supported by a supporting system for the soil that surrounds the excavated area. Depending on the scale and importance of the project, and how it is aimed to be used, one of the many vertical soil support systems can be chosen for this work.

For big and deep excavations, the use of reinforced concrete diaphragm walls is highly appropriate due to its high bending stiffness, the limited amount of displacement allowed for the given depth of excavation and its relatively easier application compared to some other methods. In addition, diaphragm walls cut the seepage from outer soils to the excavation pit, which creates a remarkable benefit for an underground structure that to be realized in The Netherlands, a country where soil and underground water conditions are highly challenging. They are also to be used as a structural component of the underground structure, rather than just a soil bearing system.

When these benefits of Diaphragm Walls are taken into account, their widespread use in practice is comprehensible. This field proves its varied aspects for a structural engineer to look for answers concerning the challenges of design and application of the wall. Which leads researchers to investigate these structures and their behavior more in detail with the increasing developments and requests in the field. This thesis focuses on a deep excavation work supported by reinforced concrete diaphragm walls realized with the staged excavation method.

The project includes an excavation work to be encased by structural diaphragm walls. The top view of the excavation can be seen in Figure 1.1. This type of configuration uses a mix of two types of diaphragm walls. Circular and straight diaphragm wall configuration are connected to each other by construction joints at both ends of the pit marked by red circles.

FIGURE 1.1: Top View of Construction Pit: Green Panels Straight; Blue Panels Circular; Critical Connections Marked By Red



1.1.1 Problem Description

As will be explained in detail in Section 1.1.2, there is theoretical and practical knowledge to estimate the deflection behavior of the two different wall shape configurations when they are built separately. From a literature survey it is seen that there is a lack of knowledge to estimate the behavior of walls which are a combination of different load transfer mechanisms (see explanation of these mechanisms in 1.1.2).

From a structural point of view, estimating the performance of the contact surface between two types of panels (construction joints marked with red circles, see Figure 1.1) during staged excavation and service life is needed, to be able to continue with the execution of the project. The reasoning behind this problem description will be elaborated in sub chapter 1.1.2.

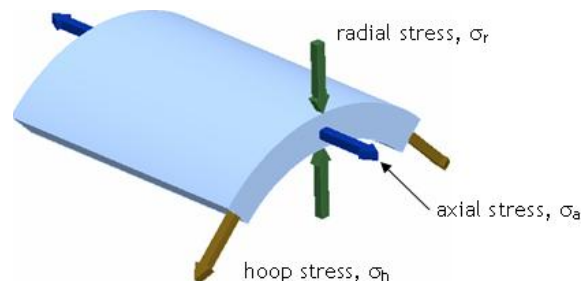
1.1.2 Problem Background

The two different types of wall configuration used together decreases the predictability of the behavior of the wall and soil behind it, which prevents the designer to also benefit from previous experiences and empirical data.

For a cylindrical diaphragm wall, it can be assumed for the theoretical axi-symmetrical circular shaped wall for uniform inwards soil pressure at a given depth shown by green arrows in Figure 1.2. The hoop forces occur in the tangential direction of the cylinder. An additional force occurs in the axial direction of the wall (Compression). These forces can be seen as brown arrows in Figure 1.2.

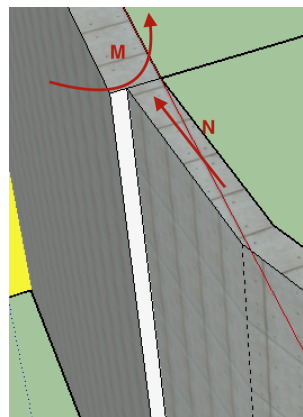
- A circular diaphragm wall is characterized by a predominantly horizontal balance of loading via normal force and arc operation under uniform loads. A straight diaphragm wall is characterized by a predominantly vertical balance of loading via bending under uniform loads. On the transition of a round to a straight diaphragm wall deformations of both systems are not compatible. This leads to additional moments and lateral forces in the horizontal direction that might result in the opening of the *unarmed joints* between the diaphragm wall panels and possibly succumb. This can lead to leakage of the joints.

FIGURE 1.2: Tangential Forces Due To Inwards Pressure



- A particular aspect at the investigated connection of the circular part and the straight part of the diaphragm wall is that it has a straight part thickness of 1200 mm and the round part a thickness of 800 mm see Figure 1.3. Because the interior sides of the round and the straight part are connected at the same level, alignment of the two parts becomes eccentric and introduces the transfer of the normal force from the round part with an additional moment in the straight diaphragm wall. It should be remembered that cylindrical type load bearing causes less deformations compared to bending type of bearing of straight walls.

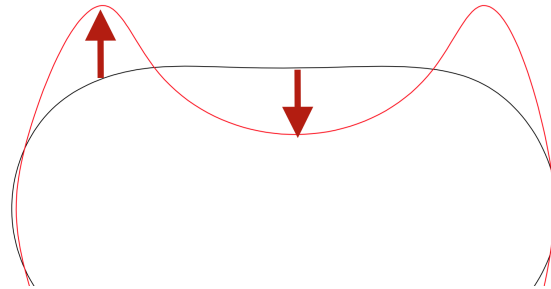
FIGURE 1.3: Eccentricity at the Particular Joint



- The circular cross section is subjected to ovalisation by an asymmetric load see Figure 1.4. This ovalisation depends on the stiffness of the surrounding soil. This leads to additional moments and lateral forces in the horizontal direction which is expected to give rise to the opening of the *unarmed joints* between the diaphragm wall panels and possibly failure. This will increase the distortion of the diaphragm wall and can lead to leakage of the joints.

The mechanics described above refers clearly to a 3-dimensional problem. Namely, the combination of round and straight diaphragm wall panels complemented by a phased stamping and excavation. Horizontal distortions will lead to greater vertical loading issues, that is complex by nature. It is not possible to implement this into a 2-D Model.

FIGURE 1.4: Expected Deformations Due To Ovalisation:
Red shows the deformed wall[Top View]



Due to the questions revealed about the load transfer and deflection mechanisms between two different wall types, the construction joint that is connecting them becomes critical and requires further investigation.

For a reliable analysis three aspects of this problem will be in focus, namely:

- An easy yet realistic simulation of soil behavior.
- Linear elastic estimation of reinforced concrete wall behavior and modeling of concrete wall panels.
- Focusing on the construction joints and clarification of different joints. Modeling realistically the behavior of joints.

These aspects are the main focus point of this dissertation. The soil part is necessary to estimate a realistic behavior. On the other hand, there will not be a detailed explanation of soil theories. Well used and suggested methods will directly be applied to the model.

1.1.3 Target of Thesis

Target of this thesis is not only to see if the mentioned construction joints can withstand the external pressures without failure. As mentioned earlier there is a theoretical knowledge gap on the behavior of walls that combine different load transfer mechanisms. And especially since these structures are geotechnical structures, the modeling of soil is more taken into detail by geotechnical engineers and the structural point of view is neglected or taken ideally. This thesis aims to focus less on soil and apply previously tried and suggested models. Thus, the focus is more on the structural joint.

1.1.4 Approach

For the determination of the behavior of construction joints under service loads, during phased excavation, different number of research aspects are revealed:

- Realistic simulation of the physical non-linear behavior of the soil and simplistic linear elastic modeling of the diaphragm wall.

- Clarification of mechanisms of the panels and their load transfer and modeling of expected behavior.
- Clarification of the mechanisms within joints and modeling of expected behavior.
- Clarification of the behavior of joints after analysis. (deflection, loading - resulting force conditions) of transition joints under service conditions.

In order to answer these research aspects, a diaphragm wall will be modeled according to a project that is waiting to be constructed. Material properties, geometrical data and soil properties will be based on this project and will be shared in Chapter 3. For the analysis of the problem two different computer programs will be used:

- D-Sheet: For preliminary analysis and recuperating soil stiffness diagrams.
- Diana 10.1: For realizing a simple yet effective model to analyze the problem and determine the deflections. Confirm them with previous preliminary analyses.

The procedure is briefly described below as it is represented in the thesis report:

Chapter 1 introduces the subject and sets the aim for thesis.

Chapter 2 reveals the literature survey that is carried out for clarifying the method of construction and its important aspects that have to be taken into account.

Chapter 3 describes the thesis problem in detail and presentation of the project data chosen according to the literature survey. It also elaborates the method of modeling, design approach and assumptions.

Chapter 4 illustrates 2-D analysis using the D-Sheet program, in order to estimate deflections. And to see the amount of mobilized passive pressures, and to calculate the spring parameters of the soil for each level of construction in every different construction stage.

Chapter 5 illustrates the preparation for a Diana 10.1 finite element model, decision of the elements to be used and application of the material properties derived from theoretical research.

Chapter 6 illustrates the engineering model to be used for the detection and analysis of the most critical structural joint at the connection of two different wall mechanisms.

Chapter 7 concludes the thesis and enlists the limitations, examines the possible effects of these limitations to results and suggests critical points that could be interesting for future research.

Chapter 2

Theoretical Background

In this section, the most crucial aspects of the general background and the construction method of diaphragm walls are presented. The aim of the section is to respectively represent the General background information of the subject and the definition of a diaphragm wall, Requirements of construction and execution, fundamentals of the construction and finally monitoring of the work during and after execution.

In order to clearly illustrate the different aspects of the survey, they will be presented in several sub chapters as follows:

1. General Background
2. General Construction Requirements
3. Construction Method and Sequencing
4. Design, Quality Control, Monitoring

2.1 General Background

For the different depths and sizes and the purpose of use of the excavation work, required and/or suggested walling or paneling technique is different. According to Puller, 2003 these different techniques are listed as below:

Plate and Anchor Walls: Useful for soil support during construction.

King Post Wall: Useful for only soil support during excavation.

Soldier Pile: Useful for only temporary works.

Steel Sheet Piling: Useful mostly for soil retention during excavation but with increased thickness and additional methods (combi or high modulus walls), it can be used as a permanent structure.

Contiguous Bored Piling: Both for temporary and permanent walls. It creates problems due to vibrations.

Secant piling: Similar method to above, only one pile is reinforced and the next intersecting is unarmed, higher impermeability can be achieved. The problem of vibration exists for this method too.

Diaphragm Walls: Useful for deep excavations where deflections are supposed to be limited. It can be done in different methodologies as reinforced cast in-situ, pre-cast reinforced and finally post-tensioned. According to the ease of use, the reinforced concrete cast in-situ method is highly appropriate for the construction of the scale of big projects.

As can be seen from the categorization above, for deep excavation works where depth is above 10 m, a steel sheet piling with embedded depth or a diaphragm wall with relatively smaller embedded depth is the most appropriate. When the method of increasing the stiffness of steel sheet piling is considered with the additional construction additions it requires a diaphragm wall proves its usefulness for this project. Since, the decision for diaphragm wall is made, the clear definition and advantages of diaphragm walls will be shared.

FIGURE 2.1: A Circular Diaphragm Wall Application



According to Kurian, 2013, diaphragm walls as can be understood from their names, are relatively thin soil retention structures embedded in soil. They are constructed in panels. At each panel, excavation of the trench, supporting of the trench with slurry, placement of the reinforcement cage, and filling of the trench with structural concrete, are executed.

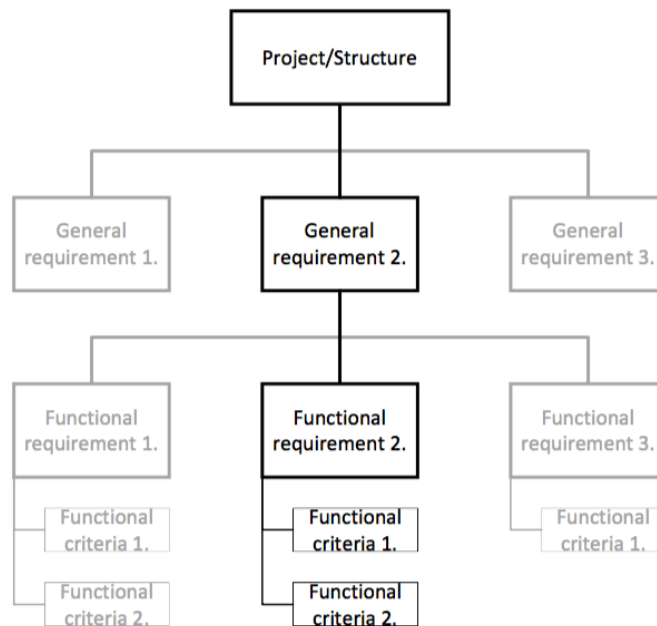
In addition Puller, 2003 enlists the benefits of diaphragm walls on the focus on aspects as listed below:

- its efficiency on cost and construction time. Diaphragm walls can be used for both permanent and temporary underground retention for walls of medium or greater depth.
- Diaphragm walls allow effective transfer of vertical load from the building superstructure to the subsoil below basement level.
- Diaphragm wall construction causes minimum noise and vibration disturbance.

2.2 Requirements and criteria

Requirements and criteria are separated into three categories according to their ranking (see Figure 2.2) in the following list respectively:

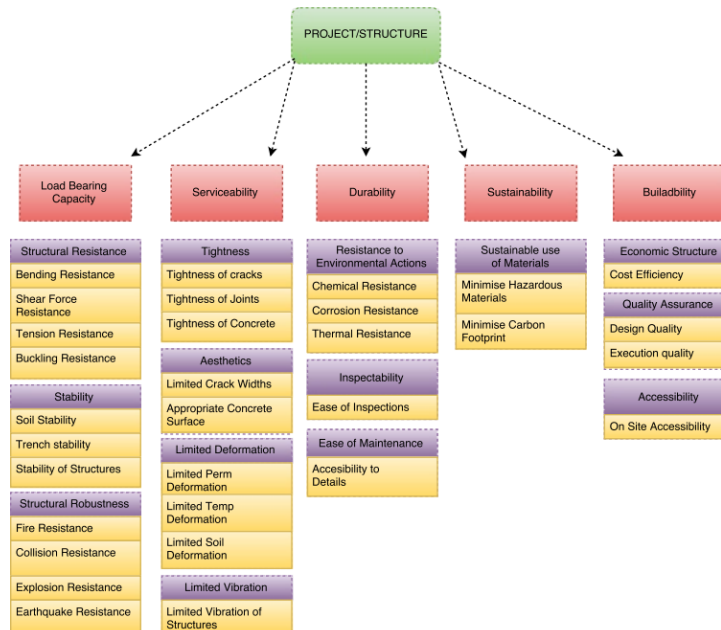
FIGURE 2.2: Difference of Ranking Between Requirements



- General Requirements: General and complete performance of the structure.
- Functional Requirements: Detailed Performance of the structure.
- Functional Criteria: verifiable specific performance of structure

The general requirements of diaphragm wall design and construction have been enlisted by Gudjonsson et al, are split into in five branches which are represented as red boxes in Figure 2.3:

FIGURE 2.3: General Requirements: Red, Functional Requirements: Purple, Functional Criteria: Yellow



2.3 Construction Method and Sequencing

As described , the total construction process of a diaphragm panel consists of five stages:

1. Excavation Of The Trench (Including Guide Wall)
2. Supporting Of Trench With Slurry
3. Placement Of The Reinforcement Cage
4. Filling Of Trench With Structural Concrete
5. Sequencing and Construction Joints

2.3.1 Excavation of Trench

The conventional construction procedure for slurry trenches, is described by Boyes, 1975. *Guide Walls* are constructed in advance of the slurry trenching operation. These walls are going to be used as the guides to the excavation process and there a significant high effect on the satisfaction of tolerances prevention of deviations from original geometry.

A trench using satellite mapping or electronic theodolites is excavated around 1 to 2 meters for the construction of the lightly reinforced guide walls. In case of having problems to find firm ground in the first 2 meters, the depth of the guide walls can be increased. Guide walls are constructed at a clearance between 25 mm to 50 mm to the finished surface of the diaphragm wall, see Figure 2.5 and Figure 2.6. The clearance distances are

FIGURE 2.4: Execution Of One Panel

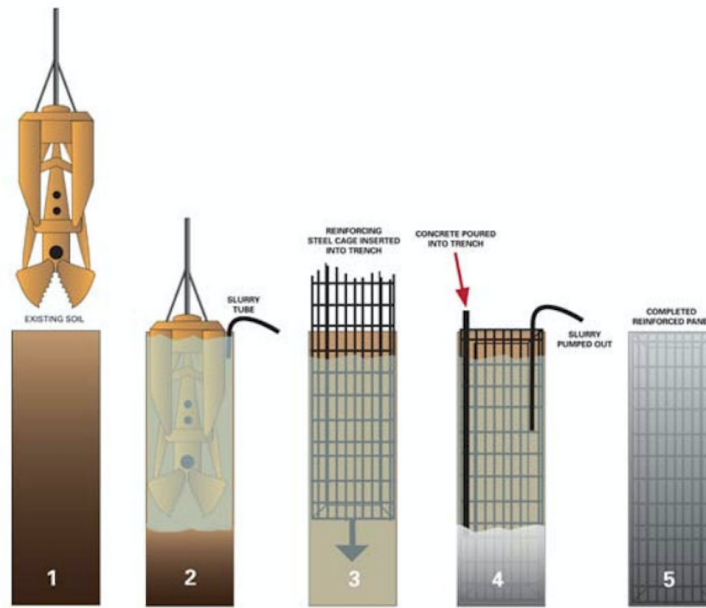


FIGURE 2.5: Two Parallel Rectangular Guide Walls Separated By Timber struts

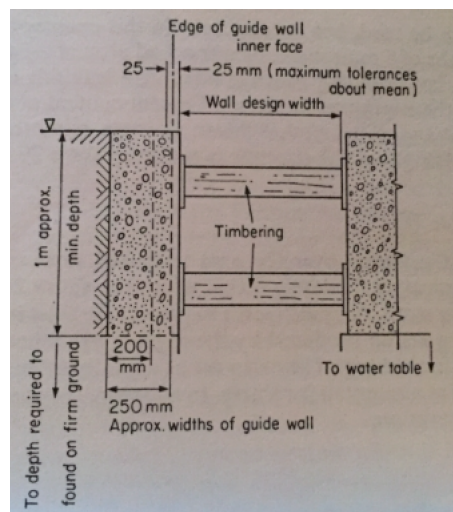


FIGURE 2.6: Two Parallel Rectangular Guide Walls Separated By Timber struts



required to be higher for curved walls.

The finished face of the guide wall towards the excavation should be vertical and deviation shouldn't be higher than 15 mm in 3 m. Existence of firm soil under the toes of the guide walls decreases the risk of slip failures due to surcharge loads on the soil adjacent to the outer side of guide wall. If the construction site is located on a soil with low bearing capacity, back-filling to guide walls should be avoided if possible. For instance, grab excavators can easily be used for guide wall excavation which is shallow meaning that deviations are still controllable.

Boyes, 1975 describes the purpose of the guide walls as follows: "They support the trench over the area subjected to heavy construction surcharge pressures, at the levels within which the slurry fluctuates during the course of the work. They also serve to protect the sides of the excavation against scouring action produced by the digging equipment or during the pumping in of fresh slurry. They also act as a guide to the grab during the excavation and as a reservoir for slurry. In addition, they define the planned path of the excavation." In addition, guide walls are used to support the hangers of reinforcement cages until the concrete is hardened.

After completion of the guide wall construction, *Excavation* work is carried out with different types of excavators for different site conditions and works. For the excavation of diaphragm walls special excavation equipment is needed because of the depth of excavation and to succeed a good finishing on excavated surface. Clam shell excavators and trench cutters are useful for this type of work and used in practice. In case of soil with boulders, specialized equipment might be needed.

During excavation, existence of sloped clayey stratus should be taken into consideration because it can affect the alignment of the clam shell excavator. In order to prevent misalignment during excavation preboring of piles at joint positions and later execution of excavation can be preferred. If there are limitations on sound and vibrations, guide pile boring might be less favorable, that is why a trench cutter can be preferred.

Excavation equipment should not cause severe fluctuations in the slurry height and create vacuum effect while leaving the trench see Figure 2.7. This requirement limits the speed of excavation and again increases the use advantage of trench cutters that are fully equipped to remove slurred soil through rotating cutter heads.

2.3.2 Supporting Of Trench With Slurry

During excavation, the trench will simultaneously be filled with slurry in order to keep the trench surface balanced with the liquid pressure caused by the bentonite water mixture in the trench. During this procedure, slurry height over water table should be kept in a stable manner. Slurry surface should be within the guide walls height. A regular slurry circulation system will be as shown in Figure 2.8.

FIGURE 2.7: Filter Cake Effect Due To Displacement Of Soil Particles. Caused By Slurry Flow Reversing While Clam Shell Excavator Pulls Up

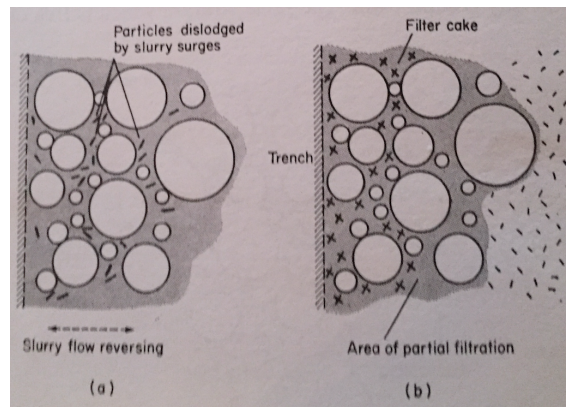
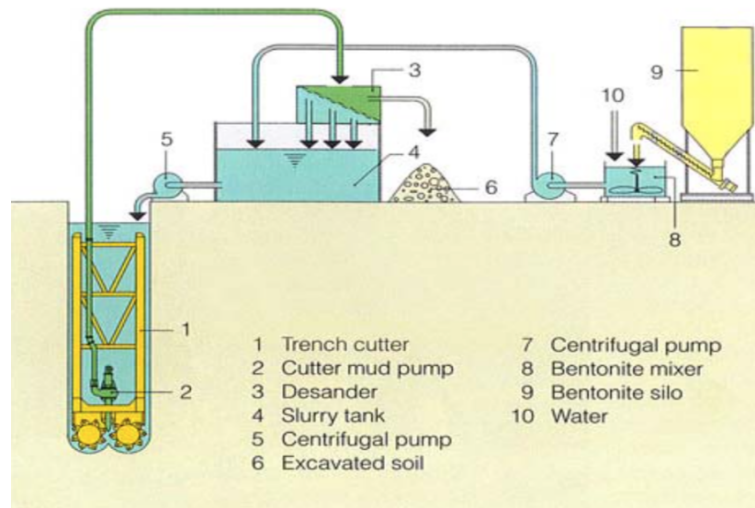


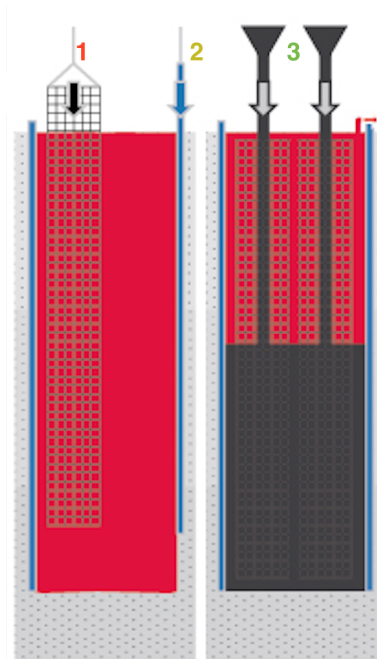
FIGURE 2.8: Bauer Catalog: Slurry Circulation System With Trench Cutter Method



Bentonite is a specific variety of clay named Montmorillonite. There are two types of bentonite: Natural sodium bentonites and calcium bentonites. Bentonite is a spongy rock with a soap like surface. And after mulling and milling it becomes a fine, dry cement like powder. There have been further developments by usage of clay in *Slurry* mixture. Additives can be used to increase performance *i.e.* *Polymers, Laponite*.

Slurry Mixture requires to satisfy different functional criteria to prevent many problems as inclusions, filter cake effect and rapid hydration of slurry. The lower limit to bentonite concentration in slurry mixture is 4-7%. This concentration is generally used in soils that support themselves without slurry yet used for extra precaution. For more difficult excavation works this concentration is expected to be higher.

FIGURE 2.9: Sequencing of Cage Installation, End Tube Installation, Concreting



2.3.3 Placement of Reinforcement Cage

Reinforcement cages are fabricated horizontally on site and lifted by cranes to a vertical direction and submerged into slurry and hanged by hangers to guide walls. Reinforcement cages must satisfy numerous requirements:

- Cages should also be resistant against deformations due to crane lifting, placement and especially tremie concreting.
- Round plastic or concrete spacers can be used in order to ensure the correct positioning of the cage.
- According to EN 1538, 2010 clause 8.2.2 the tolerance on the width of the reinforcement cage should be ± 1 cm. The tolerance on the elevation of inserts (starter bars) after concreting shall be ± 7 cm. The tolerance on the elevation of top of cage after concreting shall be ± 5 cm. The tolerance on the horizontal position of the cage along the axis of the wall after concreting shall be ± 7 cm.
- Bar spacing is suggested around 1 – 1.5 cm.

2.3.4 Filling Of Trench with Structural Concrete

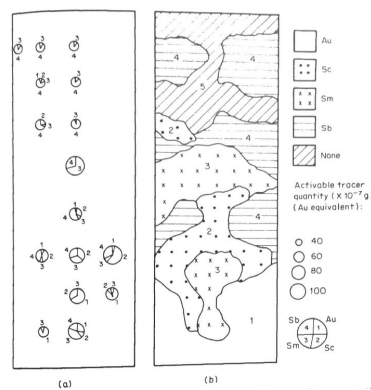
This part of the execution and design is highly crucial for the scope of the thesis, that is why, a detailed explanation of different aspects of the structural concrete walls will also be shared within this subsection. *Tremie Concreting* should be performed with a very steady continuity where, casting of poured concrete does not start before the completion of pouring in order to prevent discontinuities in the mechanics of the wall. Concreting of a continuous part should not exceed 6 to 7 hours. If not stabilized slurry concrete inclusions will form under newly poured fresh concrete. A standard

concreting pour is around $30 - 35 \text{ m}^3/\text{hr}$. Additives to increase the workability and the retard of setting can be highly useful. Aggregate should not be larger than 3.2 cm or one fourth of the maximum aggregate size. In EN 1538, 2000 clause 6.5.3 table 2 minimum cement content for Maximum grain size is given. For maximum grain size 3.2 cm , minimum cement content is suggested to be $350 \text{ kg}/\text{m}^3$.

For placement of the concrete with tremie pipes, Xanthakos, 1994 gives the following guide lines:

- The most common way of placing is done with pipes. In this method pipes are lifted simultaneously with the rising concrete height. The bottom of the trench should be cleaned by using special methods such as air lifts.
- There is a simple rule of thumb for the usable tremie dimensions, this rule is to use tremie pipes with a diameter at least 8 times bigger than the maximum aggregate size of the used concrete. If concrete with $size_{agg;max} = 3.2 \text{ cm}$ is used a tremie around 25 cm should be used to not to affect the flowability of the concrete.
- It should be remembered that for the flow motion of concrete, research has been carried out to trace the different batches of concrete and their position within the panel. It is seen from Figure 2.10 that the theory of first batch always rising above new coming batches until placement is finished is not true. This creates an emphasis on good pouring that will prevent *cold joints*.

FIGURE 2.10: Tracing Of Concrete Batches In The Panel



- In addition, the mixture of different batches changes with depth but not along thickness. That is why panels can be considered as uniform in their thickness direction, yet this can not be said along the depth.
- Attainable concrete strength along depth and cracked stiffness of the wall in vertical direction becomes important for the analysis and should be included in research.

Attainable Concrete Strength

Due to execution and operational factors designed concrete strength is difficult to reach in reality which leads us to estimate an attainable concrete strength. This strength is affected by multiple factors. These factors are listed as:

- Flow motion during placement: First batch since it is placed moves in the pit until whole pouring procedure is completed. For deep and long panels this can take many hours. That is why special care to prevent premature setting should be considered and taken into account.
- Changes in water-cement ratio: Concrete pour performed in the slurry filled pit, might cause the water content of the placed concrete to rise, which will decrease the attainable strength. Many methods of prevention have been discussed in related chapters to slurry.
- Introduction of bentonite and slime: If somehow intermixing of concrete with bentonite and slime is not prevented, the attainable strength of concrete reduces. This should especially be well monitored in joint sections.
- curing conditions: Curing is highly important to achieve a good hydration of placed concrete, it also has great effect on the surface quality of the concrete element, which has a high effect on the durability of the structure. The pouring should be performed during a time where the heat in soil depths are higher and moist compared to outside temperatures. This way, it can be maximally benefited from the underground pouring and its positive effect on curing. This is why, creep and shrinkage effects are out of this thesis scope.

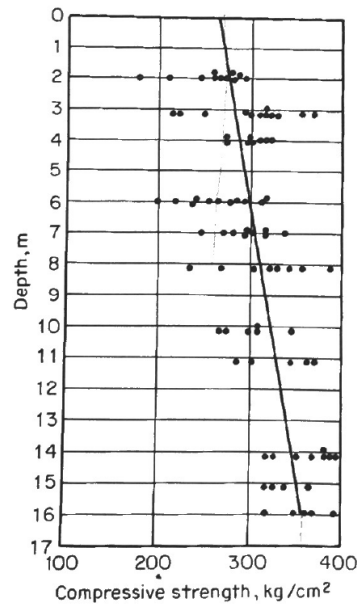
For the selection of minimum axial concrete compression strength f_c , Xanthakos, 1994 gives the following rule of thumb: For walls of nominal thickness 60 – 75 cm the suggested minimum design strength of concrete should be 21 MPa to 35 MPa. If higher concrete classes are aimed to be used, it should be justified clearly. Otherwise, it is unnecessary to use higher classes.

Recommended Concrete Strength

Many factors influence the concrete strength as mentioned earlier, yet a good estimation of the concrete strength is related to experience, well monitoring of execution procedures and pursuit of recommended checks and tests. Taking into account the favorable (good curing, increasing strength along depth...) and unfavorable (bentonite and slime infiltration...) effects, a good estimation is considered by Xanthakos, 1994 by relation 2.1 where f'_{ca} is the adjusted design strength:

$$f'_{ca} = 0.90 * f'_c \quad (2.1)$$

FIGURE 2.11: Rising Concrete Strength Along Depth



Bond Stress And Strength: Deformed Bars

Two different types of bars are available in practice, plain and deformed bars. These both systems have different load transfer mechanisms. Plain bars transfer the load from steel to concrete with adhesion and friction of the contact surface. On the other hand, deformed bars not only use adhesion and friction but also includes mechanism of bearing of reinforcement lugs by concrete. If the bars were deformed further, either the concrete between two adjacent lugs will crush due to compression or the dent of concrete between lugs will crack of shearing. In addition, deformed bars tend to show a better smeared cracking behavior this is why, using of deformed bars is highly suggested with the use of adequate splices (reinforcement laps). Splices should be prevented in zones of maximum stresses. If splices are unpreventable to use, it is recommended to use 1.5 to 2 times the splice length suggested by codes.

2.3.5 Sequencing And Construction Joints

Stop End Tubes are withdrawn when the concrete is hardened and a panel has been completed. The sequencing of the panels can be performed in two different options that are used in practice and in addition have different advantages and disadvantages:

- Successive panel construction as can be seen in Figure 2.12
- Alternative method with primary and secondary panel construction as seen in Figure 2.13 and Figure 2.14

Successive sequencing decreases the risks of entrapped end tubes during concreting since only end tubes in one side is used during sequencing,

FIGURE 2.12: Successive Sequencing

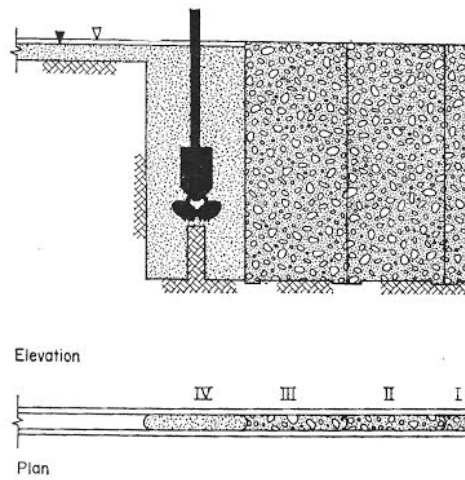


FIGURE 2.13: Execution Of Primary Panels

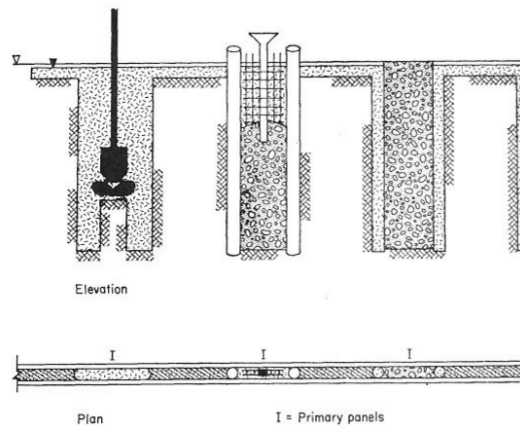
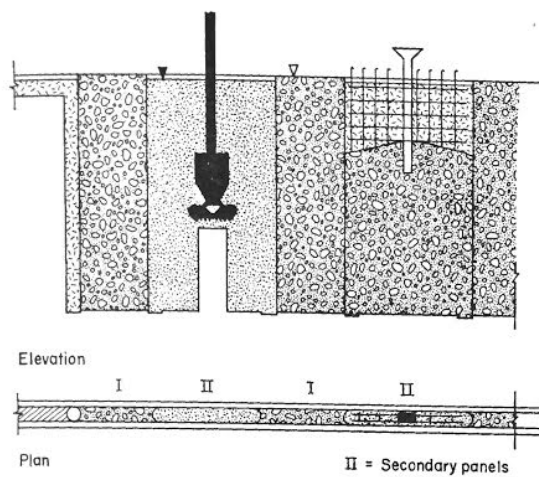


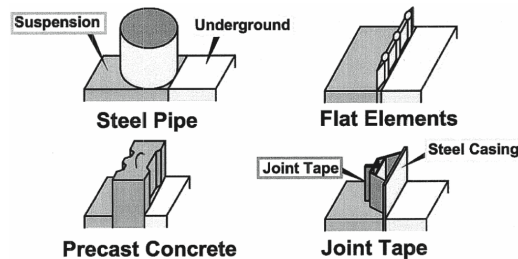
FIGURE 2.14: Execution Of Secondary Panels



which also increases the speed of construction. On the other hand, successive sequencing, insufficient hardening of the previous panel during the excavation of the next is a bigger risk. Alternative method sequencing is more

laborious and time consuming, on the other hand, according to Vlachioti, 2010, first methodology is more appropriate for straight wall configuration and the second methodology is more appropriate for circular walls.

FIGURE 2.15: Different Types of Vertical End Stops



As can be seen in Figure 2.15 different end stop types are available. Using precast concrete joints with their interlocking pockets can withstand immense shear and out of plane bending but the application and tolerances becomes more sensitive. Flat elements cannot create the effect of interlocking of successive panels in case of serious shear and out of plane bending effects on the joints. In practice, steel pipes and steel casing types of stop ends are preferred due to their ease of application.

In case of paneling where the joints need to be horizontally continuous to withstand out of plane bending additional methods might be needed. Because traditional methods are using unarmed joints. Xanthakos, 1994 describes the round tube joints as seen in Figure 2.15 (a), as solutions that can transfer lateral shear forces but can not transfer the bending stresses since the reinforcement is not horizontally continuous along the joint. If horizontal continuity is needed different methods such as *Steel Plate And Vinylon Sheet Method*, or in very special cases some joint types developed by specialist contractors, to allow structural continuity. These methods can be named: *TEBA Joints*, *TECA Joints*, *Steel Plate Casing Joint*, *Casing Joint By Franki*, *Locking Box By Takenaka*. During execution and design of joints some aspects should be taken into account for the ease and quality of joint execution. These remarks are Xanthakos, 1994:

- The joint forms and plates should withstand the pressure of fresh concrete without deflecting or slipping.
- If required the joint should be designed and built to transfer shear and possible other forces, and should be water tight according to the requirements.
- The joint should not collect slime and bentonite.
- The feasibility of construction should always be kept in mind and simple methods should be preferred.
- The joint should be economically feasible for the intended function of the wall.

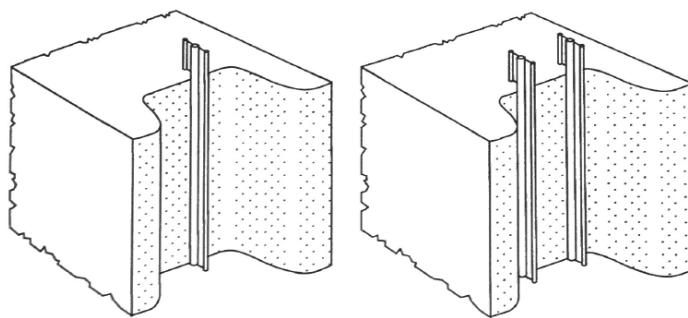
- Physically the joint should not disturb the previously poured section yet must also accommodate the excavation of the following panel without causing restrictions the use of equipment.
- While the joint is executed there should be no leakage of fresh concrete in to the slurry.

For decision of usable stop ends following CWS stop ends please check Figure 2.16. from this analysis it can be seen that Vinyl and/or PVC water stops are the most preferable within other options, due to their ease of installation yet they are one of the worst type of stop ends when long term costs are considered. swelling water stops can be preferred if the difficulties in application is considered and accepted. PVC water stops are highly used in practice and easy to procure. Figure 2.17 shows the use of 1 line or 2 lines of water stops in order to prevent leakage. For critical sections 2 lines of cws can be used to increase reliability.

FIGURE 2.16: Cost Analysis For Different Aspects Of Different Stop Ends According to Brinckerhoff, 2008: 1-low cost, 2-below average cost, 3-average cost, 4-above average cost, 5-high cost

System	Difficulty in Installation	Initial Cost	Long Term maintenance	Success Rating
Vinyl& PVC Waterstops	3	3	4	2
Swelling Bentonite Strips	4	4	5	1
Reinjectable Waterstops	5	5	5	2
Swelling rubber Waterstops	4	2	1	5

FIGURE 2.17: Water Stop Methods: 1CWS or 2 CWSs



2.4 Design, Execution, Quality Control And Monitoring

2.4.1 Design and Execution

For the design and execution of the diaphragm walls different levels of site information and analysis of the tolerances and information on limitations needed. For instance from *Executional* point of view, following information is needed:

- Topography of the construction site.
- Previous purpose of use of site.
- Geo-technical data as specified by In EN 1538, 2010 clause 5
- Information on the adjacent structures (Roads, Buildings, Infrastructure Works)
- Location and type of services such as gas, electricity, sewers.
- Presence of obstruction to construction (Old structures, Archaeological remains, Polluted ground...)
- Information on labor regulations.
- All specific requirements that are mentioned in subsection 1.3.2
- Previous experience

For the *design* aspect, general considerations to be taken into account can be listed as:

- Design shall take into account tolerances specified by EN 1538, 2010 clause 8.2.
- The panel dimensions should take into account the information in the previous list. In addition, the excavation system and equipment to be used will also decide the panel dimensions.
- The panels should be designed as uniform shaped vertical elements.
- The design of the wall shall take into account the horizontal discontinuity.
- A capping beam is required on the top side of the diaphragm wall.
- Panel Instability
- Requirements for reinforcement cages.
- Recesses and perforations.
- Concrete cover.

2.4.2 Quality Control

Quality control of a construction is the main reassurance of its execution that is carried out in such a way that, the assumptions in design procedure are met in reality. A well carried out quality control procedure would ensure the intended design life of a structure with minimum repairs. In addition, quality controllers have the main work frame so that they can also be highly useful for the other colleagues in their company and for certification of the work executed. Puller, 2003 describes different aspects of quality control work of diaphragm wall construction as follows, these considerations are also implemented in standards:

The need for continuous construction

It is highly crucial to maintain a stable cycle of execution. For a stable cycle of execution, planning of the project shall take into account the limitations on allowable excavation and concrete pouring, in addition the number of hours that workers can work per day. Additional planning for the transportation of fresh concrete should be kept in mind in order to estimate realistically the amount of concrete that can be poured per day and estimate the risks caused by traffic, waiting.

Panel instability

Panel instability does not directly have an increasing risk factor with increasing depth. It is more related to the obstructions during excavation and also to the soil profile that is excavated. Panel instability is related to the arching capacity of surrounding soil during all stages of panel excavations; the properties of slurry, the level of slurry, the length of panels, the time during which the trench is open are important factors to be monitored to prevent *concrete overbreaks*. The overbreaks should be cut and cleaned, but this procedure would risk the loss of contact between soil and wall at the given depth. The most important caution to prevent this type of problem, slurry should be kept at a height of 1.5 m above the water level and additional additives such as polymers can be used to reduce the risks of instability. If a difference of 1.5 m height can not be achieved directly between slurry and water table, lowering the water table to a level can be considered.

Inclusions

Inclusions might occur because of many factors, a slurry that is designed within requirements will limit the risks of inclusion but yet will not ensure it. For instance in the case of a badly planned and non continuous concrete pour (see section 1.3.3.4) will increase the risks of slurry inclusions within the concrete. Low slump and non-cohesive concrete also increases the risk of inclusions. On the point of view of planning the tremie work, tremie pipes should not be too far away from each other, because this can also increase the risks of inclusions. Some additional suggestions are listed as

follows:

- Prevention of large box-outs.
- For deep walls, especially the ones excavated by a cutter, it is suggested to use of different type of slurries for excavation and concreting.
- If heavy slurry used for panel stability is changed with lighter slurry right before concreting, risks of inclusions would decrease remarkably.
- Reinforcement spacing should comply with the standards. It shouldn't prevent the flow-ability of the concrete.

Tolerances

Different aspects of the work require and limit tolerances differently. These tolerances should be in harmony with the standards. An overall enlistment of tolerances is as follows:

1. Guide Walls: Vertical to within 1:200; minimum clear distance between the faces of the guide walls shall be wall thickness plus 2.5 *cm* and the maximum distance shall be wall thickness plus 5 *cm*, line of the finished face nearest to excavation should be 1.5 *cm* in 3 *m*.
2. Diaphragm wall: Exposed wall face and panel ends shall be vertical within a 1:100 tolerance.
3. Box-outs. Vertical and horizontal tolerances of 7.5 *cm* .
4. Reinforcement: Tolerances of reinforcement is shared in section 1.3.3.3 in detail.
5. Concrete: Where the final trimmed level of the diaphragm wall is up to 1 *m* below the top of the guide wall, the casting tolerance will be 60 *cm* above the trim level; for each additional 1 *m* depth of final trim level, allow an additional 15 *cm* level tolerance.

Concrete quality

Large concrete pours are required for deep diaphragm walls. Mass concrete has many risks that can be named as: over heating of the hydration process, segregation... These effects can reduce the strength of the wall remarkably. That is why, concrete pouring job for some aspects of the mixture should be stringently specified. "EN1538" 2010 Clause 6.5 describes the requirements to be satisfied as follows:

- Clause 6.5.1 sets the guideline for the concrete properties required to achieve correct execution. Its water tightness should also be kept in mind.

- Clause 6.5.2 sets the limitations for maximum aggregate size.
- Clause 6.5.3 sets the guideline for minimum cement content that is required for the chosen maximum aggregate size.
- Clause 6.5.4 sets the guideline for maximum water/cement ratio, the minimum ratio is decided by different factors such as intended strength, level of hydration, desired permeability etc.
- Clause 6.5.5 sets the guidelines for the use of admixtures.
- Clause 6.5.6 sets the guidelines for the fresh concrete and its workability. Slump test is required for the decision of the applicability of the procured concrete. a slump value between 1.6 – 2.2 *cm* is suggested. In addition, flow test may also be used instead of slump test, it should be performed right before placement and should has a value of 5.2 – 6.3 *cm*.

Water resistant construction

Water resistance is a core important aspect of diaphragm walls and its reassurance is a must for these types of work. No diaphragm wall can achieve full water tightness but it should be kept under a certain rate of flow for reasons like: stability, failure and also serviceability. Following aspects of water resistant underground construction should be kept in mind:

- Soil and underground water conditions: Loose soils with high water tables increases the risk of deflection from water resistant construction.
- All the aspects of work should satisfy the required standards and control quality procedure should be detailed accordingly.
- Avoiding of walls with thickness lower than 0.6 *m*.
- There are some literature survey that proves that joints with return angles has higher risks for not satisfying tightness requirements.
- The greater the depth of excavation, the greater the risk of leakage.
- Shorter panels can increase the amount of joints which is not suggested but on the other hand it might reduce the risk of inclusions.
- In case of using cutters the vibration can be minimized, if in addition, improved verticality tolerances are implemented, better finishing and quality of wall can be achieved.
- Excessive reinforcement increases the risk of worse water tightness.
- Top Down construction reduces the risks of leakage.
- Systems such as CWS are essential to stop the leakage.
- Precautionary grouting can be used in critical joints.

2.4.3 Monitoring

Monitoring is the key to reassure the quality of a construction and can also provide data to analyze the performance of the structure. Monitoring can be separated in three groups depending on the nature of the work. First group of monitoring suggestions are about monitoring of the earthworks and related measures. Second group is about execution of panels and continuous wall. Last group is performance monitoring of the structure.

(i) First Group Of Monitoring Work

"EN1997-1" 2005 Annex J Clause j.2.1 describes the check points as: "Verification of ground conditions and of the location and general lay-out of the structure. Ground-water flow and pore-water pressure regime; effects of dewatering operations on ground-water table; effectiveness of measures taken to control seepage inflow; internal erosion processes and piping; chemical composition of ground-water; corrosion potential. Movements, yielding, stability of excavation walls and base; temporary support systems; effects on nearby buildings and utilities; measurement of soil pressures on retaining structures; measurement of pore-water pressure variations resulting from excavation or loading. Safety of workmen with due consideration of geotechnical limit states." Clause j.2.2 describes the points to be monitored about water flow and pore pressure as: "Adequacy of systems to ensure control of pore-water pressures in all aquifers where excess pressure could affect stability of slopes or base of excavation, including artesian pressures in an aquifer beneath the excavation; disposal of water from dewatering systems; depression of ground-water table throughout entire excavation to prevent boiling or quick conditions, piping and disturbance of formation by construction equipment; diversion and removal of rainfall or other surface water. Efficient and effective operation of dewatering systems throughout the entire construction period, considering encrusting of well screens, silting of wells or sumps; wear in pumps; clogging of pumps. Control of dewatering to avoid disturbance of adjoining structures or areas; observations of piezometric levels; effectiveness, operation and maintenance of water recharge systems, if installed. Settlement of adjoining structures or areas. Effectiveness of sub-horizontal borehole drains."

(ii) Second Group Of Monitoring Work

"EN1538" 2010 Table 3 gives an overall description of the monitoring works to be performed for in-situ diaphragm walls and the suggested frequency of monitoring for each different work. These monitoring works can be separated in five groups namely, about lowering reinforcement cages, concreting, extracting stop ends, trimming, exposed face.

(iii) Third Group: Performance Monitoring

These monitoring are for collecting experience from the structure under service conditions. Also threatening conditions such as intensive settlement

around pit can be early detected with well conducted performance monitoring. "EN1997-1" 2005 Annex J Clause j.3 describes the performance monitoring of the construction as "Settlement at established time intervals of buildings and other structures including those due to effects of vibrations on meta stable soils. Lateral displacement and distortions, especially those related to fills and stockpiles; soil supported structures, such as buildings or large tanks; deep trenches. Piezometric levels under buildings or in adjoining areas, especially if deep drainage or permanent dewatering systems are installed or if deep basements are constructed. Deflection or displacement of retaining structures considering: normal backfill loadings; effects of stockpiles; fills or other surface loadings; water pressures. Flow measurements from drains. Water tightness. Vibration measurements."

Chapter 3

Problem Description And Method Of Simulation

From the problem description and theoretical background chapters the following aspects of the work should be chosen for the development of the thesis methodology. These aspects can be separated into subsections such as the geometrical and material properties of the construction, the modeling methodology of soil behavior and the structural assumptions that are used.

3.1 Construction Properties

3.1.1 Soil Properties

During field tests, CPT measurements have been carried out in multiple positions according to standards, and the soil properties that to be derived from cone penetration tests are taken conservatively according to the methodology in "EN1997-1" 2005. Two types of soil came to attention due to their soil parameters, but CPT number 15 is the most appropriate due to its well presenting characteristic values of soil parameters and its closeness to the location of the diaphragm wall to be constructed. In order to be able to analyze the structure, a detailed soil profiling is needed.

Analyzed soil properties will be chosen according to the requirements of CUR method. These required properties are listed as:

- Unsaturated and saturated total unit weights γ_{ur} γ_s
- Cohesion c
- Internal friction angle ϕ
- Delta friction angle $\delta \approx 2\phi/3$

The cone penetration test is performed by a cone that penetrates the soil at a constant rate. During this penetration procedure, forces on the cone and friction sleeve are measured. Cone penetration tests are used to determine the in-situ stress conditions, shear strength parameters, soil density, soil type and especially soil stratification. The stratification of soil can be seen at Figure 3.1.

FIGURE 3.1: Soil Stratification According To CPT Measurement 15

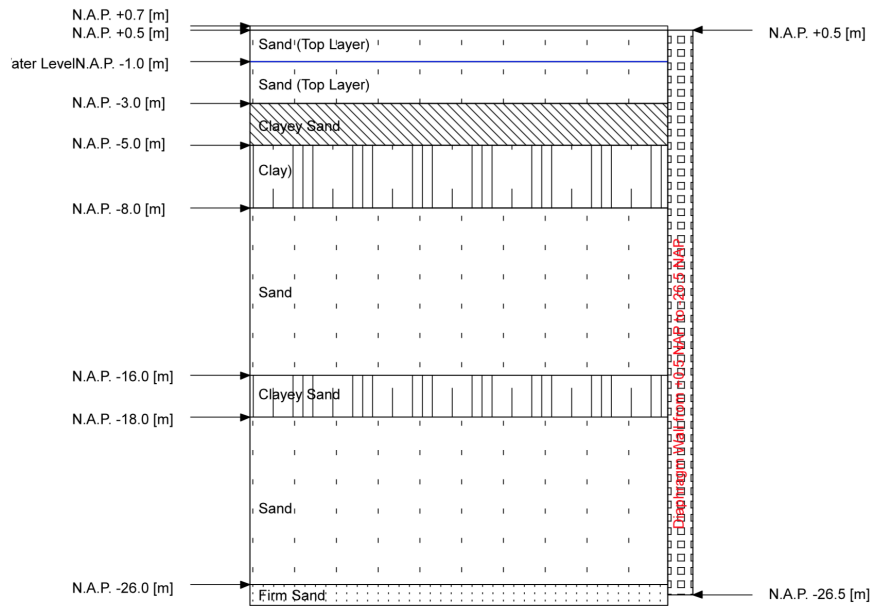


TABLE 3.1: Soil Properties

<i>SoilType</i>	<i>TopLevel</i> <i>mNAP</i>	$q_{c,av}$ kN/m^2	γ kN/m^3	c kN/m^2	ϕ °	δ °
Sand (Top Layer)	+ 0.5	4.0	17/19	0	32.5	20.0
Clayey Sand	-3.0	3.5	18/18	0	25.0	16.7
Clay	-5.0	1.0	17/17	5	17.5	11.7
Sand	-8.0	8.0	18/20	0	32.5	20.0
Clayey Sand	-16.0	4.0	18/18	0	25.0	16.7
Sand	-18.0	15.0	18/20	0	32.5	20.0
Firm Sand	-26.0	23.0	19/21	0	35.0	20.0
Gravel	-17.75		20/22	0	37.5	20

As can be seen From Table 3.1, q_c values have been analyzed according to methodology of EN7, and the cone penetration test results are averaged according to lower bound case to increase the reliability of the analysis. It should also be noted that *water level* is accepted to be situated at -1 *mN.A.P.*.

3.1.2 Construction Method

Staged and Struted and paneled construction is decided to be the most appropriate method for the work. The reasons for this methodology can be discussed in different aspects. Using struts can be explained by different reasons:

- In order to decrease the expected deflection differences between straight and circular walls.

- In order to design the walls by satisfying the requirements for maximum allowable deflection.
- Reducing the unpredictability and the risks during excavation stages that might rise from unexpected deflections and the rupture of the walls.
- Circular hollow core struts will be used due to their uniform properties. And the higher stiffness they have against buckling compared to the open sections.

Construction will be realized with staged method. D-Sheet allows the user to set the stages of construction and according to the analysis method, all stages will be confirmed step by step to reassure the stability of the excavation work in each step of construction. According to the CUR 166, the construction stages one by one should be analyzed to secure the integrity of work throughout the construction and later on during service life. Diana 10.1 also allows user to perform a staged excavation analysis.

The construction stages will be total number of six stages as follows:

- **Stage 1:** Water Level in the pit will be lowered to -2.7 mNAP and the pit will be dry excavated until -2.5 mNAP .
- **Stage 2:** The strut at -1.5 mNAP will be placed, the water table will be released again back to -1 mNAP and wet excavation up to -10 mNAP will be carried out.
- **Stage 3:** The second strut at level -9 mNAP will be placed and the wet excavation until -18.5 mNAP will be carried out.
- **Stage 4:** Leveling, Gravel and Under Water Concrete will be placed and the excess water will be pumped out of the pit which will make the new water table level at -17.75 mNAP and the pit surface will be at -16.75 mNAP .
- **Stage 5:** The floors -5, -4, -3, -2 will be placed meanwhile the strut at level 9 mNAP will be removed.
- **Stage 6:** The floor -1 and the deck will be placed meanwhile the strut at -1.5 mNAP will be removed.

3.1.3 Structural Data

Reference Period and Durability

The design must be determined on the basis of a design life of 100 years and a reference period of 50 years. Durability of the structure becomes highly important due to its constant contact with underground water. In addition, as mentioned previously the walls and joints are required to be water tight. When considering the challenging saline water content in The Netherlands required environmental classes for inside and outside of the wall becomes (EN1992, 2005):

- Outer side of wall: XC2 -> $c_{nom} = 4 \text{ cm}$ and preferred cover thickness $c_{app} = 10 \text{ cm}$.
- Inner side of wall: XC3

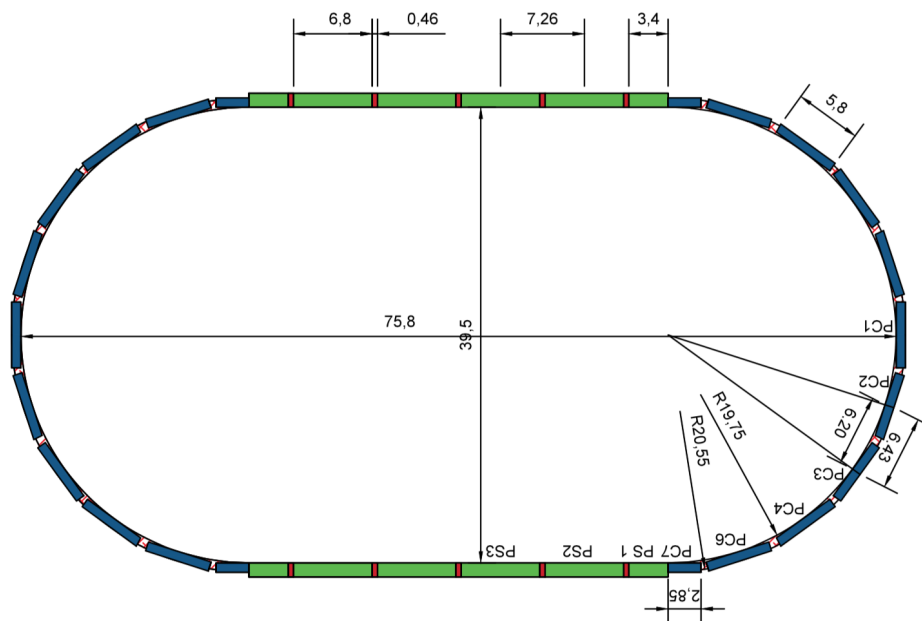
Structural Geometry

The geometry of the structure is decided by taking into account of couple of aspects as listed:

- Requirement for minimum depth of embedding.
- Maximum allowable deflection of the wall.
- Requirements on wall dimensions
- Required thickness of Under Water Concrete to withstand basal heave.
- Required bending stiffness of the floors due to the displacement of the wall.

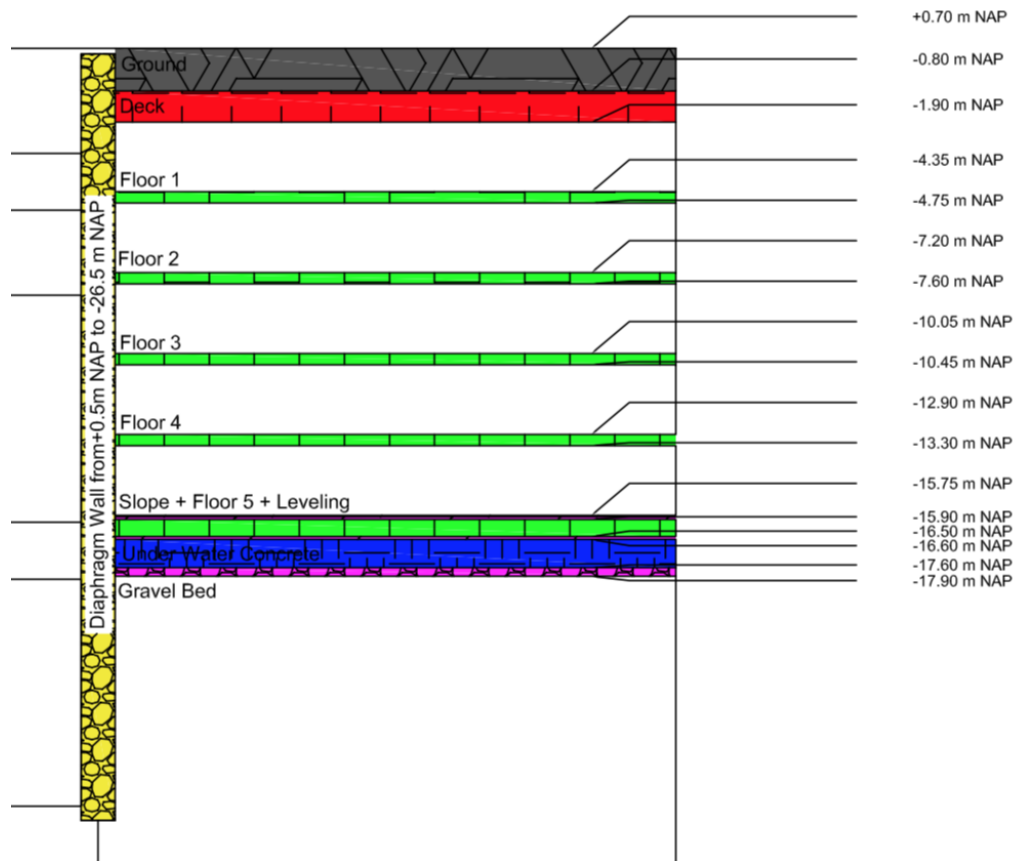
The top and side view of the construction pit can be seen respectively from Figures 3.2 and 3.3.

FIGURE 3.2: Top View And Dimensions Of Excavation Pit, Including Panel Lengths



Ground level: NAP + 0.5 m, Ring bar: NAP -1.0 m to -2.5 m, Diaphragm wall: NAP -2.5 m to NAP -27.0 m, Underwater concrete floor: NAP -16.6 to -17.6 m, Deepest excavation-level: NAP -17.9 m.

FIGURE 3.3: Side View Of the Construction and Levels of Floors [mNAP]



Diaphragm Walls

Diaphragm Walls will be built by the use of C28/35 concrete (C35 according to old method of labeling). The diaphragm walls will be two different types, Figure 3.4. Different information on panels according to their types can be listed as in Table 3.3.

As mentioned earlier, wall thickness at circular part is smaller than the wall thickness in the straight section. This is caused by the difference of deflection mechanisms for both wall types: Straight walls deform due to bending, on the other hand, circular walls deform due to arching caused by normal forces, which leads to smaller deformations. Designing the circular parts with higher thickness would be uneconomical, in addition heavily constrained deflections in circular part might increase the deflection incompatibility between straight and circular sections. Straight walls are designed thicker due to their relatively low stiffness against deflections compared to a circular section with same thickness. Further explanation will be done in related chapters.

TABLE 3.2: Material Properties Of Concrete Strength Class C28/35

<i>Property</i>	<i>Value</i>
	<i>MPa</i>
f_{ck}	28.00
$f_{ck,cub}$	34.2
f_{cm}	36.00
f_{ctm}	2.78
$f_{ctk,0.05}$	1.92
$f_{ctk,0.95}$	3.60
E_{cm}	$32.8 * 10^3$

FIGURE 3.4: Top View Of Two Different Panels

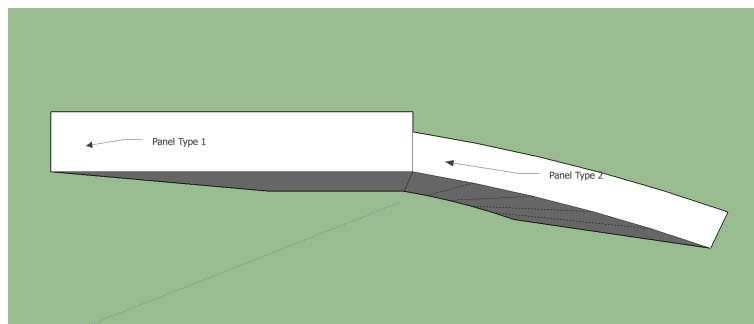


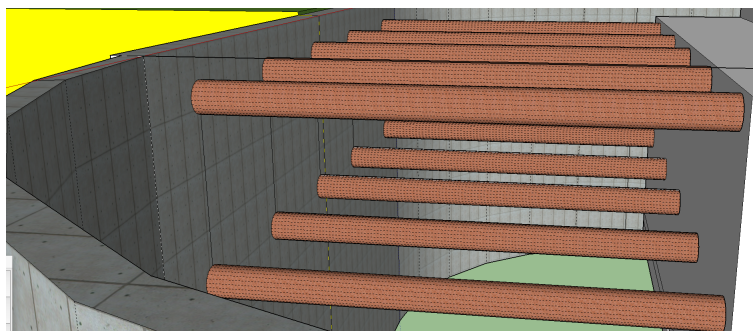
TABLE 3.3: Geometrical Data On Panels

<i>Name</i>	<i>PanelLength</i>	<i>Thickness</i>
	<i>m</i>	<i>m</i>
Panel 1	6.32	1.2
Panel 2	7.26	0.8

Struts

The struts will be used as steel grade S355, this steel grade is highly used in deep excavation where big lateral support is needed. The lateral (steel hollow core) struts that are decided to be used in the lateral supporting of the excavation has following properties see Figure 4.2 :

FIGURE 3.5: Two Rows Of Hollow Core Struts



- Outer Diameter $D=1.32\text{ m}$
- Thickness $t=13\text{ mm}$
- Steel Grade S355
- Length $l=19.75\text{ m}$

The struts will be located at every 6.8 m in the horizontal direction. Thus, we can calculate the buckling force of the struts per meter of supported area. According to Eurocode 3 *clause 3.2.6(1)* the Young's Modulus for structural steel $E = 2.10 \times 10^8\text{ kN/m}^2$. By using the Euler buckling force relation and above mentioned properties, the input properties of struts are found.

Floors

Floors support the wall in lateral direction after construction stage 4. Increased lateral support prevents the structure from deflecting more and allows the constructor to empty the water in the construction pit without causing instability. During analysis there are multiple methods for simulation of floors. These methods can be explained as *Lateral Springs, Rotational Springs or Rigid Elements*. Rigid elements due to their big stiffness values are causing small deflections. This is not wanted.

Theoreticians suggest that the best modeling of floors can be expressed as either lateral or rotational spring elements. According to analysis to be performed how they are modeled will be explained in related chapters. the geometrical information on slabs can be described as:

TABLE 3.4: Floor Geometrical Properties

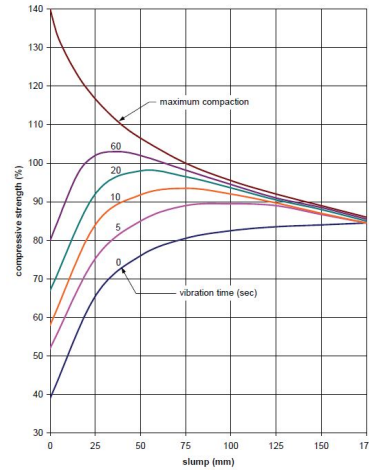
	<i>TopLevel</i>	<i>BottomLevel</i>	<i>Thickness</i>
<i>Name</i>	<i>NAPm</i>	<i>NAPm</i>	<i>m</i>
Floor 1	-4.35	-4.75	0.40
Floor 2	-7.20	-7.60	0.40
Floor 3	-10.05	-10.45	0.40
Floor 4	-12.90	-13.30	0.40
Floor 5	-15.90	-16.50	0.60
Deck	-0.80	-1.90	1.10

Under Water Concrete

Under water concreting is a method of pouring concrete underwater. Many aspects of the concrete becomes highly important while executing this experience requiring work. Yao, Berner, and Gerwick, 1999 lists the important aspects to be checked for a good underwater concrete mix design, these factors are: *Flowability, Self-Consolidation, Cohesion*. For instance in site conditions, it is impossible to compact the concrete under water. That is why the concrete should be able to flow by itself and fill the area without trapping water, later it should compact itself and reach characteristic strength due to its self-consolidation capacity and it should be cohesive during this

procedure and later. As can be seen for Figure 3.6 for the good realization of meeting the strength requirements of concrete, either it should be vibrated during placement, which is not a liable option, or concrete with slump value around 175 should be chosen in design.

FIGURE 3.6: Effect Of Vibration And Slump For Strength Of UWC

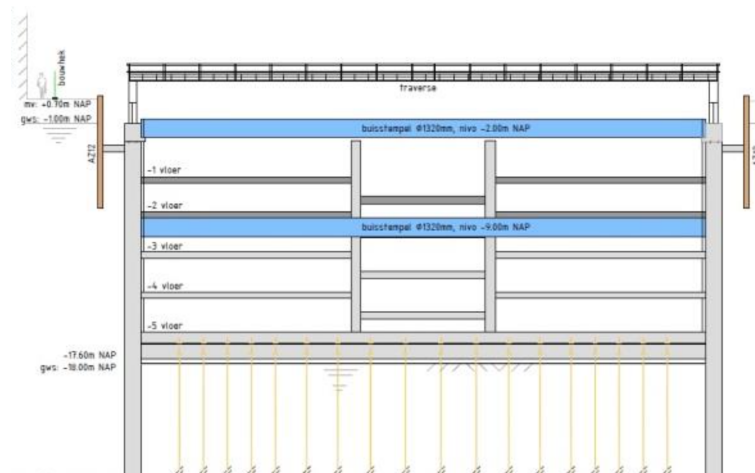


Underwater concrete placement is also highly crucial for a good quality construction. The concrete should be placed at a nearly constant rate, which requires a well detailed planning. This is highly important to prevent cold joints. For the placement sequence, there are two main methods. Doing tremie concreting with multiple tremie is not useful for big area of pourings. (The project that is under investigation of this thesis is a big area of cover). Thus, second method *Advancing Slope Method* is preferred in which multiple tremies are used but they do not execute pouring simultaneously. when the concrete poured by first tremie reaches to desired height and the concrete height in adjacent tremie rises above 0.3m first tremie stops pouring and the adjacent tremie starts the pouring. In this way the risks of entrapped water and forming of cold joint can be prevented for big areas. Under water concrete should also balance the basal heave and uplift pressures caused by the uneven earth and water. The pressure that is caused by the uneven water level can not only be balanced with the dead weight of concrete and gravel bed, as can be seen from figure 3.7 the pressure difference is also stabilized by the axial work of piles under the UWC. This effect is not in the scope of this thesis. the conclusions from this section shows that, the impermeability and cohesion of UWC are the most important aspects to understand the effect of UWC.

TABLE 3.5: Soil Properties

	<i>TopLevel</i>	<i>BottomLevel</i>	<i>Thickness</i>
	<i>NAPm</i>	<i>NAPm</i>	<i>m</i>
UWC*	-16.60	-17.60	1.0
Gravel	-17.60	-17.90	0.3

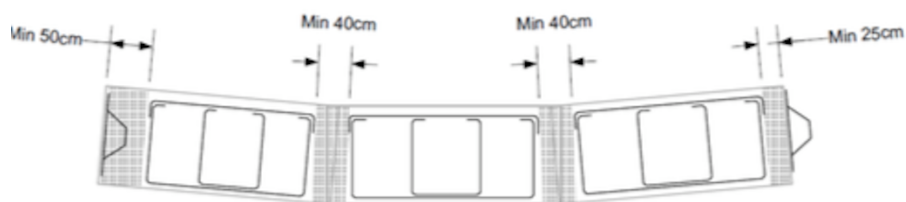
FIGURE 3.7: Basal Heave Balanced With UWC and Piles(Yellow)



Construction Joints

Due to the sequencing of panel constructions there will be vertical construction joints between panels. Requirements for construction joints mostly refer to the ease of installment factor. Complicated joints will increase the time of construction and quality control measures might be challenged. In addition, construction joints should withstand extreme pressures and stay water tight. In practice, construction joints with continuous horizontal reinforcement are very difficult to execute. Unarmed joints are highly easy to execute using end stops and trimming and pouring fresh concrete. But they are unarmed, so they have a limited shear and bending resistance. That is why a clear engineering model for the analysis of the construction joints will be shared in the last chapter of this dissertation.

FIGURE 3.8: Requirements For Spacing Between Joint Tape And Cage And Two Cages



As can be seen from Figure 3.8 Three different types of unarmed sections exist in the structure. Further illustration of construction joints can be seen from Figure 3.9 and Figure 3.10

FIGURE 3.9: Straight Panels [m]

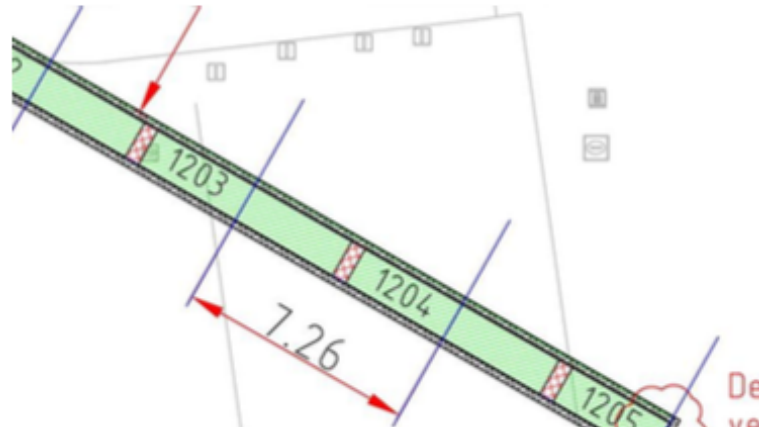
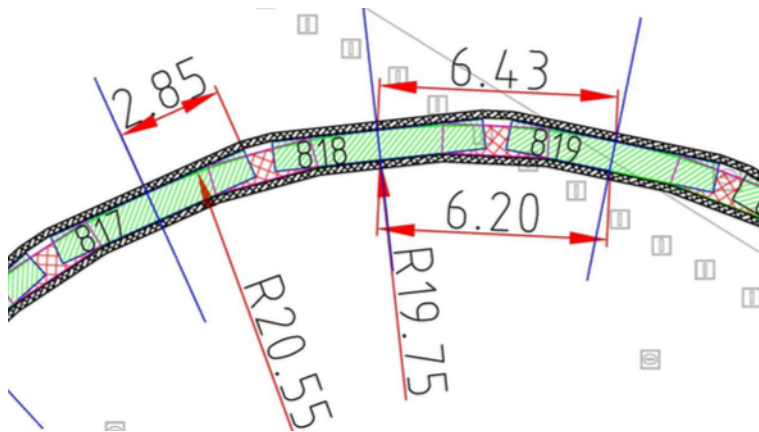


FIGURE 3.10: Curved Panels [m]



3.2 Decision For Soil Model

Referring to "EN1997-1" 2005 Clause 2.4.1.(3) the calculation model shall estimate the expected behavior of the ground for the limit state assumed. In case of inestimable deformations and behavior, alternate methods should be implemented. Any type of model should either be accurate or in the safe side.

In practice, three different types of calculation methods are widely used. These are:

- Analytical Models
- Semi-empirical Models
- Numerical Models

Analytic and semi-empirical simple models such as stress analysis or movement analyses are suggested for flexible systems such as steel sheet piles. On the other hand, the phased analysis would increase the complexity further.

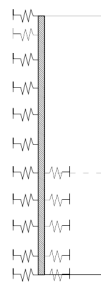
Since the construction is going to be realized in stages as described in section 1.4.4, *numerical analyses* would be the most beneficial to use. Pressures from soil particles and underground water would be the representative value and external loads should also be representative values of actual loads, not upper bound loads. These models can also model soil-structure interaction that has a changing effect according to the soil pressure at a given depth. Thomas D. Richards, 2006 enlists possible numerical analyses and focuses on the last two options:

- Equivalent Beam Model
- Beam On Elastic Foundation Method
- Finite Element Method

3.2.1 Beam On Elastic Foundation Method

In this 2-D method, soil is modeled according to Winkler soil model, and is applied at both sides of the wall as seen in Figure 3.11. At the start of the model spring are compressed to represent at rest earth pressures. With the each excavation steps external loads from soil, water and supports cause changes in the spring loads, thus displacements occur.

FIGURE 3.11: Wall Modeled With Soil as Winkler Springs

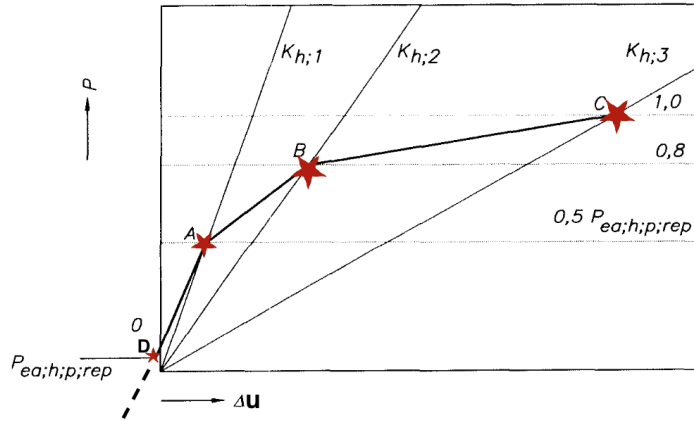


According to Jones, 1997, Winkler introduced the concept of modeling soil as elastic spring elements. Earth modeled with springs consist of different challenges. Because soil normally behaves as a spring with changing stiffness (subgrade reaction) during displacement. And this behavior is dependent on the site conditions of the soil at considered depth and water-table level. CUR166, 2012 Table 3.3 manual gives a method for choosing subgrade reaction according to the site conditions as seen in Table 3.6 and the force displacement curve can be seen from Figure 3.12.

This reference allows us to estimate subgrade reaction moduli according to site conditions and branch (a) values are representative values for lower bound and applicable to our analysis. Relative displacements at given stress levels will be decided according to 3.12 using the relations from 3.1 to 3.5.

TABLE 3.6: Moduli Of Subgrade Reaction k_h [kN/m^3]

	$p_0 \leq k_1(a)$	$\leq 0.5pp$ $k_1(b)$	$0.5pp \leq k_2(a)$	$\leq 0.8pp$ $k_2(b)$	$0.8pp \leq k_3(a)$	$\leq pp$ $k_3(b)$
<i>Sand(qc)(MPa)</i>						
<i>Loose5</i>	12000	27000	6000	13500	3000	6750
<i>Firm15</i>	20000	45000	10000	22500	5000	11250
<i>Compact25</i>	40000	90000	20000	45000	10000	22500
<i>Clay(Cu)(kPa)</i>						
<i>Loose5</i>	2000	4500	800	1800	500	1125
<i>Firm15</i>	4000	9000	2000	4500	800	1800
<i>Compact25</i>	6000	13500	4000	9000	2000	4500
<i>Peat(Cu)(kPa)</i>						
<i>Loose10</i>	1000	2250	500	1125	250	560
<i>Firm30</i>	2000	4500	800	1800	500	1125

FIGURE 3.12: p - Δu Curve of Soil: CUR166

$$u_A = \frac{0.5 * \sigma'_{hp}}{k_{h1}} \quad (3.1)$$

$$u_B = \frac{0.8 * \sigma'_{hp}}{k_{h2}} \quad (3.2)$$

$$u_C = \frac{\sigma'_{hp}}{k_{h3}} \quad (3.3)$$

$$k_{ha} = \frac{0.5\sigma'_{hp} - \sigma'_{h0}}{u_A} \quad (3.4)$$

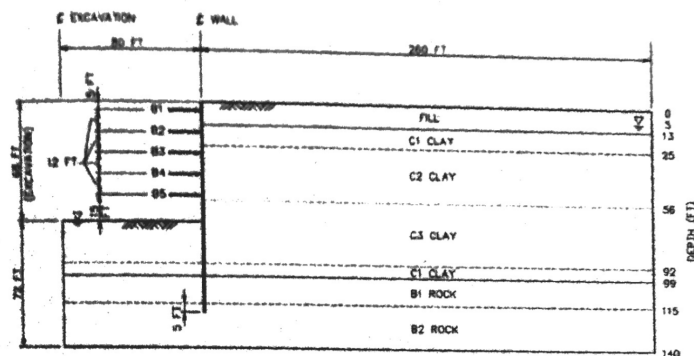
$$u_D = \frac{\sigma'_{h0} - \sigma'_{ha}}{k_{ha}} \quad (3.5)$$

The BEF (Beam On Elastic Foundation) model can provide useful insights into the behavior of the wall and the wall-soil boundary, and the automated computer programs make it easy to perform multiple analyses for optimizing the design and evaluating sensitivity to input parameters.

3.2.2 Finite Element Method

Continuous Finite Element Models are models that can include the soil mass surrounding the structure into the model. Strain response of the soil is modeled with constitutive equations. Constitutive equations are mathematical models that can vary according to the Finite Element computer programs capacity. The most used constitutive model in practice is Mohr-Coulomb model, which can model the failure and yield of the soil especially for materials like sand. But this model behaves as linear elastic upon where it becomes directly fully plastic. Diana 10.1 allows the user to use Modified Mohr-Coulomb model which has certain modification syntax to add additional parameters to model soils different than sand. But still this model needs the estimation of the mobilization of passive pressures. This information can be taken from previous D-Sheet analysis and be applied on the soil. But this method has certain disadvantages, it is difficult to run the model, it requires heavy computational space and also a big part of soil is needed to be modeled, SEI/ASCE, 2000, see Figure 3.13. This is not favorable and also as mentioned before, the analysis does not count for the non-linear elastic behavior of soil. Staged excavation will also cause additional complication.

FIGURE 3.13: Required Vastness Of Soil For A Reliable Continuum Model



3.2.3 Modeling Method Of This Thesis

According to SEI/ASCE, 2000, the comparison of soil-spring model and a regular finite element continuum soil method shows similar deflection patterns, on the other hand soil-spring analysis and the deflections it gives are highly dependent on subgrade reactions. That is why, a good methodology to determine good subgrade reactions that simulate the realistic behavior of soil, shall be chosen. The methodology of CUR166, 2012 subgrade reaction can be used in this analysis. By choosing this methodology, the nonlinear behavior of the soil can easily be included in the analysis without the implementation of a complex continuum soil model. In order to analyze the situation without building a 3-D pit model in Diana 10.1, the following methodology will be followed. The different wall sections is considered

separately as straight panels and cylindrical panels. In the conclusion a simplistic engineering model will be suggested for the combination of two different analyses.

- Run preliminary D-Sheet Analysis for the straight wall section for estimation of the wall displacements and caused section forces in the wall panel.
- Perform a simple cylinder under pressure (Ko) Analysis to estimate the wall deflections and the caused section stresses in the cylindrical wall panel.
- Run a 2D Plane Strain Diana 10.1 FE analysis for the straight wall panel and compare the results with the D-Sheet analysis results.
- Run an 2D Axi-Symmetric Diana 10.1 FE analysis for the cylindrical section of the wall and compare the results with previously performed Ko analysis.
- Find the most critical construction stage and apply the found section forces to the simplistic engineering model that estimates the connection of two different wall sections.

By this methodology time and computational complications that a full 3-D constitutive model might cause will be minimized, yet the 3-D effects of the construction pit can be investigated without building a 3D mesh. For the detailed explanation of mesh geometry, modeling of structure and properties that are assigned please see the related part. For D-Sheet analysis Chapter 4, for Diana Analysis Chapter 5 will be useful. In section 3.3, a detailed explanation for structural and soil assumptions will be explained before setting the analysis method in full depth.

3.2.4 Geotechnical Design Approaches

In order to perform a steady analysis, compatible geotechnical design approaches shall be used. For The Netherlands type of soil, CUR166 methodology is highly suggested. And the modeling of the soil according to CUR166 will also allow us to perform simplistic 2D models.

1. Eurocode 7 NL method can be explained as follows: Design of geotechnical structures will be done according to EN7 in European Union countries, that is why verification of EN7 method is highly important. Explanation of different methods for EN7 including design approaches can be revised from section 1.4.1. Yet *Dutch National Annex* describes the methodology that is suggested by CUR166, 2012 with different partial factors. That is why in this chapter first the partial factors required for EN7 verification analysis will be shared. Later the methodology of CUR166, 2012 and the partial factors suggested will be shared so a detailed comparison can be illustrated.
2. CUR 166 methodology can be described in two different ways. Method Class III analysis method A has been realized. Class III type of design is required for the design of underground structures of which failure

will cause excessive economical and/or social damage. Method A takes the principle of confirming the stability of the pit at every stage of construction by using material and load factors. this method is exactly same method suggested by “EN1997-1” 2005. Since we can not be sure at this time which stage might have excessive risk, confirming all the stages will be appropriate.

The material and load factors suggested by EN7-NB can be seen in table 3.7. The material and load factors used suggested by CUR166 can be seen in table 3.8. Different factor values deviating from EN7 will be shown with red::

TABLE 3.7: Partial Factors And Geometrical Deviations For EN7 RC3

<i>LoadFactor</i>	<i>Value</i>	<i>MaterialFactor</i>	<i>Value</i>	<i>Geom.Modif</i>	<i>Value[m]</i>
$\gamma_{perm,un}$	1.00	$\gamma_{cohesion}$	1.40	ΔGL_{pas}	-0.50
$\gamma_{perm,fav}$	1.00	$\gamma_{tan\phi}$	1.20	ΔWL_{pas}	-0.25
$\gamma_{var,un}$	1.25	$\gamma_{subgrade}$	1.30	ΔWL_{act}	+0.05
<i>OverallStability</i>	<i>Value</i>	<i>VerticalBalance</i>	<i>Value</i>	—	—
$\gamma_{drivingMom}$	1.10	$\gamma_{m;b4}$	1.00	—	—
$\gamma_{cohesion}$	1.60	—	—	—	—
$\gamma_{tan\phi}$	1.30	—	—	—	—

TABLE 3.8: Partial Factors And Geometrical Deviations For CUR166 Method:III-A

<i>LoadFactor</i>	<i>Value</i>	<i>MaterialFactor</i>	<i>Value</i>	<i>Geom.Modif</i>	<i>Value[m]</i>
$\gamma_{perm,un}$	1.00	$\gamma_{cohesion}$	1.10	ΔGL_{pas}	-0.35
$\gamma_{perm,fav}$	1.00	$\gamma_{tan\phi}$	1.20	ΔWL_{pas}	-0.25
$\gamma_{var,un}$	1.25	$\gamma_{subgrade}$	1.30	ΔWL_{act}	+0.05
<i>OverallStability</i>	<i>Value</i>	<i>VerticalBalance</i>	<i>Value</i>	—	—
$\gamma_{drivingMom}$	1.10	$\gamma_{m;b4}$	1.20	—	—
$\gamma_{cohesion}$	1.50	—	—	—	—
$\gamma_{tan\phi}$	1.20	—	—	—	—

The staged excavation analysis is realized by steps as defined in CUR166, 2012 with 11 steps. Step 6 is for checking the structural deformations for required ULS and SLS checks. An overall description of the steps can be seen in following from Figure 3.14 to Figure 3.18. Additionally in Table 3.9 different aspects of these steps are shared.

And the application of geometrical and material factors based on the different steps can be followed from Table 3.9.

FIGURE 3.14: CUR Step 6.1

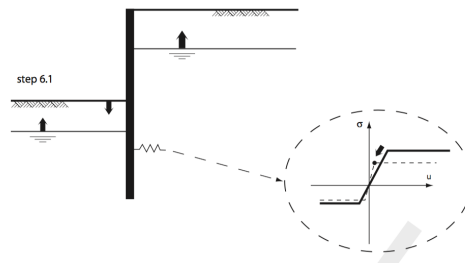


FIGURE 3.15: CUR Step 6.2

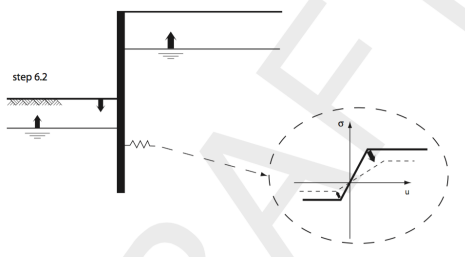


FIGURE 3.16: CUR Step 6.3

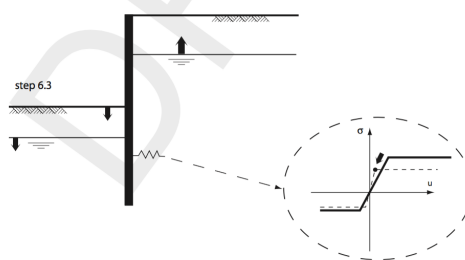
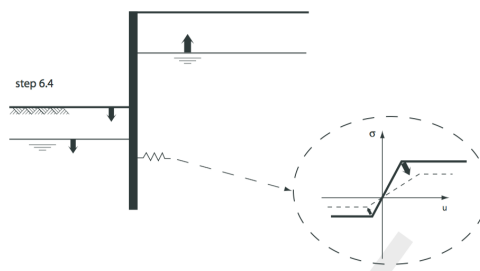


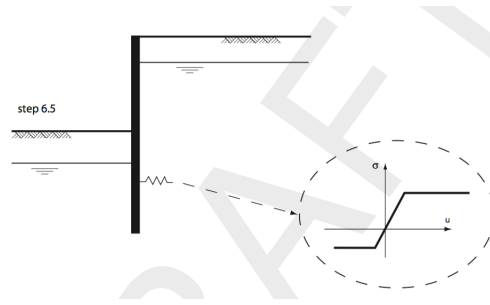
FIGURE 3.17: CUR Step 6.4



Decision

Since there are compatibility of two standards, yet incompatibility of partial factors, the most appropriate choice is to run Diana FEM analyses according to SLS with unfactored loads and soil properties (step 6.5 for CUR166). The soil spring properties should be derived from this step. Otherwise, spring behavior as in Figure 3.12, would be the outcome of factored soil parameters, yet any type of load factoring according to EN7 would be obsolete for the check of any ultimate states because material partial factors for soil in

FIGURE 3.18: CUR Step 6.5

TABLE 3.9: Design Values For Soil And Geometry Properties In CUR Steps ($k_{high,rep} = 2.25 * k_{low,rep}$)

Step	Limit	k_d	c_d	$\tan\phi_d$	$\tan\delta_d$
6.1	ULS	$\frac{k_{low,rep}}{\gamma_k}$	$\frac{c_{low,rep}}{\gamma_c}$	$\frac{\tan\phi_{low,rep}}{\gamma_{\tan\phi}}$	$\frac{\tan\delta_{low,rep}}{\gamma_{\tan\phi}}$
6.2	ULS	$\frac{k_{high,rep}}{1}$	$\frac{c_{low,rep}}{\gamma_c}$	$\frac{\tan\phi_{low,rep}}{\gamma_{\tan\phi}}$	$\frac{\tan\delta_{low,rep}}{\gamma_{\tan\phi}}$
6.3	ULS	$\frac{k_{low,rep}}{\gamma_k}$	$\frac{c_{low,rep}}{\gamma_c}$	$\frac{\tan\phi_{low,rep}}{\gamma_{\tan\phi}}$	$\frac{\tan\delta_{low,rep}}{\gamma_{\tan\phi}}$
6.4	ULS	$\frac{k_{high,rep}}{1}$	$\frac{c_{low,rep}}{\gamma_c}$	$\frac{\tan\phi_{low,rep}}{\gamma_{\tan\phi}}$	$\frac{\tan\delta_{low,rep}}{\gamma_{\tan\phi}}$
6.5	SLS	$k_{low,rep}$	$c_{low,rep}$	$\tan\phi_{low,rep}$	$\tan\delta_{low,rep}$
		<i>PassiveSide</i>	<i>PassiveSide</i>	<i>Activeside</i>	
6.1	ULS	$GL_{rep} - \Delta GL_{pas}$	$WL_{rep} + \Delta WL_{pas}$	$WL_{rep} + \Delta WL_{act}$	
6.2	ULS	$GL_{rep} - \Delta GL_{pas}$	$WL_{rep} + \Delta WL_{pas}$	$WL_{rep} + \Delta WL_{act}$	
6.3	ULS	$GL_{rep} - \Delta GL_{pas}$	$WL_{rep} - \Delta WL_{pas}$	$WL_{rep} + \Delta WL_{act}$	
6.4	ULS	$GL_{rep} - \Delta GL_{pas}$	$WL_{rep} - \Delta WL_{pas}$	$WL_{rep} + \Delta WL_{act}$	
6.5	SLS	GL_{rep}	WL_{rep}	WL_{rep}	

EN7 is different than CUR. In addition, SLS check allows engineer to investigate aspects such as deflections and cracking, which is highly compatible with the scope of this thesis. Namely, the performance of joint. From practical point of view, underground load bearing structures in The Netherlands is designed following CUR methodology.

3.3 Assumptions on the Soil and Structure Behavior

In this section assumptions that are taken into account will be elaborated in detail respectively for soil modeling and structural assumptions. If there were points that were taken into account in previous sections, they again will be shared here to remind reader and clear the overall outline of the analysis.

3.3.1 Executional Assumptions

- Uplift pressure due to uneven water levels on both side of the wall will be stabilized by the combined action of piled under water concrete. Concreting will be done by the tremie method of *Advancing Slope*. Figure 3.7

- Panel construction will be sequenced differently for circular part with primary-secondary panel method Figure 2.13, straight part will be performed with successive method Figure 2.12
- Slurry will be accepted as properly applied according to warnings requested in section 2.3.2. And the effects of excessive filter cake or instabilities or execution mistakes will be neglected in the main analysis.
- 3 types of construction joints will be accepted. First group of joints which are predominantly working in compression between circular panels that can easily be executed by steel end pipes. Second type of joints that might work in compression in combination of shear and bending, which can most preferably be executed by joint tape ends. Figure 2.15.

3.3.2 Assumptions On Behavior Of Soil

- The soil will be modeled as smeared spring elements rather than continuum elements for FEM analysis. This choice has been done to limit the computational load of the model, in addition increase the ease of steering the model.
- No factoring on soil and loads will be used, the structure first will be checked according to SLS conditions.
- Lateral earth pressure coefficient for neutral state will be followed from Jaky, 1948 and can be followed for coarse and fine grains respectively from Equations 3.6 and 3.7.

$$K_0 = \sqrt{OCR} * (1 - \sin\phi) \quad (3.6)$$

$$K_0 = OCR^{(1-\sin\phi)} * (1 - \sin\phi) \quad (3.7)$$

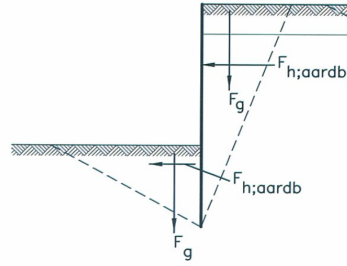
- Lateral earth pressure coefficients for active and passive state will be followed from Müller-Breslau, 1906 and can be followed from Equations 3.8 and 3.9. δ is the angle of wall friction and ϕ is the soil friction angle.

$$K_a = \frac{\cos^2\phi}{(1 + \sqrt{\frac{\sin\phi * \sin(\phi+\delta)}{\cos\delta}})^2} \quad (3.8)$$

$$K_p = \frac{\cos^2\phi}{(1 - \sqrt{\frac{\sin\phi * \sin(\phi+\delta)}{\cos\delta}})^2} \quad (3.9)$$

- Slip surfaces of the soil is thus considered according to straight slip surface theory suggested by Müller-Breslau, 1906. this assumption can be seen from Figure 3.19.

FIGURE 3.19: Straight Slip Surface Assumption



- Limiting earth pressures will be calculated according to D-Sheet, 2014 Manual as seen in Equations 3.10 and 3.11. Equation 3.12 is taken from CUR166, 2012.

$$\sigma'_a = K_a * \sigma'_v - 2c * \sqrt{K_a} \quad (3.10)$$

$$\sigma'_p = K_p * \sigma'_v + 2c * \sqrt{K_p} \quad (3.11)$$

$$\sigma'_v = \gamma_{d;z} * z - u_{d;z} \quad (3.12)$$

- Dilatancy angle δ will be accepted as 0.67ϕ . This also implies that wall has either very rough or rough surface as it will be the case for a concrete wall panel. This is a good estimation of reality where the soil is mostly made of sand layers.
- Lateral Pressure $\sigma_{h,sur}$ due to *Surcharge load* Q on the required side of the wall will be calculated according to $\sigma_{h,sur} = K_i * Q$ where K_i is the lateral earth pressure coefficient at given depth and given deflection situation chosen from Equations 3.6, 3.7, 3.8, 3.9.
- The underwater concrete and the gravel bedding under it will be modeled as soil layers with appropriate stiffness parameters, the chosen values will be represented in Chapter 4.

3.3.3 Assumptions On Wall Structure

- With correct planing and steady concrete placement, forming of cold joints within the panels will be controlled and prevented. Thus, for modeling of the walls will not take into account the effects of possible cold joints to structural behavior.
- While modeling the structure a simple modeling first have to be accepted to check the reliability of the soil model prepared by interface elements.
- Normally, diaphragm walls show increasing stiffness property along the depth according to Xanthakos, 1994. This effect will not be taken into account, because increasing stiffness will limit deflections, by not taking into account this realistic behavior, the deflections that will be

found by analysis will already be bigger than structures deflections in service conditions.

- The wall panels will be modeled by 2D configuration. The effect on the critical joint will be performed by a simplistic hand calculation with the results derived from Diana 10.1 analyses.
- Main model of the construction pit will not take into account execution faults and wont consider the additional effects of deviations and unsymmetrical conditions.
- Properties of the concrete and required parameters will be taken from EN1992, 2005. Since the finite element modeling will be of complex nature, firstly linear elastic isotropic concrete properties will be used. For future researches, more complex wall behavior can be modeled. But the scope of this thesis is mostly concerned on how to model a complex underground structure without modeling the full 3D continuum model.

Chapter 4

Preliminary D-Sheet and K0 Analyses

4.1 D-Sheet Analysis

For the straight wall panels a theoretical method is needed for being able to compare with the Diana model to be built. As a commercial software package D-Sheet Piling allows the user to apply CUR166 methodology in a layered soil during staged construction. This is a perfect fit for the preliminary analysis of the straight wall panels. On the other hand, D-Sheet is unable to calculate the deformations of an axi-symmetric wall. For the given reason, the cylindrical part of the wall will be checked by a simplistic K0 analysis.

4.1.1 Applied Soil Properties

According to the methodology of CUR represented in previous chapter different k_1 , k_2 , k_3 parameters are chosen following the Table 3.6, these values can be seen in 4.2:

TABLE 4.1: Soil properties CPT15

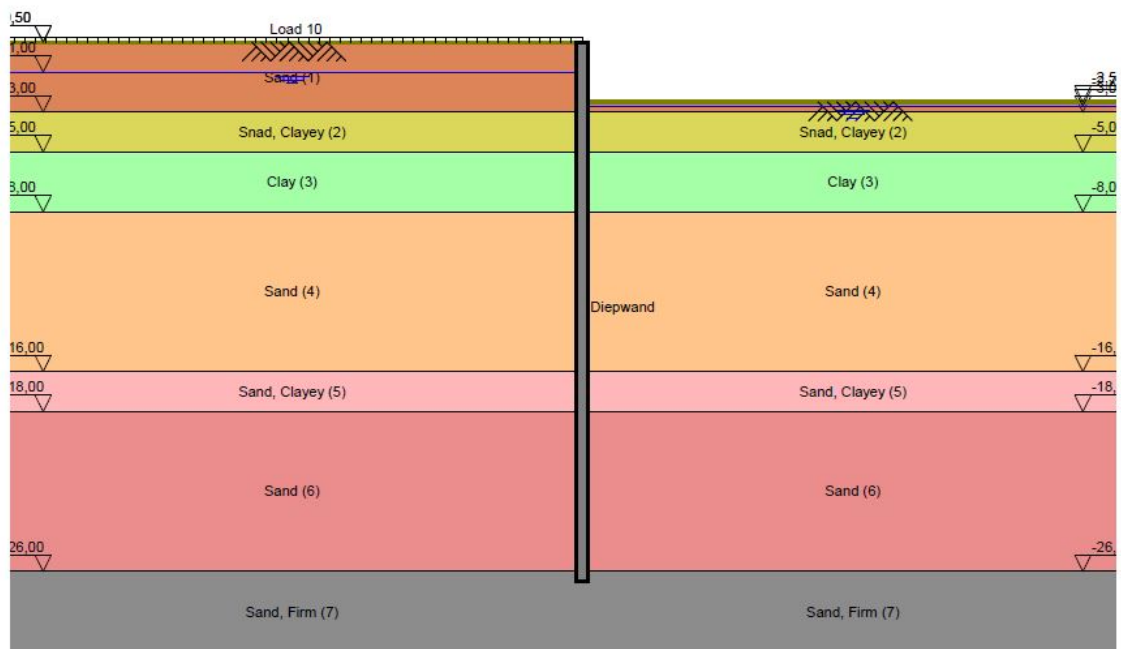
<i>SoilType</i>	<i>TopLevel</i>	$q_{c,av}$	γ	c_u	ϕ	δ
	[mNAP]	[kN/m ²]	[kN/m ³]	[kN/m ²]	degree	degree
Sand (Top Layer)	+ 0.5	4.0	17/19	0	32.5	20.0
Clayey Sand	-3.0	3.5	18/18	0	25.0	16.7
Clay	-5.0	1.0	17/17	5	17.5	11.7
Sand	-8.0	8.0	18/20	0	32.5	20.0
Clayey Sand	-16.0	4.0	18/18	0	25.0	16.7
Sand	-18.0	15.0	18/20	0	32.5	20.0
Firm Sand	-26.0	23.0	19/21	0	35.0	20.0
Gravel	-17.75		20/22	0	37.5	20
UWC*	-16.75		0.01/0.1	15000		

The gravel layer that is mentioned in the tables 4.1 and 4.2 is the layer of gravel that is going to be placed as a leveling below the underwater concrete. The underwater concrete properties can be seen from UWC (underwater concrete) in Tables 4.1 and 4.2. With the chosen soil properties, a soil stratification similar to the site conditions has been modeled in D-Sheet. The model can be seen in Figure 4.1:

TABLE 4.2: Lateral Displacement Stiffness Parameters

<i>SoilType</i>	k_{h1}	k_{h2}	k_{h3}
	[kN/m^3]	[kN/m^3]	[kN/m^3]
Sand (Top Layer)	1.2×10^4	6×10^3	3×10^3
Clayey Sand	1.2×10^4	6×10^3	3×10^3
Clay	4×10^3	2×10^3	8×10^2
Sand	1.6×10^4	8×10^3	4×10^3
Clayey Sand	1.2×10^4	6×10^3	3×10^3
Sand	1.6×10^4	8×10^3	4×10^3
Firm Sand	2×10^4	1×10^4	5×10^3
Gravel	4×10^4	2×10^4	1×10^4
UWC	1×10^6	1×10^6	1×10^6

FIGURE 4.1: Soil Stratification Representation



The soil stratification is represented in four different soil profiles prepared in the D-Sheet. The reason to use four different soil profiles can be explained due to the differences in the pore water pressure in soil layers for different construction stages. For instance, at the first construction stage, the pore water pressure under clay(3) layer will be 14.71 kN/m^2 but when at the second construction stage the water level in the pit is raised back to its natural(field) value, the pore pressure under the clay layer will be 0 kN/m^2 . After the placement of the UWC and the removal of the water in the construction pit, the pore water pressure under the under water concrete will rise to 164.32 kN/m^2 due to the imbalance of the water levels on both sides of the wall.

4.1.2 Applied Structural Properties

Lateral supports can be modeled by four different options in D-Sheet, these four different methods are:

- Anchors
- Struts
- Spring supports
- Rigid supports

The struts that are located at -1.5 mNAP and -9 mNAP will be modeled as struts. The required properties to define a strut are listed as:

- Level of support [mNAP]
- E modulus (Young's modulus) [kN/m^2]
- Cross section [m^2/m']
- Length [m]
- Design buckling force [$\text{kN/m}'$]

The slabs that are laterally supporting the wall can not be modeled as rigid supports because they will flex and rotate with the lateral load pressing the diaphragm wall inside, and these support points will deflect through the inside of the excavation pit. Assuming the slabs as rigid supports will decrease the lateral deflection results and will give unreliable results.

Thus, modeling the slabs as spring supports is the most applicable option and through the literature review it is a highly accepted method. Required spring support parameters are listed as:

- Level of support [m]
- Translation spring constant [$\text{kN/m/m}'$]
- Rotation spring constant [$\text{kNm/rad/m}'$]

Decision of above mentioned parameters will be explained in the following subsections:

Strut Properties

The struts will be located at every 6.8 m in the horizontal direction. Thus, we can calculate the buckling force of the struts per meter of supported area as requested in D-Sheet input file. According to Eurocode 3 *clause*3.2.6(1) the Young's Modulus for structural steel $E = 2.10 \times 10^8 \text{ kN/m}^2$. By using the Euler buckling force relation 4.1 and above mentioned properties, the input properties of struts are found as in table 4.3.

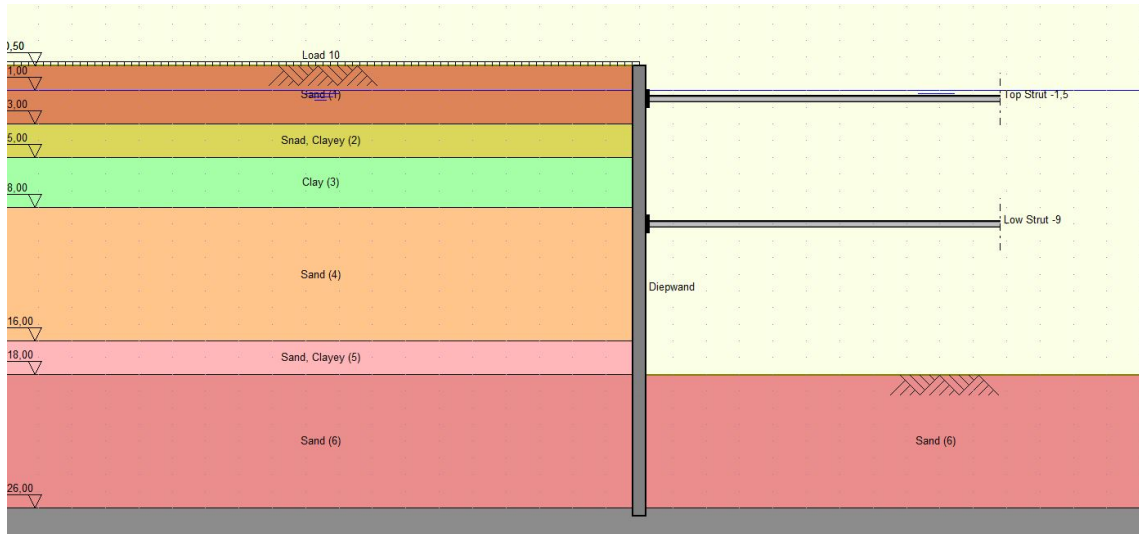
$$F_{buc} = \frac{EI\pi^2}{L_{eff}^2} \quad (4.1)$$

TABLE 4.3: Struts Structural Properties

Name	Level mNAP	E kN/m ²	CrossSection m ²	Length m	Angle °	DesignBuck.Force kN
Strut 1	-1.50	2.1×10^8	4×10^{-3}	19.75	0.00	1120.00
Strut 2	-9.00	2.1×10^8	4×10^{-3}	19.75	0.00	1120.00

Placed struts can be seen in the Figure 4.2.

FIGURE 4.2: Position of Struts in Excavation



Floors and Under Water Concrete Properties

The floors in this analysis are modeled as translation springs.

The relation when used with the data given in Table 4.4 gives the results in table 4.5

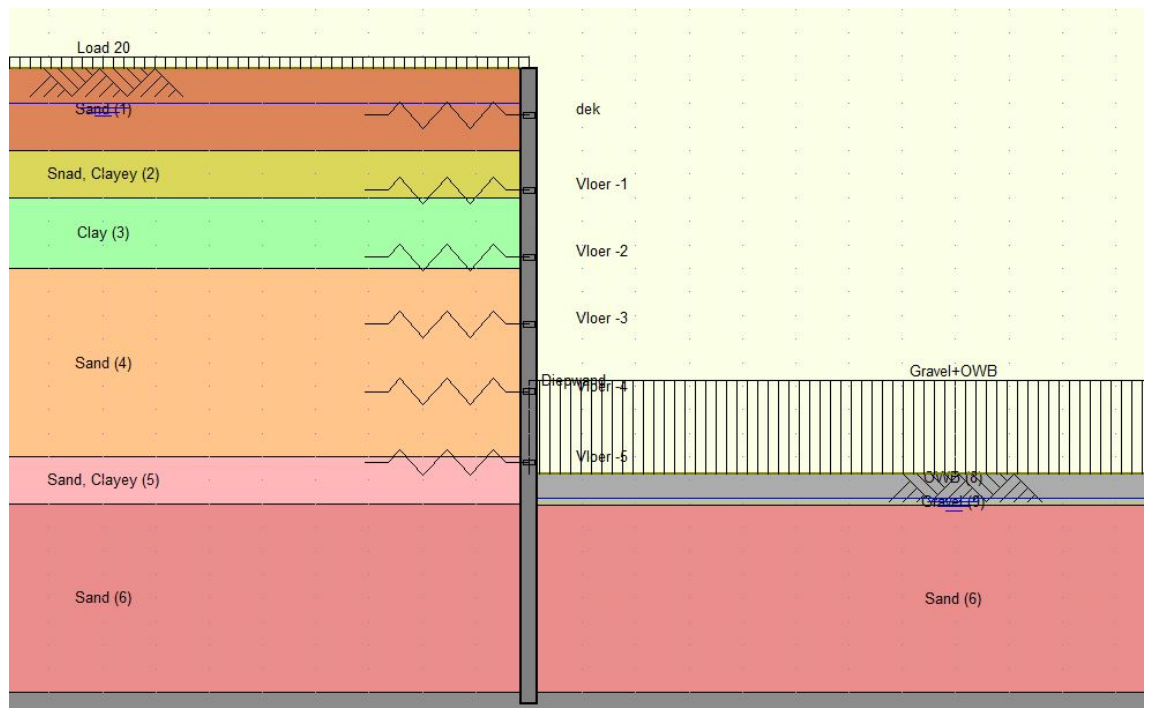
TABLE 4.4: Properties of Floors

<i>Name</i>	<i>Level</i> <i>mNAP</i>	<i>E</i> <i>kN/m²</i>	<i>Thickness</i> <i>m</i>	<i>Length</i> <i>m</i>
Deck	-1.50	3×10^6	1.10	19.75
Floor 1	-4.68	3×10^6	0.40	19.75
Floor 2	-7.53	3×10^6	0.40	19.75
Floor 3	-10.38	3×10^6	0.40	19.75
Floor 4	-13.23	3×10^6	0.40	19.75
Floor 5	-16.25	3×10^6	0.60	19.75

TABLE 4.5: Spring Constants of Floors

<i>Name</i>	<i>Level</i> <i>mNAP</i>	<i>k</i> <i>kN/m</i>
Deck	-1.50	1.7×10^7
Floor 1	-4.68	6.1×10^6
Floor 2	-7.53	6.1×10^6
Floor 3	-10.38	6.1×10^6
Floor 4	-13.23	6.1×10^6
Floor 5	-16.25	9.1×10^6

FIGURE 4.3: Floors Modeled as Springs



Diaphragm Wall Properties

The diaphragm walls will be two different types. First group is the circular walls with 0.8 m thickness, second group will be the straight walls with 1.2 m thickness. Calculating the 0.8 m thick walls assuming that their thickness is relatively lower compared to straight walls thus would be more critical,

is not correct. The axial forces exerted from the circular cross-section actually increases the strength of the wall, reducing the deflections. That is why, only the straight walls will be analyzed in this part of the thesis. The properties of the diaphragm wall(Wall Type 1) used in D-Sheet can be seen in table 4.6

TABLE 4.6: Diaphragm Wall Properties

<i>WallType</i>	<i>TopLevel</i> [<i>mNAP</i>]	<i>E</i> [<i>kN/m²</i>]	<i>I</i> [<i>m⁴</i>]	<i>E_{corr}</i> [<i>kN/m²</i>]	<i>Thickness</i> [<i>m</i>]
Wall Type 1	0.50	32,80.10 ⁶	0.144	4,7230.10 ⁶	1.2
Wall Type 2	0.50	32,80.10 ⁶	0.0427	1,399.10 ⁶	0.8

Staged Construction Geometrical Properties

Staged construction in this analysis will define the loading conditions that are applied to the wall along the execution of the project. During the problem description in section 3.1.3, the geometry of staged excavation was explained in detail. For the ease of understanding same geometrical variations are represented in Figure 4.4. In the figure WL stands for Water Level, SL stands for Soil Level and finally STL stands for Strut Level. The water level difference on both sides of the wall at the first and fourth stages will cause additional water pressure distribution under the clay layer positioned between -5 mNAP and -8 mNAP , see Figure 4.1.

FIGURE 4.4: Stage 1 Verification Step 6.5: Unit [*mNAP*]

Staged Construction	Stage No	Left Side m NAP		Right Side m NAP	
	1	WL	-1	WL	-2,7
		SL	0,5	SL	-2,5
				STL	-
	2	WL	-1	WL	-1
		SL	0,5	SL	-10
				STL	(-)1,5
	3	WL	-1	WL	-1
		SL	0,5	SL	-18,05
				STL	(-)1,5/-9
	4	WL	-1	WL	-17,75
		SL	0,5	SL	-16,75
				STL	(-)1,5/-9
				<i>OWB</i>	(-16,75to-17,75
				<i>Gravel</i>	(-17,75to-18,05

4.1.3 Analysis Results

Bending Moment, Shear And Displacement Charts

From the staged analysis following displacement and section forces results are calculated. These results will be the basis for checking the reliability of the Diana Analysis that is performed in the following chapter.

FIGURE 4.5: Stage 1 Verification Step 6.5

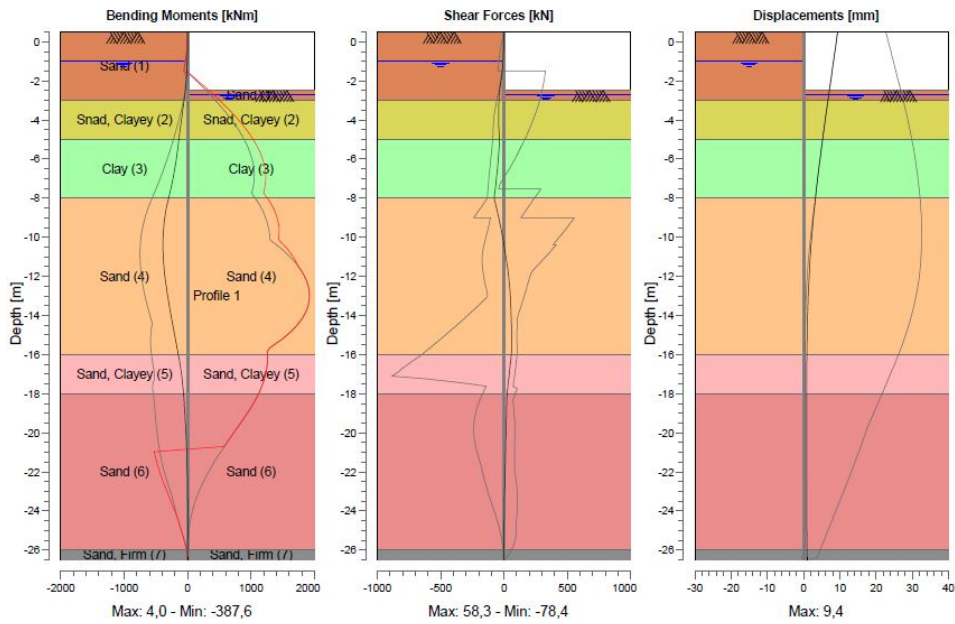


FIGURE 4.6: Stage 2 Verification Step 6.5

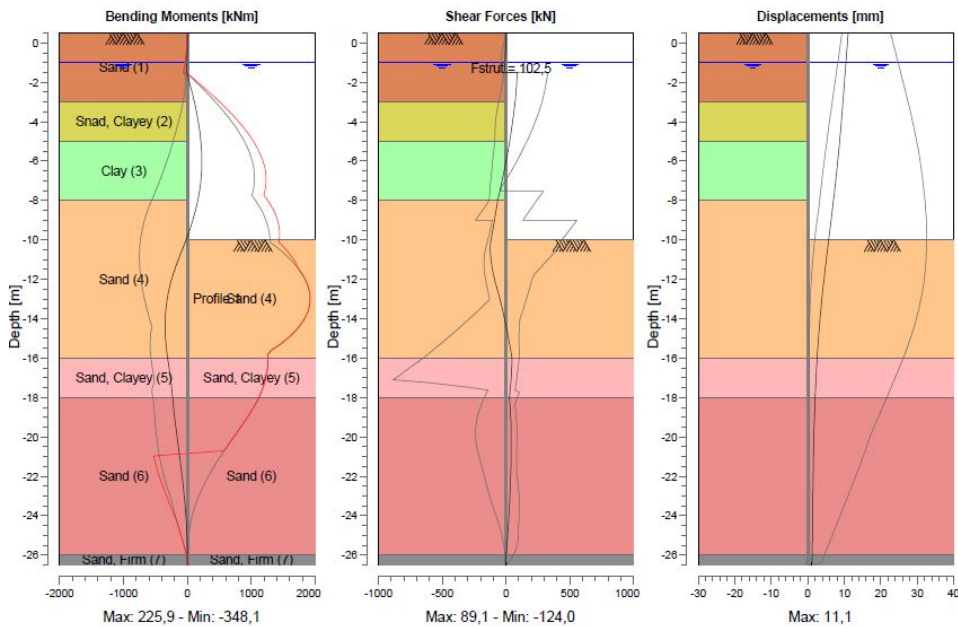


FIGURE 4.7: Stage 3 Verification Step 6.5

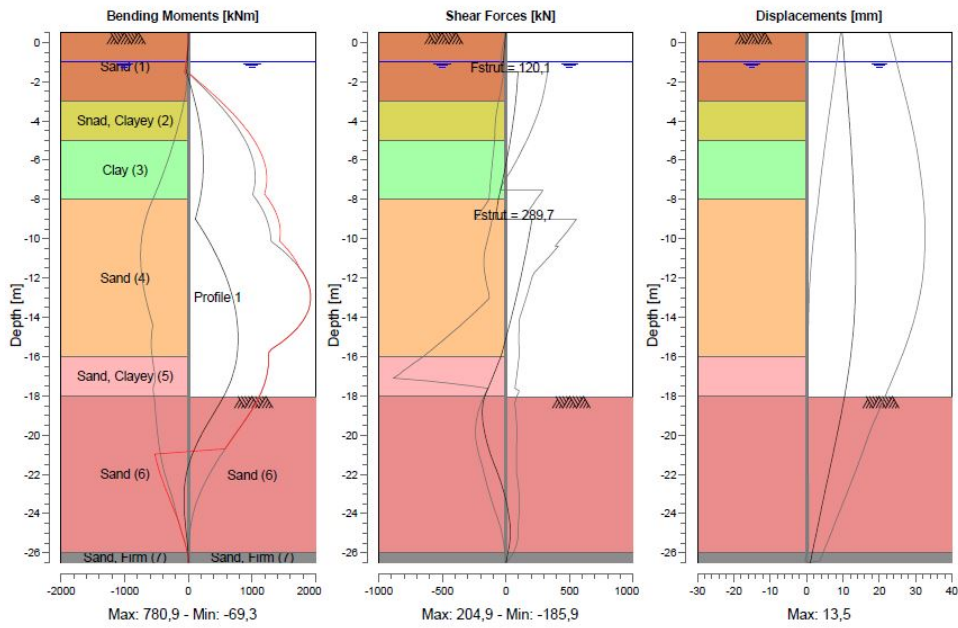


FIGURE 4.8: Stage 4 Verification Step 6.5

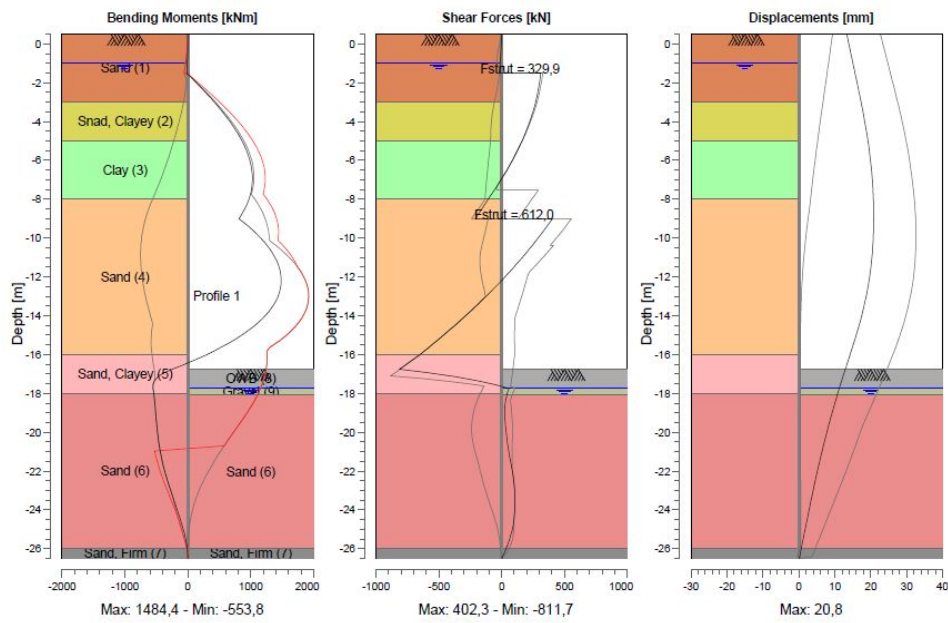


FIGURE 4.9: Stage 5 Verification Step 6.5

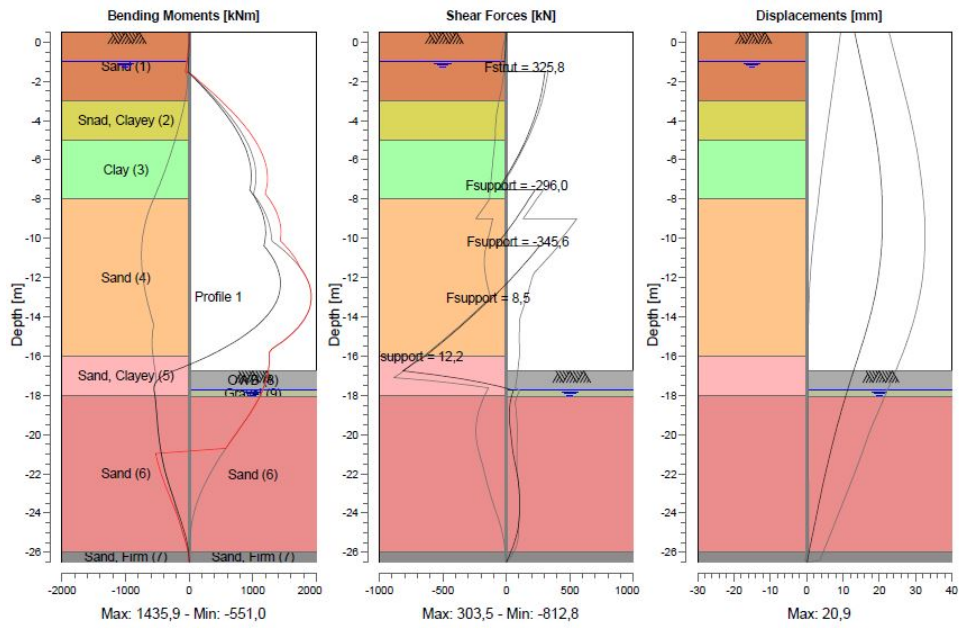
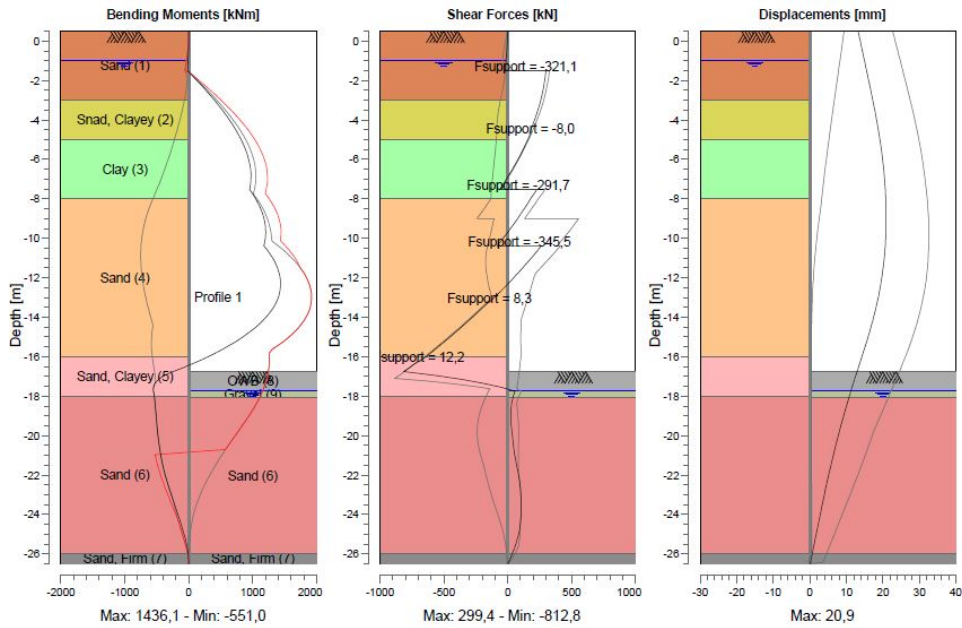


FIGURE 4.10: Stage 6 Verification Step 6.5



Conclusions

The D-Sheet analysis results will be shared in order of the construction stages realized. For all the stages CUR verification step 6.5 is shared.

As can be seen from the results of analysis from Figure 4.5 to Figure 4.10 the last stages are the most critical stages concerning the lateral deflections of the wall. And clearly, it can be seen from Figure 4.11 that the deflections and section forces are more or less stabilized after placement of Under Water Concrete and emptying of the water in pit.

FIGURE 4.11: Comparison Of Deflections For Different Stages

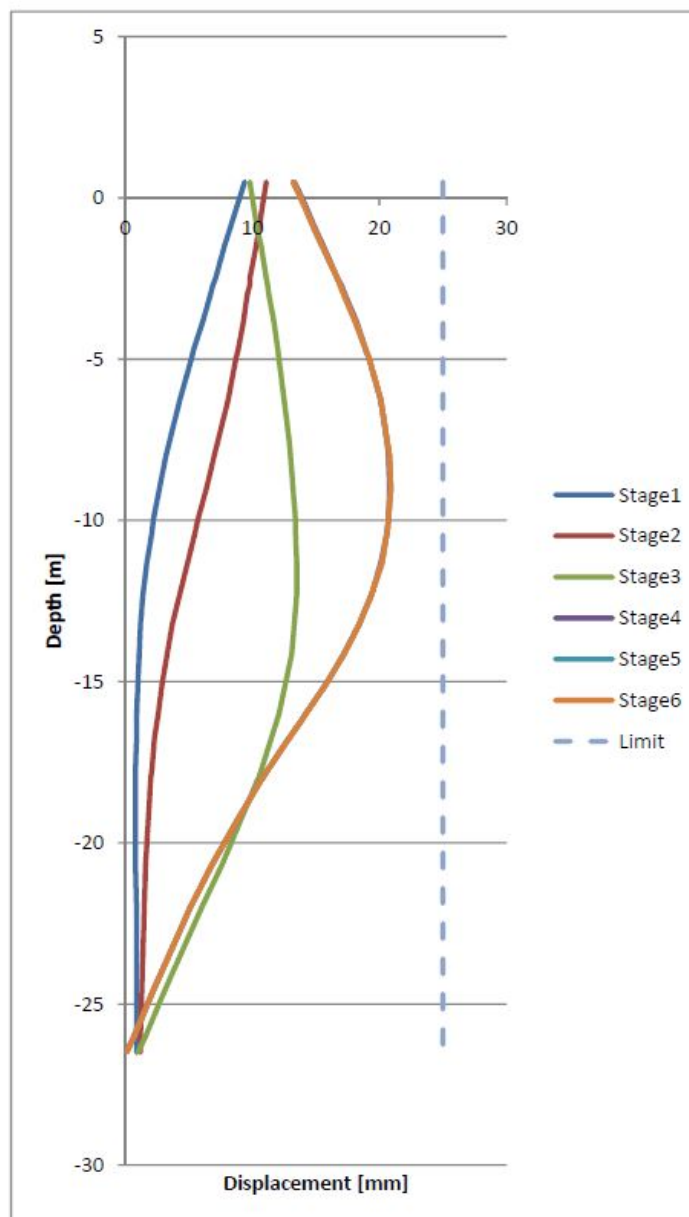
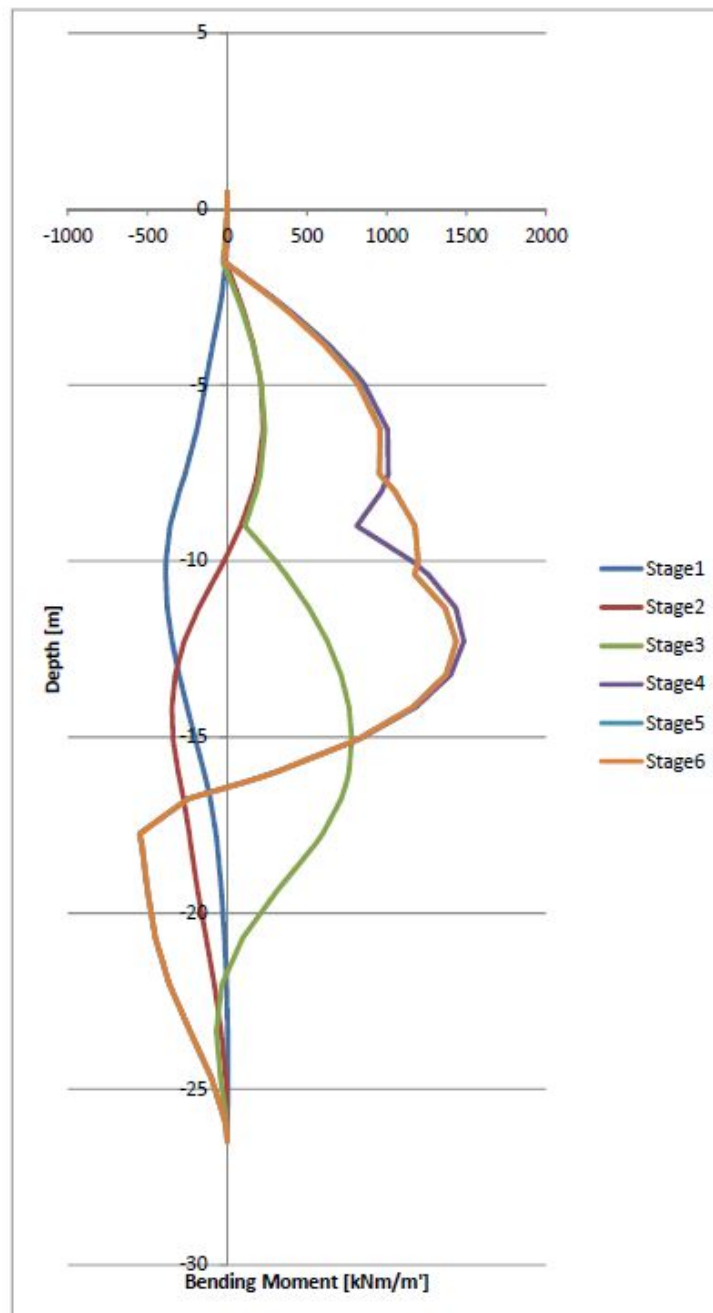


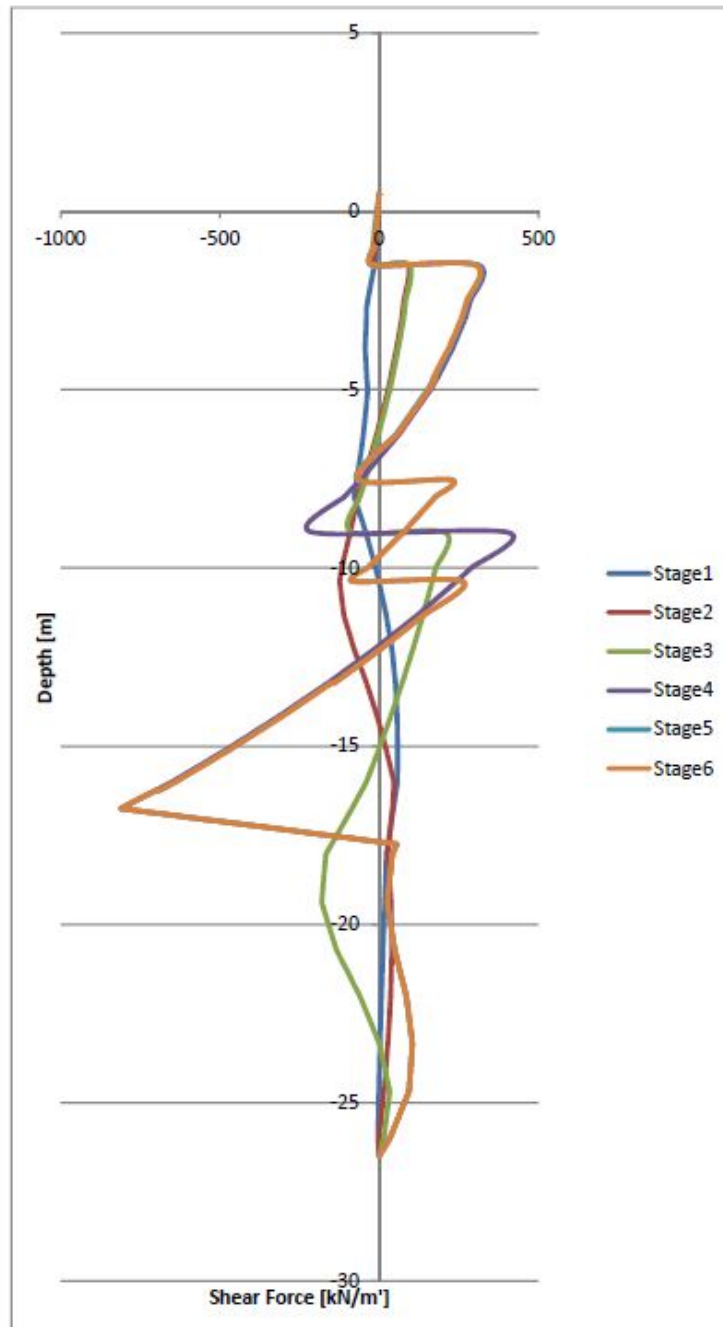
FIGURE 4.12: Comparison Of Bending Moments For Different Stages



In addition the bending moments and lateral strut forces are also seem to be stabilizing after the placement of the Under Water Concrete and the emptying of water in pit (See Figures 4.12 and 4.13). Additional floors and removal of temporary struts do not effect the construction pit heavily, thus the diaphragm wall. From these observations, it can be pointed out that the properties (*assumptions*) of Under Water Concrete during analysis are very important and can cause serious changes in the results.

- **Lateral Strut Forces at Stage 4** When the Figure 4.8 is examined it is

FIGURE 4.13: Comparison Of Shear Forces For Different Stages



seen that the top strut is exerted to -329.9 kN , the bottom strut is exerted to -612.0 kN , which in total makes a lateral force of -941.9 kN at total.

- **Lateral Support Forces on Slabs at Stage 6** When the Figure 4.10 is examined it is seen that the floors from 5 to deck are respectively exerted to $+12.2 \text{ kN}$, $+8.3 \text{ kN}$, -345.5 kN , -291.7 kN , -8.0 kN , -321.1 kN , which in total makes a total lateral force of -945.8 kN .

When the two lateral forces for both stages are compared the difference

in the total support load is 0.414%, a very acceptable error. For the detailed explanation of transforming D-Sheet results to a Diana model will be explained in detail in Chapter 5.

4.1.4 Analysis Results: Points To Take For Diana Analysis

- Stress conditions of adjacent soil to circular part and straight part will be considered similar even though the behavior of soil will be different. This is out of the scope of this thesis.
- Expected displacements at levels of strut will be taken from this analysis and be used during the modeling of Diana.
- Only first four stages will be examined. This is a valid assumption and is explained before.
- This analysis has been realized to get easy interpretation of soil without going in depth of soil mechanics and miss the structural point of the thesis scope.
- The loads caused by soil and under water pressure will be taken from D-Sheet analysis because other methods like Mohr-Coulomb requires the estimation of developed passive stresses.

4.2 K_o Analysis: Cylinder Under Pressure

K_o analysis is a simplistic theoretical method to estimate the radial displacements of a cylindrical section subjected to inner and outer pressures. A simple free body diagram of such perfectly symmetrical cylinder can be seen in Figures 4.14 and 4.15.

FIGURE 4.14: Top View Cylindrical Wall

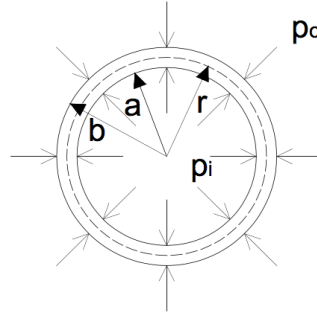
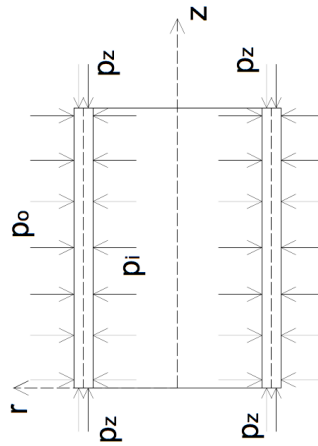


FIGURE 4.15: Side View Cylindrical Wall



The formulations that relate the inner and outer pressuring to the radial wall displacement can be seen from Equations 4.2 to 4.5. The outer and inner pressures will be decided from the natural pressures at the given excavated pit. In other words, the effect of the excavation from one stage to the other wont be implemented to the developed soil pressures.

$$\sigma_{\Theta} = \frac{a^2 * b^2 * (p_o - p_i)}{(b^2 - a^2) * r^2} - \frac{a^2 * p_i - b^2 * p_o}{b^2 - a^2} \quad (4.2)$$

$$\sigma_r = -\frac{a^2 * b^2 * (p_o - p_i)}{(b^2 - a^2) * r^2} - \frac{a^2 * p_i - b^2 * p_o}{b^2 - a^2} \quad (4.3)$$

$$\rho_r = \frac{1 + \nu}{E} * \left[\frac{a^2 * b^2 * (p_o - p_i)}{(b^2 - a^2) * r} - \frac{a^2 * p_i - b^2 * p_o}{b^2 - a^2} * (1 - 2\nu) * r \right] + \frac{\nu * r}{E} * \left[p_z + \frac{2 * \nu * p_i * a^2 - p_o * b^2}{b^2 - a^2} \right] \quad (4.4)$$

$$P_{c,hoop} = P_o * b - P_i * a \quad (4.5)$$

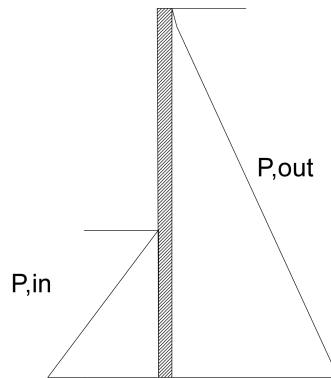
Where:

- a is the internal radius of the wall [m]
- b is the external radius of the wall [m]
- r is the average radius of the wall [m]
- E is the elasticity modulus of concrete [kN/m^2]
- ν is the Poisson's ratio of concrete []
- P_z is the axial pressure on the wall due to self weight. [kN/m']
- P_c is the compression on the wall due to hoop effect. [kN/m']
- σ_θ is the tangential stress at the central axis of the cross-section. [kN/m^2]
- σ_r is the radial stresses at the radial axis of cross-section. [kN/m^2]
- P_o is the soil pressure on the wall from the side that is not excavated. [kN/m^2]
- P_i is the soil pressure on the wall from the side that is excavated. [kN/m^2]

FIGURE 4.16: Geometrical and Material Properties that are used in the K_o Analysis

	[m]
a	19,75
b	20,55
r	20,15
	[kN/m^2]
E	32800000
ν	0,2

FIGURE 4.17: Inner and Outer pressures subjected to a diaphragm wall supporting an excavation



The data used in this analysis can be seen in Figure 4.16. The loading on the wall can be seen from the Figure 4.17. For the analysis, the effective neutral pressures on both sides of the wall have been calculated for all different 4 stages. And the different water table loads are also included in to the load combinations. Effective pressures of the soil layers are calculated according to Equation 3.12, while neutral earth pressure coefficients K_o of different layers are found according to Equation 3.6. The neutral pressures at the given depth will be found with the following equation 4.6 The water load at the given depth is added to the effective pressures and the load charts are prepared. P_z in Equation 4.4 is calculated from the self weight of C28/35 concrete class. The volumetric weight of the concrete is chosen $\gamma_{conc} = 2.4 \text{ Tons}/m^3$

$$\sigma'_o = K_o * \sigma'_v \quad (4.6)$$

During the comparison of theoretical methods it is seen that K_o analysis overestimates the hoop forces. This overestimation prevents the researcher to assess the reliability of FEM analysis results. In order to have a second opinion, an additional 3-pinned arch analysis is performed for estimation of hoop forces. The main idea of this analysis is to use an engineering model of an arch pinned at connections which represents the two consecutive panels of circular part of diaphragm wall. The graphical representation can be seen from Figure 4.18. The calculation of horizontal forces (N) and Hoop forces (N) are as follows:

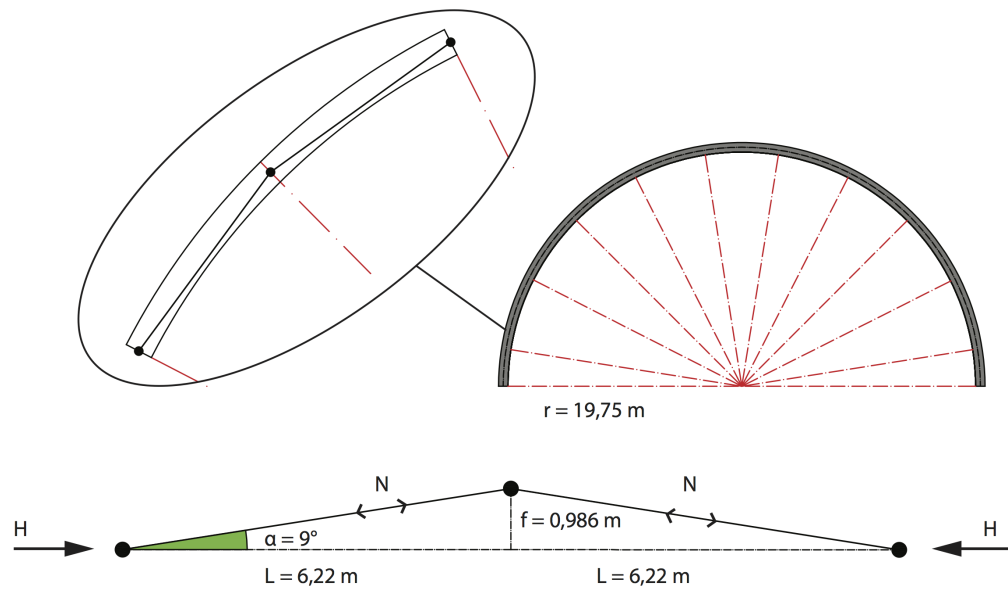
$$H = \frac{q * l^2}{8f} \quad (4.7)$$

$$N = \frac{H}{\cos\alpha} \quad (4.8)$$

Where:

- q: The resulting soil pressure [kN/m^2]
- l: Total span of the arch (2L in Figure 4.18) [m]
- f: The height of the arch [m]
- α : The angle of the panel with horizontal plane [degrees]

FIGURE 4.18: 3-Pinned Arch Graphical Representation



4.2.1 Results of K_o Analysis

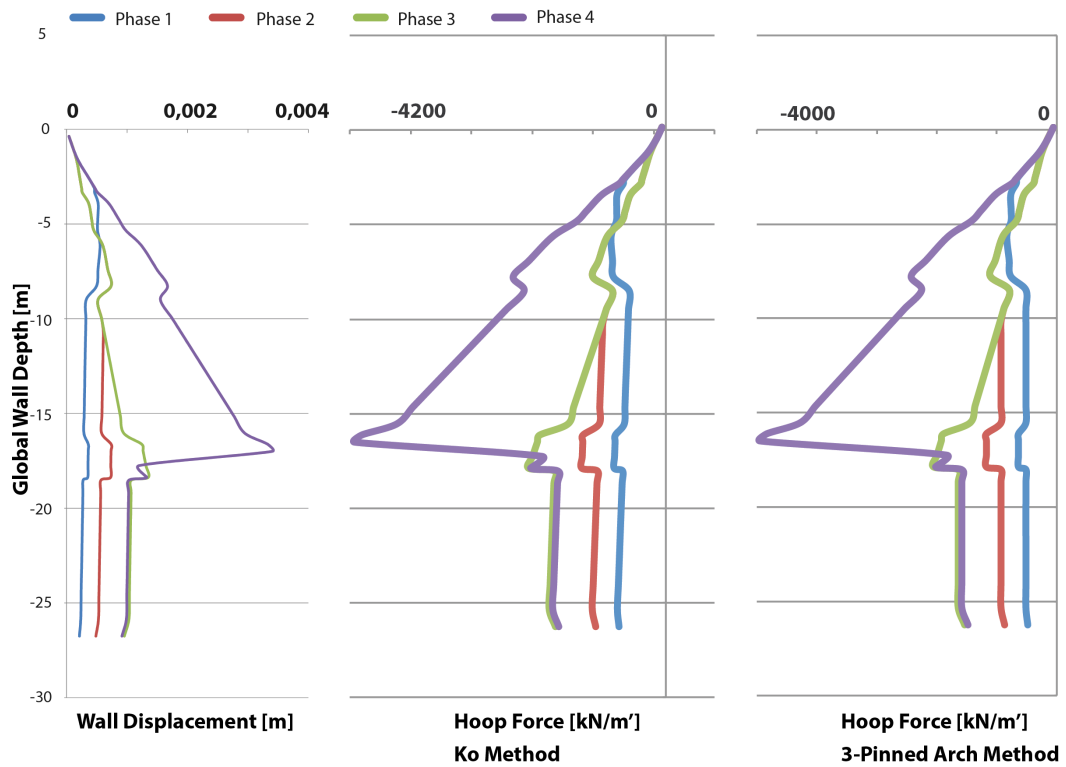
The loading of four different stages are calculated and applied to the structure according to the Equations 4.2 to 4.5. The deformation results can be seen from Figure 4.19. When the deformation results are compared of D-Sheet analysis for the straight wall in Figure 4.11 and the cylindrical wall deformations in Figure 4.19, it can be seen that there is a serious deformation expectancy difference between the two different mechanisms.

On the other hand it is under consideration that K_o analysis takes into account perfectly axi-symmetric conditions where hoop forces increase the stiffness of the cylindrical wall against out of plane bending. The walls that are subject to this thesis are not fully cylindrical that is why at the corners where cylindrical wall meets the straight wall the hoop forces will disperse, thus the stiffness of the wall will decrease against out of plane bending. This effect will cause higher deformations. But this theoretical results gives us a lower bound and can be compared with the axi-symmetrical Diana Analysis to be performed in Chapter 5.

In addition, as can be seen from Figure 4.19, the deformations on the wall is not continuous along the depth. This is caused by the uncoupled nature of the soil bedding taken in to account in the analysis. Axi-symmetrical Diana Analysis will be done with coupled springs, that is why in Diana analysis a continuous deformation pattern is expected.

The results of 3-pinned arch method also can be seen from Figure 4.19, when compared with the hoop forces found by K_o analysis, it is seen that lower values are found. Both methods will be compared with the Diana

FIGURE 4.19: Analyses Results: Displacement Results From Ko Analysis; Hoop Force Results From 3-Pinned Arch and Ko Analyses



analysis in the following chapter and the most consistent one will be compared.

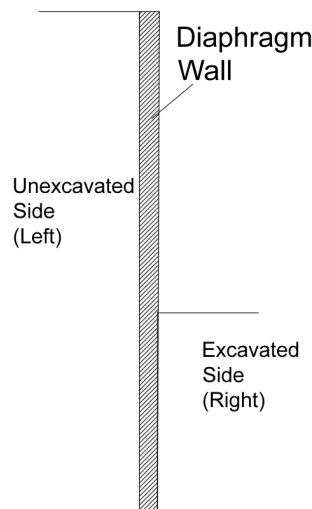
Chapter 5

Description of Diana Models: Plane Strain, Axi-symmetric Conditions

5.1 Modeling Strategy

The diaphragm wall laterally supporting an excavation pit is graphically simplified in the Figure 5.1. As can be seen from the figure, the thickness of the wall is relatively unimportant compared to its length. This reality allows us to model the wall as a shell structure. Shell elements are easy to use in Diana 10.1 models and also they allow the user to reach distributed forces and moments at applied loading. This is why for the modeling of the wall, shell elements will be used.

FIGURE 5.1: A Simple Plot Showing The Diaphragm Wall



As mentioned earlier, the soil around the wall is modeled as nonlinear springs. This is possible in Diana 10.1 thanks to the line interface elements. These interface elements behave as coupled springs (if connectivity of mesh is correctly defined) and thanks to the plot input option for stress-relative displacement curves, complex nonlinear behavior of these springs can be modeled easily.

The straight section of the wall will laterally be supported by struts. These struts are modeled by spring dashpot elements in Diana. This element is chosen to be appropriate due to the ease of application. In addition, the strut behavior is out of the scope of the thesis, that is why a simplistic modeling of the strut is considered to be convenient.

5.1.1 Definition: Plane Strain Conditions and Axi-symmetric Conditions, Phased Analysis

Diana Manual 10.1 defines the Plane Strain condition as follows: Plane strain elements are characterized by the fact that their thickness t is equal to unity and that the strain components perpendicular to the element face are zero (ϵ_{zz}) according to the global axis represented in Figure 5.2. These elements are highly appropriate for modeling the Diaphragm walls because the strains perpendicular to the element face are expected to be very small compared to the strains in other directions. In other words, the thickness of the wall won't remarkably change due to the loading. Plane strain conditions allow the user to use line interface elements. For above mentioned reasons the modeling of the straight wall will be done in Plane Strain conditions.

FIGURE 5.2: Plane Strain Element

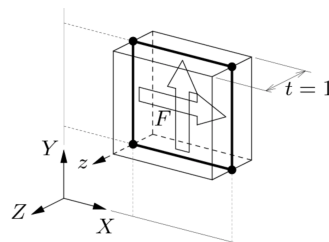
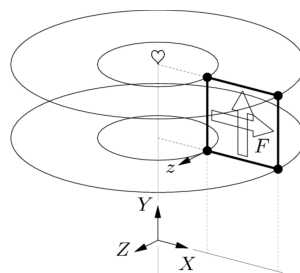


FIGURE 5.3: Axisymmetric Element



Diana Manual 10.1 defines the Axi-symmetric condition as follows: They must be positioned in the model XY plane, i.e., the Z coordinate of the element nodes must be zero. DIANA considers the Y axis as axis of rotational symmetry, therefore each element models a ring. This requires that the X coordinate of the element nodes must greater than or equal to zero. Loading F must act in the plane of the element. Typical applications for axisymmetric elements are the analysis of circular storage tanks, cooling towers, tubes and sockets. An exemplary image can be seen from Figure 5.3. similar to Plane Strain condition, Axisymmetric elements also have zero ϵ_{zz} . In addition, the line interface elements can easily be used. Since the cylindrical

section of the wall is not strutted, no spring dashpot elements are needed.

Phased Analysis

Diana 10.1 manual defined phased analysis as follows: In phased structural analysis the model may change from phase to phase. For instance, supports may be removed or added. A phased analysis comprises several calculation phases. Between each phase the finite element model changes by addition or removal of elements and constraints. Or even, the attached materials to an element can be changed from phase to phase. In each phase a separate analysis is performed, in which the results from previous phases are automatically used as initial values. These results are typically stresses, deformations, potentials, velocities etc. This type of analysis is highly appropriate for the staged excavation to be performed.

The material properties of the soil layers on the excavated side can be changed from one stage to the next. The loading also can be changed from one stage to the other. Which allows the user to model complex phased analyses taking into account material and loading and support changes (adding of Strut elements on previously deformed mesh). It shouldn't be forgotten that at the beginning of every phase the total load should be applied to model, otherwise the deformations that are found will only be the incremental change, not the final result.

5.1.2 Chosen Elements And Properties

The elements that are used in the analyses can be enlisted in three different categories. These categories are:

- Wall elements: cylindrical and straight
- Element used for the soil
- Element used for the struts

Wall Elements

For two different analyses, different shell elements are chosen. Both of the elements have the identical properties although each is only compatible with the related analysis condition. The straight wall section is modeled by CL9PE infinite shell elements. The topology of such element can be seen from Figure 5.4. The definition of variables can be seen from Figure 5.5.

FIGURE 5.4: Nodes and Local Axes of CL9PE Infinite Shell Element

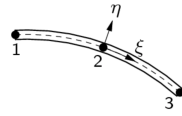
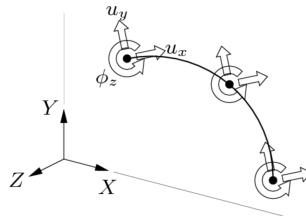


FIGURE 5.5: CL9PE Deformations and Rotation Definition



The cylindrical wall section is modeled by CL9AX Shells of Revolution element. This element basically has similar constitutive relations and integration scheme with CL9PE elements. The topology of the element can be seen from Figure 5.6 and the variables can be seen from Figure 5.7.

FIGURE 5.6: Nodes and Local Axes of CL9AX Shells of Revolution (SOR) Element

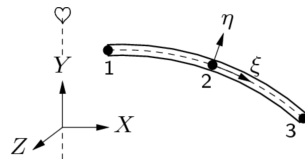
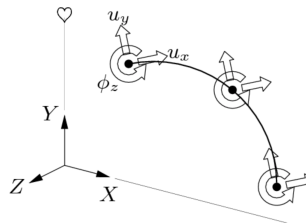


FIGURE 5.7: CL9AX Deformations and Rotation Definition



Both elements have the following interpolation polynomial for the translations, as shown in Equation 5.1. For both different analyses Gauss Integration scheme is chosen to be applied along the thickness (η) of the element. Gauss integration means that there are 2 integration points on element thickness, which can be called as 2 layers.

$$u_i(\xi) = a_0 + a_1\xi + a_2\xi^2 + (b_0 + b_1\xi + b_2\xi^2)\eta \quad (5.1)$$

The applied material and geometrical properties for two different elements are enlisted in the following Table 5.1.

TABLE 5.1: Wall Elements Applied Properties

<i>Analysis</i>	<i>Element</i>	<i>Thickness[m]</i>	<i>MaterialModel</i>	$E[kN/m^2]$	ν
<i>PlaneStrain</i>	<i>CL9PE</i>	1.2	<i>LinearElastic</i>	$3.28E + 7$	0.2
<i>Axisymmetric</i>	<i>CL9AX</i>	0.8	<i>LinearElastic</i>	$3.28E + 7$	0.2

The position of the cylindrical wall is defined according to the inner and outer radius shown in Figure 3.10. $r_{out} = 20.55\text{ m}$ and $r_{in} = 19.75\text{ m}$. As explained before in subsection 5.1.1, the rotating structure should be positioned on the right hand side of the rotating Y axis. According to this knowledge, the CL9AX SOR element will be positioned at $r_{av} = +20.15\text{ m}$ on x axis according to the axis represented in Figure 5.3. The positioning of CL9PE is not important on the results, for ease of modeling it will be positioned on Y axis itself according to the axis represented in Figure 5.5.

Soil Element

For the spring-like modeling of the soil around the wall, CL12I line interface elements are chosen to be appropriate. The topology and defined displacements of CL12I element can be seen from Figure 5.8. The CL12I element is an interface element between two lines in a two-dimensional configuration. The local xy axes for the displacements are evaluated in the first node with x from node 1 to node 2. Variables are oriented in the xy axes, Figure 5.9. The element is based on quadratic interpolation. By default DIANA applies a 3-point Newton-Cotes [$n_{\xi}=3$] integration scheme.

FIGURE 5.8: Line Interface Element CL12I

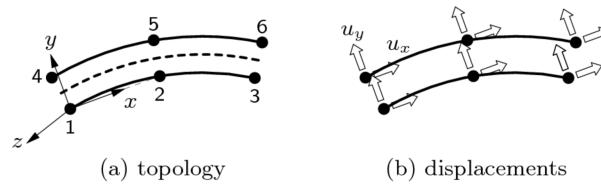
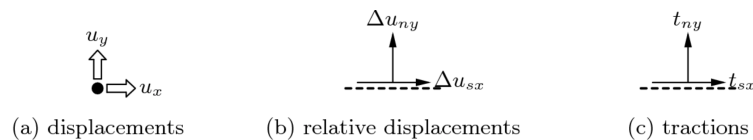


FIGURE 5.9: CL12I Element Variables



CL12I element is usable in both Plane Strain and axisymmetric conditions. This allows the user to model different models with ease, and allows the user to define material properties of the CL12I element for both different analysis identically. The only change in syntax in CL12I element definition from one analysis to other is the CONFIG syntax. For Plane strain condition CONFIG syntax of CL12I element is PSTRAI, for axisymmetric

condition CONFIG syntax of CL12I element is AXISYM.

The geometry and material properties of the soil element definition has certain prerequisites. For instance, the $p-\Delta u$ graph of the soil spring should start from negative pressures and negative displacements and end with positive pressures and positive relative displacements. That is why the yield values of soil pressures found by Equations from 5.3 to 5.5, are adjusted according to this prerequisite. Relative displacements in CUR method found by Equations from 5.6 to 5.10 are similarly adjusted. An exemplary soil element $p-\Delta u$ graph is shown in Figure 5.11. As can easily be seen, the yield active and passive yield capacity of the excavated soil decreases with the layers of soil removed from top. When the UWC is placed, the yielding limits of the soil under increases (phase 4). The $p-\Delta u$ properties of CL12I elements are inputted via DUSTNY syntax.

FIGURE 5.10: $p-\Delta u$ Graph of CUR transformed to Diana Input

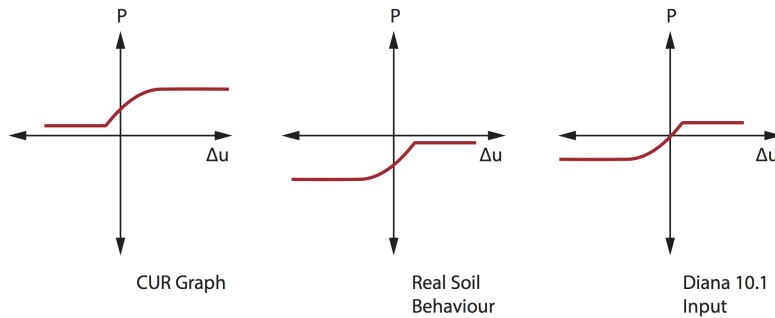
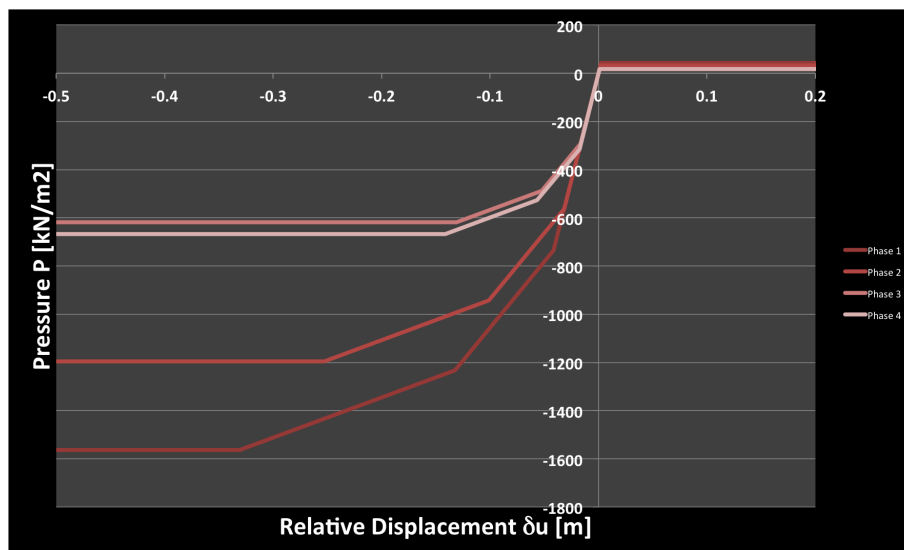


FIGURE 5.11: $p-\Delta u$ Graph Of An Exemplary Soil Layer On Excavated Side



$$\sigma'_{v} = \gamma_{sat;z} * z - u_{d;z} \quad (5.2)$$

$$\sigma'_{a} = K_a * \sigma'_{v} - 2c * \sqrt{K_a} \quad (5.3)$$

$$\sigma'_{p} = K_p * \sigma'_{v} + 2c * \sqrt{K_p} \quad (5.4)$$

$$\sigma'_{o} = K_o * \sigma'_{v} \quad (5.5)$$

$$u_A = \frac{0.5 * \sigma'_p}{k_{h1}} \quad (5.6)$$

$$u_B = \frac{0.8 * \sigma'_p}{k_{h2}} \quad (5.7)$$

$$u_C = \frac{\sigma'_p}{k_{h3}} \quad (5.8)$$

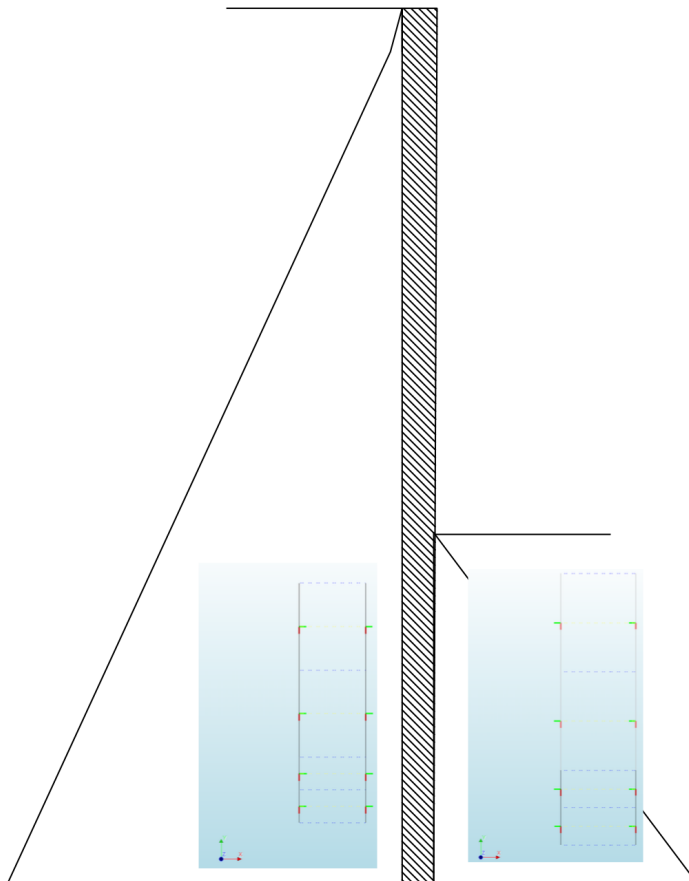
$$k_{ha} = \frac{0.5\sigma'_p - \sigma'_0}{u_A} \quad (5.9)$$

$$u_D = \frac{\sigma'_{h0} - \sigma'_a}{k_{ha}} \quad (5.10)$$

Figure 5.11 can be interpreted as follows: When the pressures on the interface are compressive the interface relatively displaces in compression, thus getting shorter [-]. When the interface element is subject to tensile stresses, it displaces in tension, getting longer[+]. The material behavior of the soil elements in local axis Y is applied via DUNY syntax of CL12I element in Material Table. The shear in local axis X values are entered via DUSX syntax. DUSX values are taken as $\frac{1}{3} * k_{h1,i}$ at given soil layer $k_{h1,i}$ values will be chosen from Table 3.6. According to this syntax, the relative displacements will occur on the local y axis of the CL12I element.

Correct geometry has to be applied in order to allow the element CL12I behave correctly. The local X axis and connectivity of elements are defined by Manual Input Interface Properties in Diana Design environment. local Z axis of the wall is defined from Geometry Table in *.dat* file. Defined local axes can be seen from Figure 5.12. Diana derives the local Y axis from the input local X and local Z axes.

FIGURE 5.12: Local Axes Of Interface CL12I On Both Sides Of the Wall: Green local y, Red local x

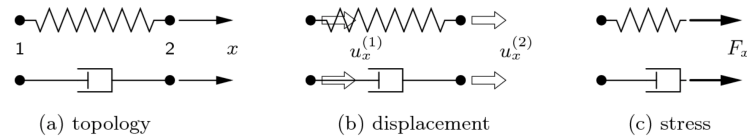


Strut Element

The struts at -1.5 mNAP that is positioned at the beginning of Phase2 and at -9 mNAP that is positioned at the beginning of Phase3 will be modeled by SP2TR Spring-dashpot element. At strut levels predefined SP2TR

elements are activated by phased analysis element activation option. And the struts are applied to deformed mesh without initial stresses. Node 1 is located on the wall, Node 2 is located at the rigid support.

FIGURE 5.13: Topology and Variables of Discrete Spring Element SP2TR



The geometry allocation of shell elements and the spring element is done automatically by Diana. On the other hand, the local axes of the soil elements requires diligence and the input of the user. The material properties of the struts is derived from D-Sheet Analysis results. In the related chapter D-Sheet strut properties are defined taking into account buckling, this is why the Force-Displacement values at strut levels at different Phases will allow us to define a spring constant k in Diana model. The Force-displacement values of D-Sheet results at strut levels can be seen from the Figure 5.14. In the bottom layer of strut it is seen that the stiffness of the strut changes, this occurs due to the loading condition and modeling of strut according to $F_{buckling}$. That is why the average values of the strut properties will be taken and applied to strut layers. These values can be seen in $K_{average}$ column.

FIGURE 5.14: D-Sheet Results of Strut Forces and Displacements: Top Strut 1st chart, Bottom Strut 2nd chart

Phase	d[M]	f[KN]	K[KN/M]	K,average
initial	0	0	0	
1	0,0078	0	0	
2	0,0103	102,2	40880	
3	0,0107	120	44500	
4	0,0156	329,93	42842,857	42740,952

Phase	d[M]	f[KN]	K[KN/M]	K,average
initial	0	0	0	
1	0	0	0	
2	0,0064	0	0	
3	0,0132	120	17647,059	
4	0,0208	329,93	27622,368	22634,714

5.2 Model, Supports, Loads, Mesh

Model

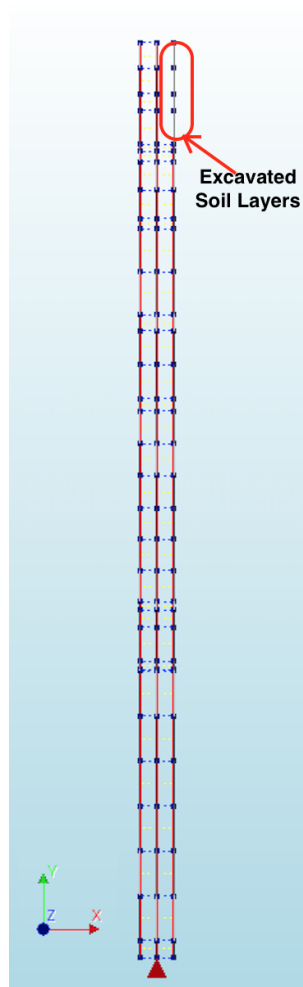
Since the elements and the material and geometrical properties to be used in the analyses are chosen, the mesh can be constructed. In order to create

a simplistic material property derivation and the comparison of the results. The wall is separated into elements in sizes that are directly same with the element sizes in D-Sheet Analysis, the mesh geometry of D-Sheet wall elements can be seen in Appendix D-Sheet Result Report. The charting of soil elements and their length and ground position is represented in Figure 5.15. The graphical representation of the geometry also can be seen from Figure 5.16. The thickness of CL12I elements in Global X axis is 0.5 m.

FIGURE 5.15: Element lengths and real life positions of shell elements [mNAP] and interface elements attached to them. Length [m], different Soil Layers Colored Separately

Elem No	m NAP	Leghth	Elem No	m NAP	Leghth	Elem No	m NAP	Leghth
1	0,5	0,75	12	-7,53	0,47	23	-16,25	0,5
	-0,25			-8			-16,75	
2	-0,25	0,75	13	-8	1	24	-16,75	1
	-1			-9			-17,75	
3	-1	0,5	14	-9	1	25	-17,75	0,25
	-1,5			-10			-18	
4	-1,5	1	15	-10	0,38	26	-18	0,05
	-2,5			-10,38			-18,05	
5	-2,5	0,2	16	-10,38	0,95	27	-18,05	1,33
	-2,7			-11,33			-19,38	
6	-2,7	0,3	17	-11,33	0,95	28	-19,38	1,32
	-3			-12,28			-20,7	
7	-3	0,84	18	-12,28	0,95	29	-20,7	1,32
	-3,84			-13,23			-22,02	
8	-3,84	0,84	19	-13,23	0,92	30	-22,02	1,33
	-4,68			-14,15			-23,35	
9	-4,68	0,32	20	-14,15	0,93	31	-23,35	1,33
	-5			-15,08			-24,68	
10	-5	1,26	21	-15,08	0,92	32	-24,68	1,32
	-6,26			-16			-26	
11	-6,26	1,27	22	-16	0,25	33	-26	0,5
	-7,53			-16,25			-26,5	

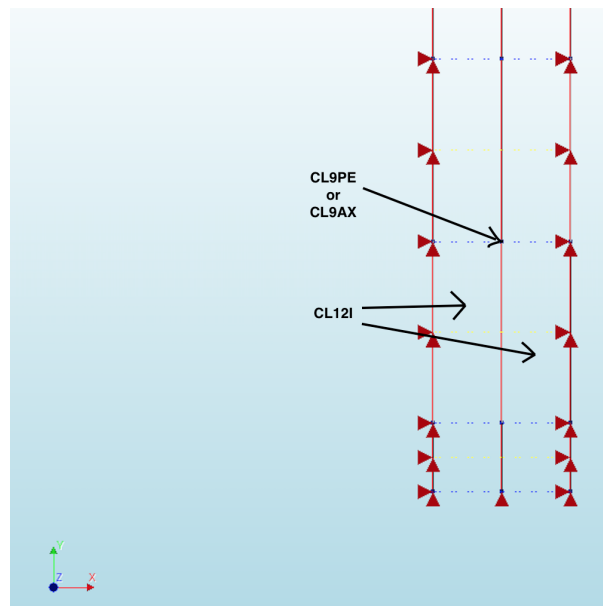
FIGURE 5.16: Graphical representation of Geometry



Supports

The supports on both of the soil and the bottom of the shell wall elements can be seen from Figure 5.17. If the base effects of the soil requires further detailing the support at the bottom of the wall can also be modeled by interface elements but this is not required for the scope of this thesis. The bottom deflection of the wall due to self-weight is highly unimportant compared to the lateral displacements due to laterally supported soil loads.

FIGURE 5.17: Bottom support defined at the bottom of the wall, Side supports defined at the end of interface elements



Loads

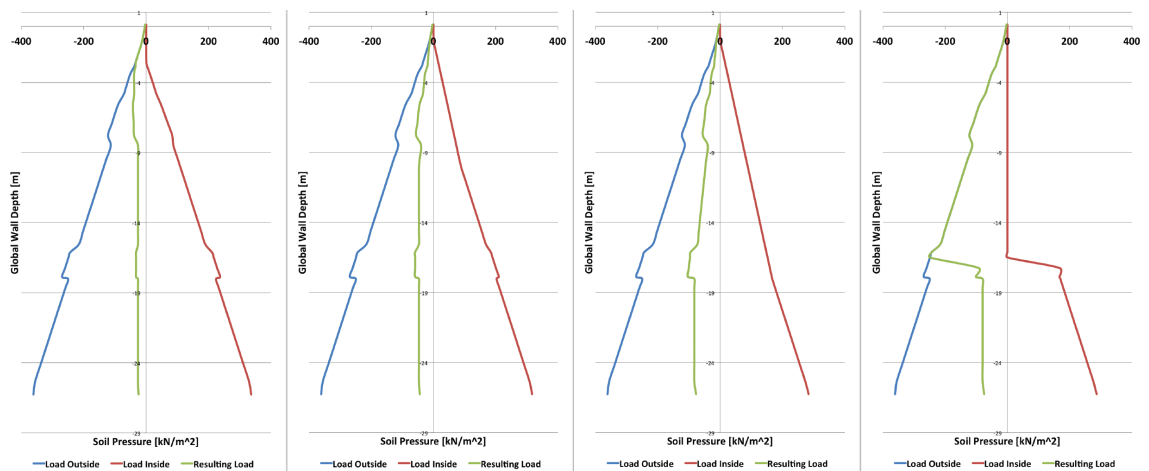
The loads applied to the model is the combination of ground water and effective soil loads on both sides of the wall. The load is applied as distributed force. In all phases, the effect of excavation on the initial soil stresses is neglected. It means that the excavation itself has no effect on the soil stresses. This is an effective assumption. As conclusion the combination of the load at a given depth can be calculated as in Equation 5.11 positive in Global X direction. The loads calculated by Equation 5.11 can be seen for different stages in Figure 5.18:

$$Load_{res} = (\sigma'_{0,out,i} + u_{out,i}) - (\sigma'_{0,in,i} + u_{in,i}) \quad (5.11)$$

Where:

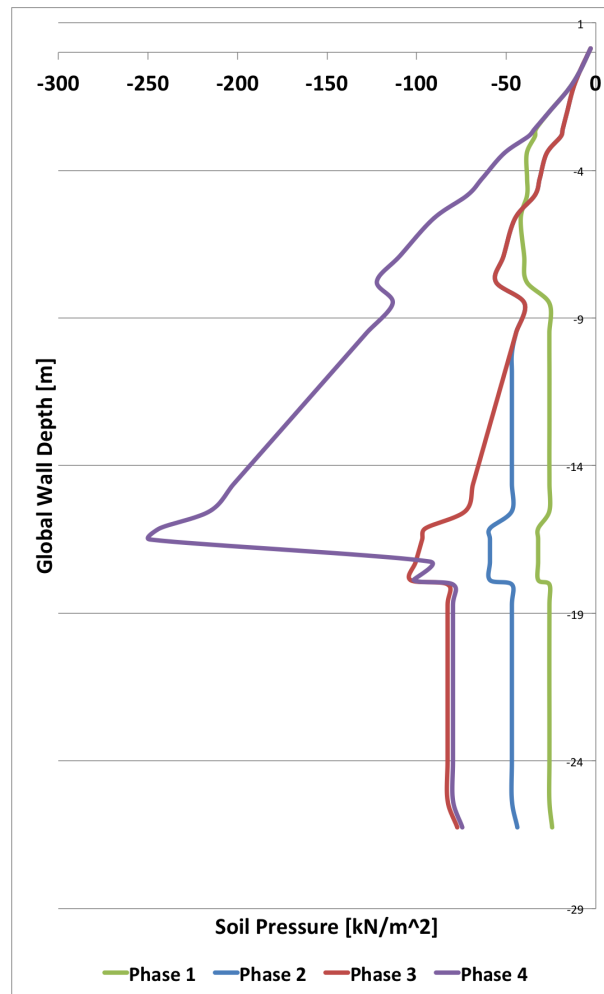
- $\sigma'_{0,out,i}$ is the effective natural pressure on unexcavated side of soil
- $\sigma'_{0,in,i}$ is the effective natural pressure on excavated side of soil
- $u_{out,i}$ is the water pressure on unexcavated side of soil
- $u_{in,i}$ is the water pressure on excavated side of soil

FIGURE 5.18: Different Phases and Applied P_{out} P_{in} and Resulting Load



The resulting applied loads in all stages are compared within the the Figure 5.19. It is seen in the figure that the soil pressures on the excavated side decreases which causes the total load to grow. In 4th phase the load grows drastically because of the dewatering of construction pit:

FIGURE 5.19: Different Phases and Applied Resulting Load



Mesh

The phased construction requires the mesh change from one phase to the other. This is possible in Diana 10.1 by phased analysis option. A symbolic representation of the mesh changes from one construction phase to the other is represented in Figure 5.21 and the graphical representation of excavation and dewatering and strutting performed is represented by Figure 5.20 .

FIGURE 5.20: Graphical Representation Of Phased Excavation: Water Level Represented Blue, Soil Level Represented Brown, Struts Represented Red, Concrete Represented Grey

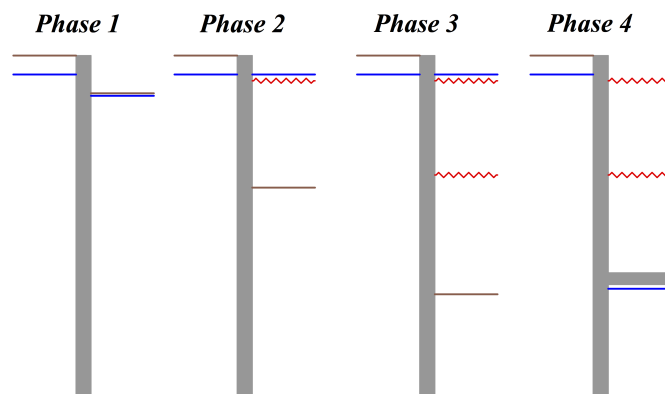
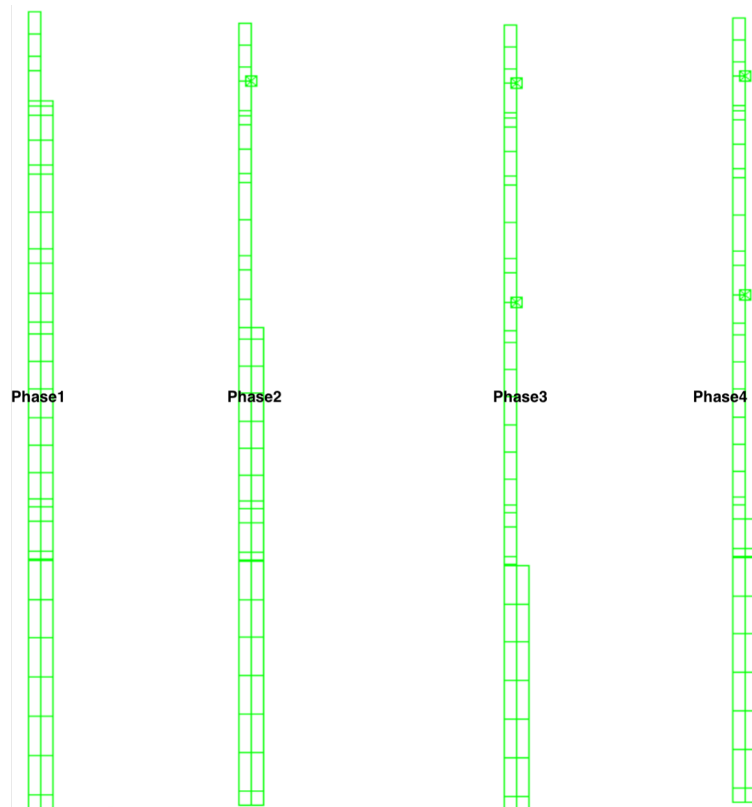


FIGURE 5.21: Different Phases: Mesh Transformation



In every phase the related calculated load is applied on the shell elements. The material properties of CL12I soil interface elements on unexcavated side does not change because there is no loading change on that side of soil. On the excavated side of the wall, the properties of CL12I elements are reassigned to new values before the next phase is calculated. Similar geometry defining and meshing strategy is used for cylindrical wall, only the analysis condition is changed from Plane Strain to Axisymmetric, which requires the change of configuration of CL12I elements. For the cylindrical section, no strut elements are defined.

5.3 Results

The results of the performed analyses will be shared in detail within this section. The results that are to be shared can be enlisted as follows:

- Wall deformations [m]
- Shear forces [kN/m']
- Bending moment [kNm/m']
- Hoop forces [kN/m']

Results are shared under four subsections. The first subsection compares the plane strain Diana model results with the preliminary D-Sheet Analysis. The second subsection compares Axi-symmetric Diana model results with the preliminary K_o and 3-pinned arch analyses. The third subsection compares plane strain and axi-symmetric Diana results. In the last section, the critical depth of section for each analysis is detected and additional results are shared. The soil condition in the results will be kept out of the scope of this thesis, the important aspect is the section results of reinforced concrete wall.

Plane Strain Diana and D-Sheet Piling Analysis Results

The results of different analyses are compared for every other construction phase from Figure 5.22 to 5.25.

FIGURE 5.22: Phase 1 Results

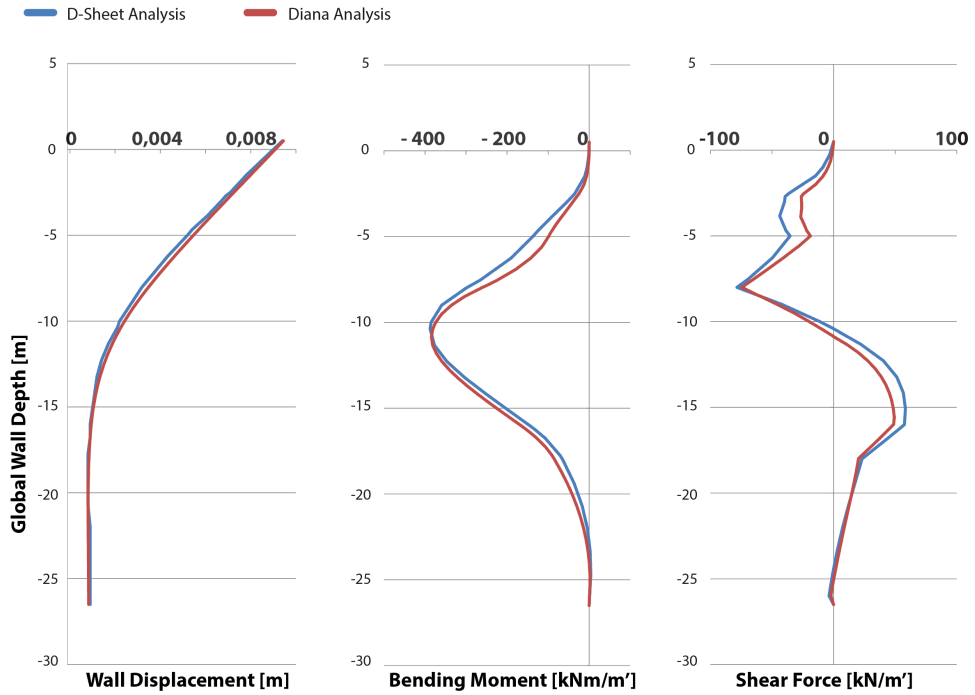


FIGURE 5.23: Phase 2 Results

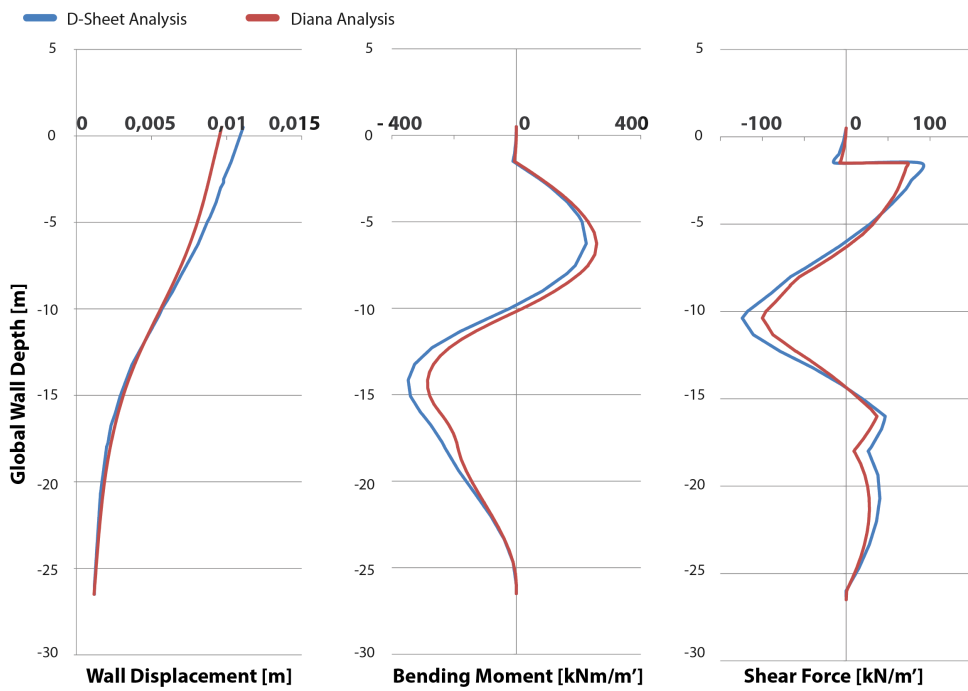


FIGURE 5.24: Phase 3 Results

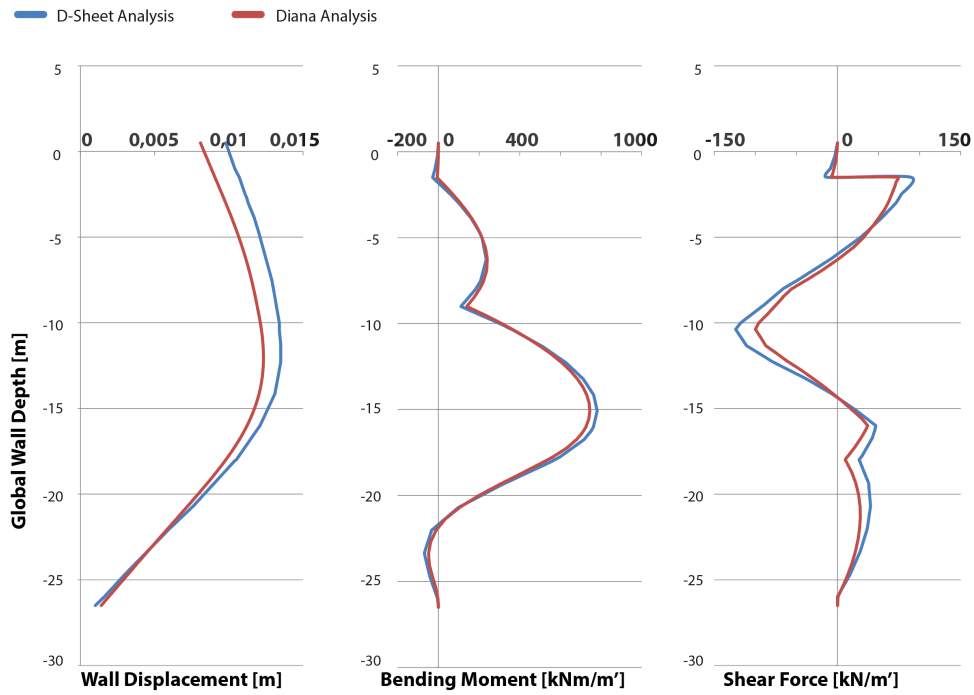
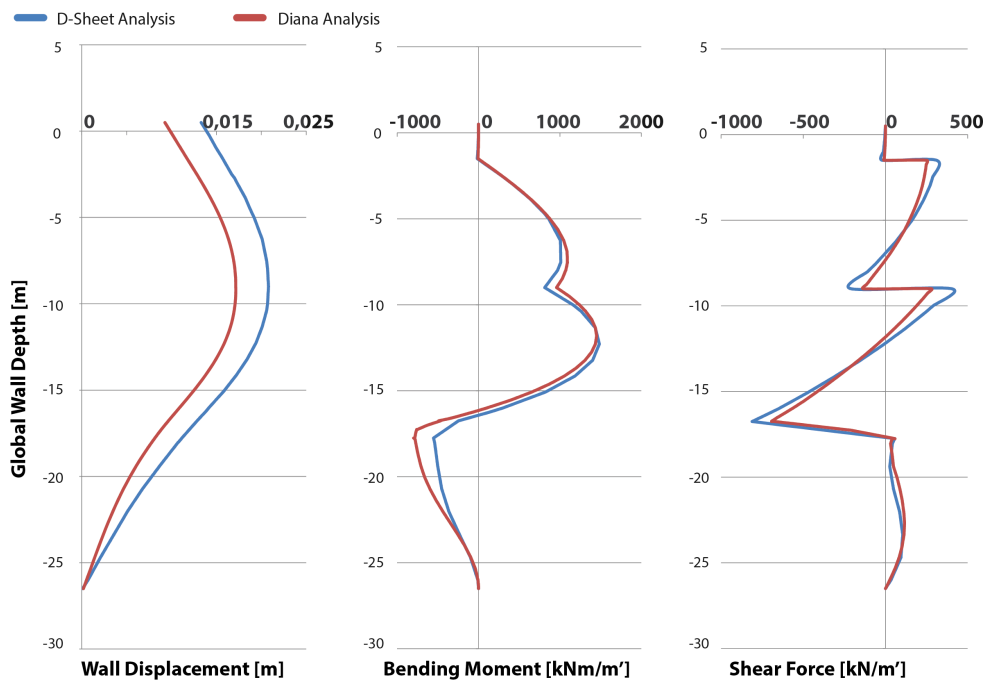


FIGURE 5.25: Phase 4 Results



In Figure 5.22, can be seen that deformation of the wall is found very similarly with a small deviation. The maximum points and values of Moment and shear graphs are also coherent. There is a small bending moment difference mostly observed towards the top of the structure, this can be due to the lack of applied surcharge load in Diana analysis. (In plane strain Diana analysis, surcharge loads applied in D-Sheet analysis are not applied.)

In Figure 5.23, similar differences are observed. In addition, at -1.5 mNAP, the maximum value of shear force is close but different. This difference in results is due to the difference of material models in both analyses for added strut. This effect can be seen in Figures 5.23 and 5.24. As can be remembered from Figure 5.14, stiffness of struts are modeled as the average stiffness of different layers of strut derived from D-Sheet analysis. For a more precise calculation: In each construction phase different strut material can be defined and assigned separately for every different phase.

It also is seen that, displacement differences in both analyses grow passing from Phase 2 to Phase 3, and grows even further from Phase3 to Phase 4. Passing from Phase2 to Phase3, there is no additional surcharge added to analysis, the deformation difference growth is due to the shear stability. In D-Sheet, the vertical shear of soil is calculated for every iteration with new stiffness of deformed soil. On the other hand, in Diana analysis the vertical stiffness of soil is chosen constant in all iterations, which creates a stiffer balanced wall against displacements. (CL12I element shear stiffness in local x direction; syntax DUSX. On the other hand, normal stiffness in local axis y direction; syntax DUSTNY changes according to soil pressures in the iteration.). For a more precise analysis, the shear behavior of the soil elements can also be modeled varying according to stress condition. This is out of the scope of this dissertation. The comparison of both analyses shows a good correlation. For this study, the Diana model results are taken into consideration for the engineering model to be described in Chapter 6.

Axisymmetric Diana and Theoretical K_o Analysis Results

The results of different analyses are compared separately for every other construction phase. In Figures 5.26 to 5.29. The results of the analyses will be shared as listed:

- Hoop Forces (N_{xy} in Diana, P_c in K_o , N in 3-Pinned Arch) [kN/m']
- Wall Displacements [m]

FIGURE 5.26: Phase 1 Results

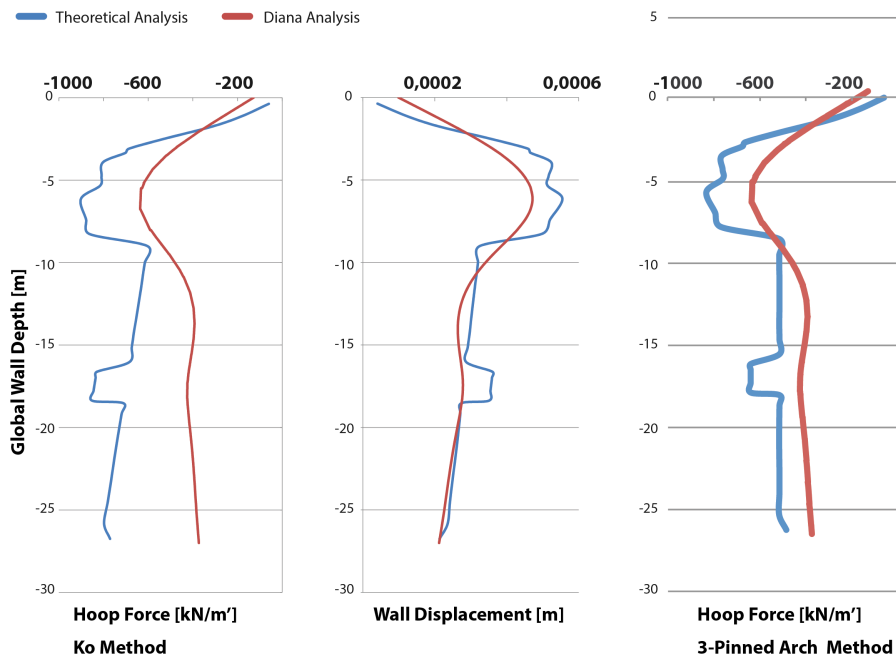


FIGURE 5.27: Phase 2 Results

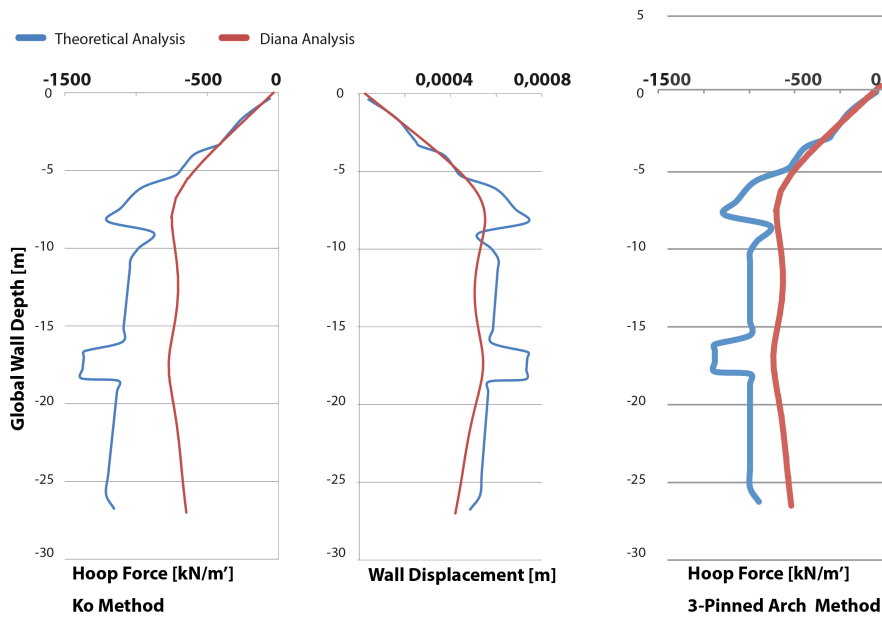


FIGURE 5.28: Phase 3 Results

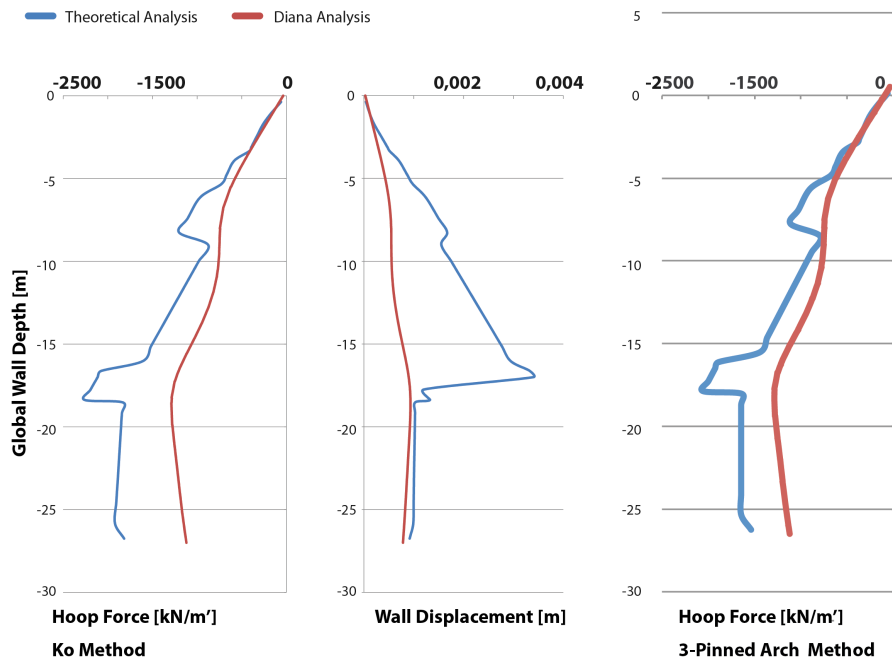
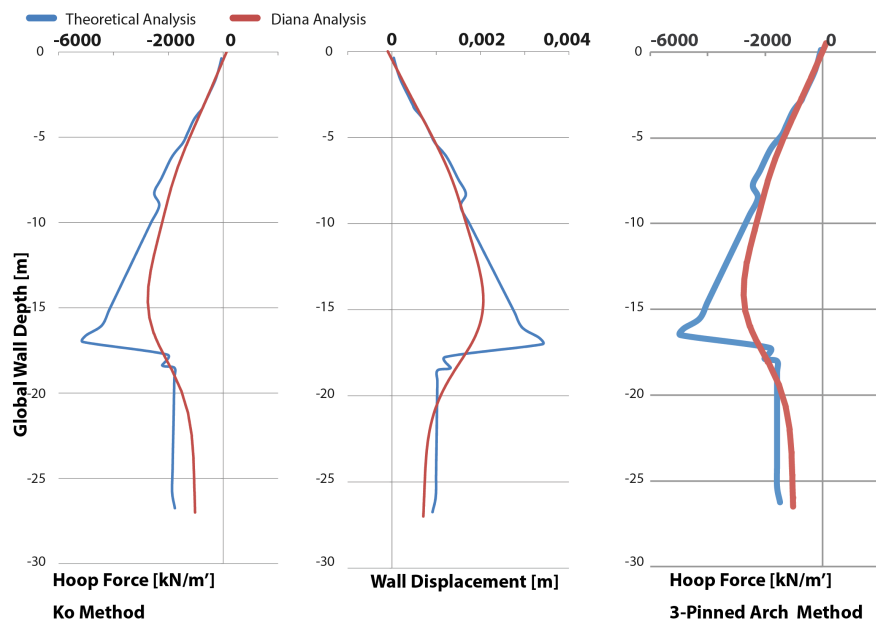


FIGURE 5.29: Phase 4 Results



The difference in wall deformations are observed in the results. This difference is caused due to the behavioral difference of soil springs for both analyses. In preliminary K_o analysis, the soil springs are uncoupled thus, causing the wall deform non continuously. Curvature changing abruptly. On the other hand, interface CL12I elements are acting as coupled springs, which deforms the wall with a smooth curvature. The coupled action of interface elements is achieved via CONNECTIVITY table of the interface elements in mesh.

The estimation of hoop stresses is highly important for the engineering

model to be introduced in Chapter 6. There is a correlation of form in the comparison of analyses but there is a serious value difference in hoop stress values in different analyses. Since the axisymmetrical Diana analysis is just a preliminary analysis for reaching a lower bound for wall displacements and hoop forces, the values of Diana analysis results will be used for the engineering model. K_o analysis is known for overestimating results, due to its model limitations. The development of displacement, forces and bending moments along the phases in both type of walls can be seen from Figures 5.30 and 5.31.

FIGURE 5.30: Plane Strain Model for 1.2 Meter Thick Straight Wall

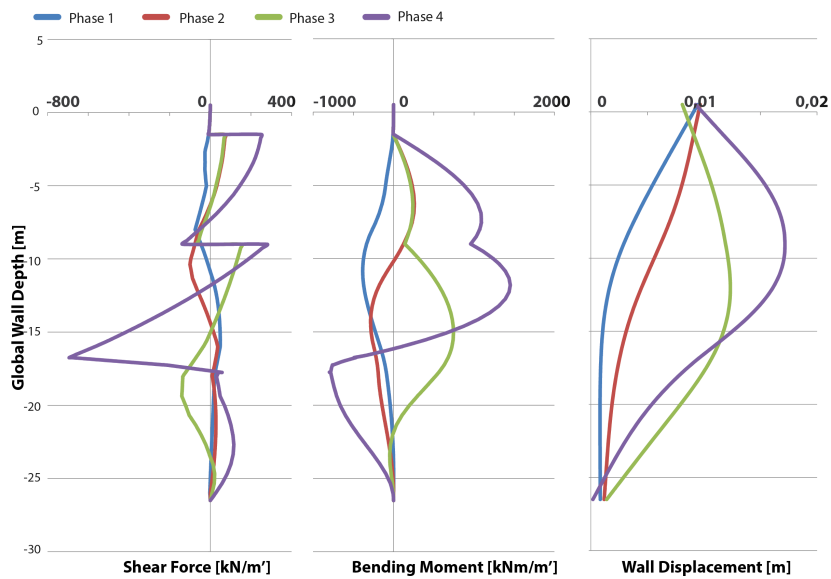
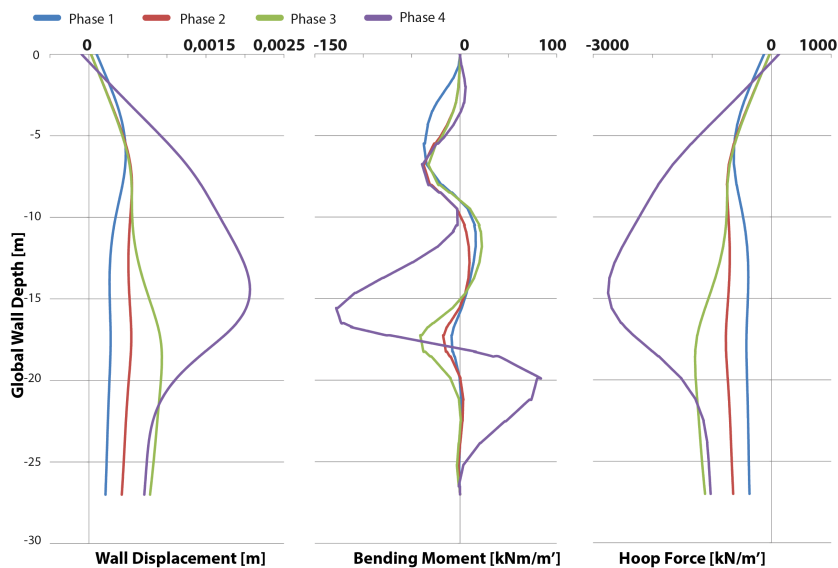


FIGURE 5.31: Idealized Axisymmetric Model for 0.8 Meter Thick Cylindrical Wall



Comparative Results of Different Wall Sections

Deformation results of two different wall sections should be compared taking into account the following aspects:

- Straight Soil Slip Surface theory overestimates the passive pressure capacity of soil. The expected wall deformations in reality will be higher towards the bottom of the walls compared to the analyses.
- Axisymmetrical analysis takes into account perfectly cylindrical walls. The half circular wall in the construction pit, will have dispersed hoop effect, thus the circular wall deformations will be higher in reality.
- The displacements in the critical joint sections at given depth, will be equal in reality on both sides of the joint. For the estimation of this behavior, the engineering model in Chapter 6 can be read.
- In addition, due to the local axes incompatibility of shell elements between both analyses, adjustment of section results are done in order to be able to compare the results correctly.

The comparison of results can be seen for every construction phase separately from Figures 5.32 to 5.35:

FIGURE 5.32: Phase 1 Comparative Results

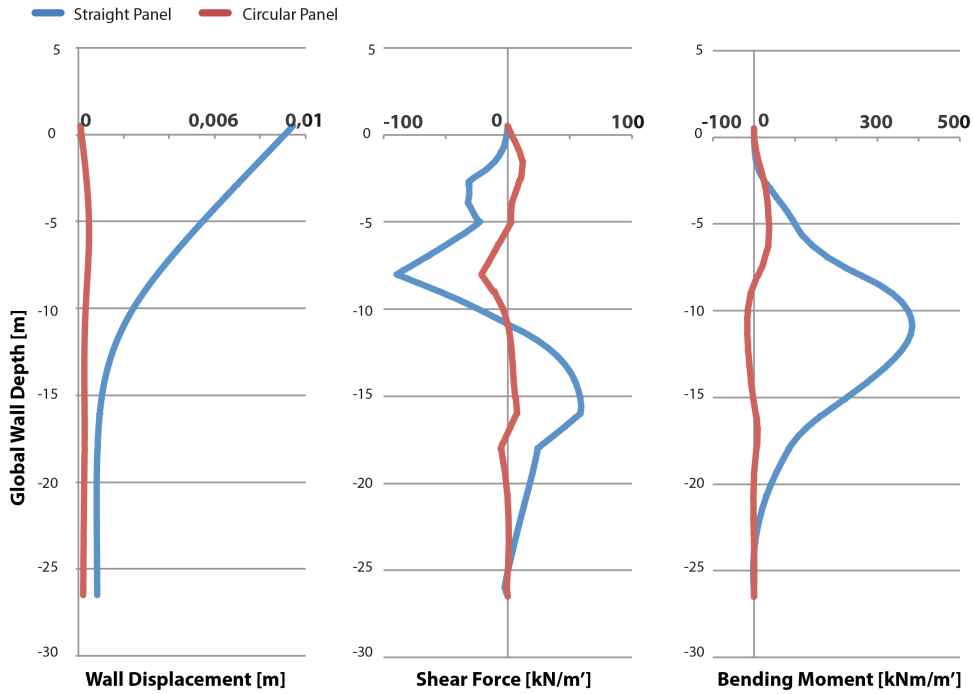


FIGURE 5.33: Phase 2 Comparative Results

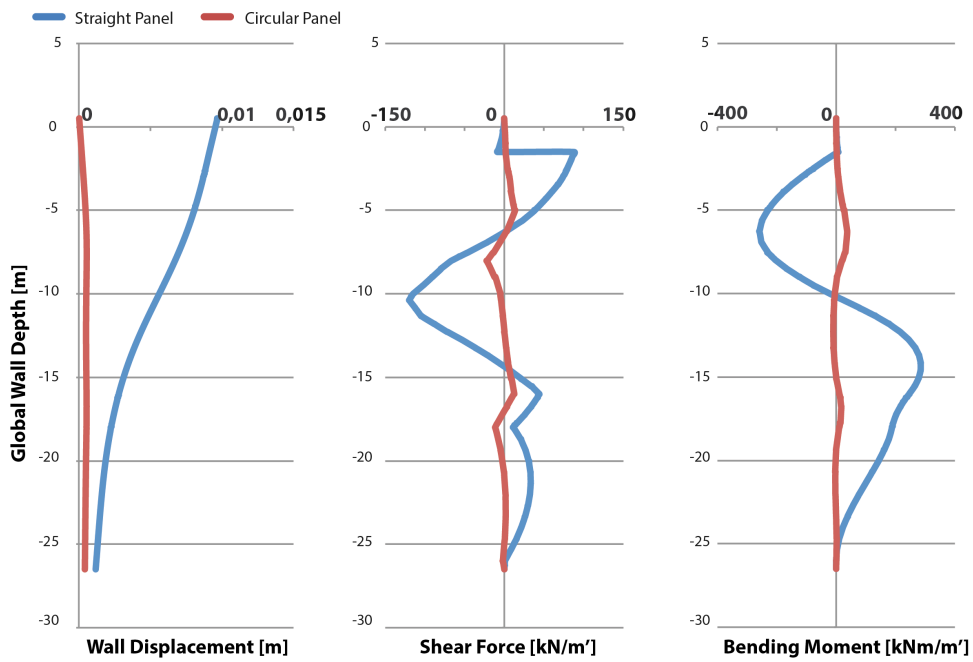


FIGURE 5.34: Phase 3 Comparative Results

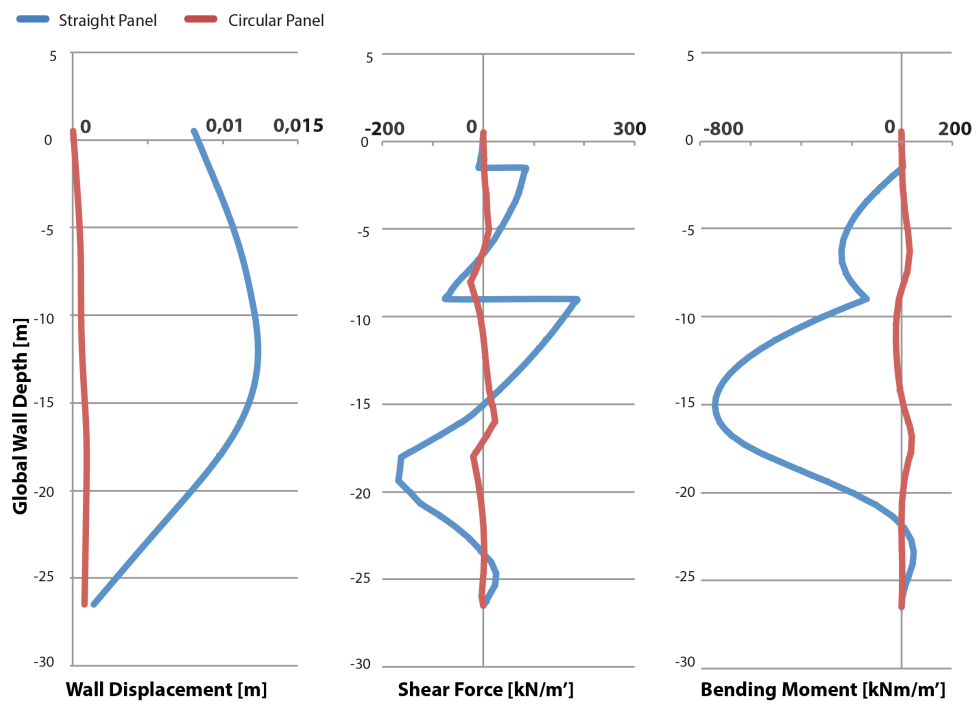
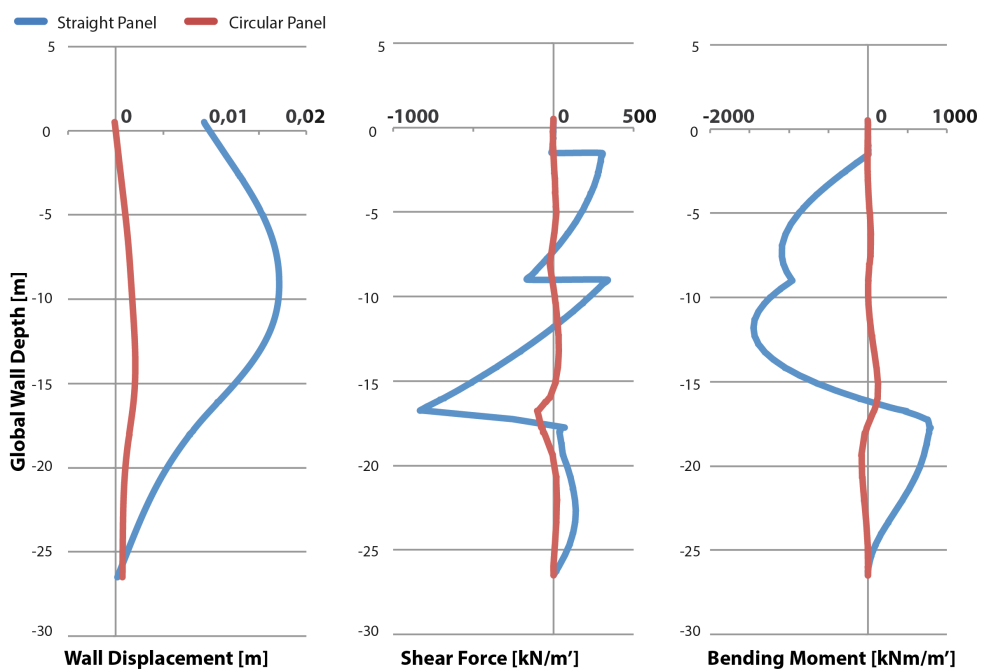


FIGURE 5.35: Phase 4 Comparative Results



Conclusions From Diana FEM Analyses

It can be seen from the graphs that the ideally plane strain and ideally axi-symmetric walls have very incompatible behavior when compared under the same loading conditions. This situation won't be the reality. Actually the resulting section forces from both idealized analyses represent a lower and upper boundary for the real behavior that will occur at the construction joint.

The axi-symmetric wall analysis takes into account perfectly cylindrical wall. On the other hand the cylindrical walls that are subject to this thesis are not perfectly cylindrical. This means that the half cylindrical walls will deform more seriously compared to the perfect axi-symmetric analysis. Yet performed Diana analysis will definitely be a lower boundary.

On the other hand, the wall deformations in the straight side of critical joint will not be able to deform as big as the idealized plane strain analysis results. The critical joint will deform evenly on both sides, which will cause more balanced section forces. And the deformation for all stages will be within the deformation envelope reached by both analyses.

In the following chapter behavioral estimation of the unarmed construction joint will be assessed elaborately. It should be reminded that the idealized analyses that have been performed gives us an envelope of deformation.

Chapter 6

Introduction Of The Engineering Model For Critical Joint

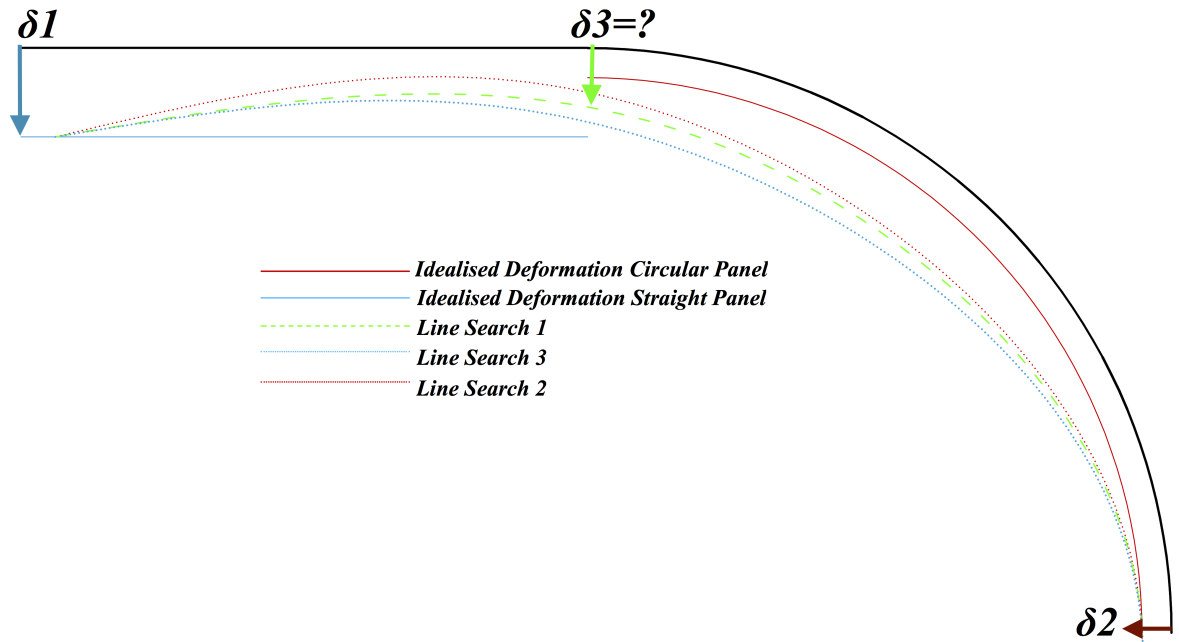
The engineering model that will give an insight on how to obtain a conclusion or interpretation on the problem description requires a multi level illustration of the problem at hand. The staged representation of the engineering model is enlisted as follows:

- Estimating the deflection at the critical construction joint.
- Estimating the resulting section forces (M, V) that will be withstood by unarmored construction joint.
- Determining the effect of eccentricity.
- Estimating the horizontal forces that will be transferred from circular panels to straight panels.
- Superposition of results obtained from above enlisted assumptions.
- Failure Mechanisms And Results.

6.1 Critical Construction Joint's Deflection Estimation

As can be seen from Figure 6.1, the deformations of the wall at three different positions will be different. Previous analyses shows that straight wall deformations will be the highest δ_1 . The wall deformations in the circular section will be the lowest δ_2 . An engineering model is needed for the estimation of δ_3 , which is expected to be in between the previously mentioned deformations.

FIGURE 6.1: Critical Joint Top View: Deformation Of Idealized Conditions Meeting At Joint, Searching For A Deformation Line



For the estimation of the deformation at critical joint, moments of inertia of different wall sections are needed. The calculations for both panels are seen as follows. Straight panel of 1 m length, 1.2 m thickness as I_1 . Circular Panel of 1 m length, 0.8 m thickness as I_2 :

$$I_1 = \frac{1 * 1.2^3}{12} = 0.144m^4 \quad (6.1)$$

$$I_2 = \frac{1 * 0.8^3}{12} = 0.4267m^4 \quad (6.2)$$

$$I_{tot} = I_1 + I_2 = 0.1867m^4 \quad (6.3)$$

Line searches for the estimation of deformation at the critical joint is done as separate three line searches as follows:

- LS1: $\delta_3 = \frac{\delta_1 + \delta_2}{2}$
- LS2: $\delta_3 = \frac{(I_2 * \delta_1) + (I_1 * \delta_2)}{I_{tot}}$
- LS3: $\delta_3 = \frac{(I_1 * \delta_1) + (I_2 * \delta_2)}{I_{tot}}$

The line searches for critical joint are calculated for all construction phases and the results can be seen respectively as follows from Figures 6.2 to 6.5. The color codes of the deformation results are compatible with the graphical representation introduced at Figure 6.1:

FIGURE 6.2: Line Searches For Phase 1

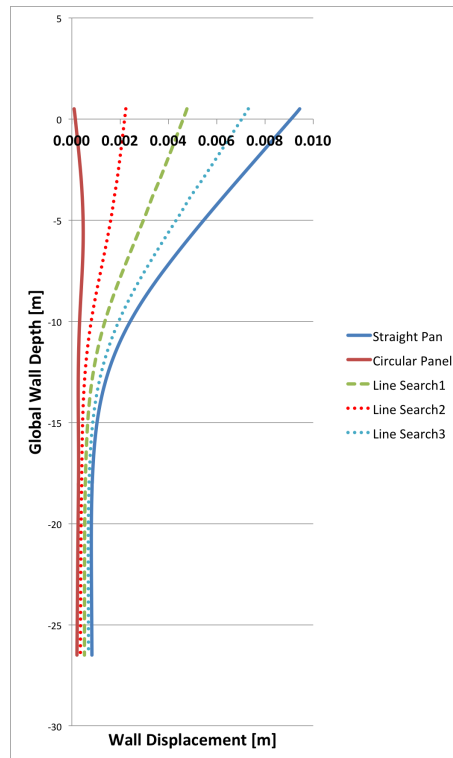


FIGURE 6.3: Line Searches For Phase 2

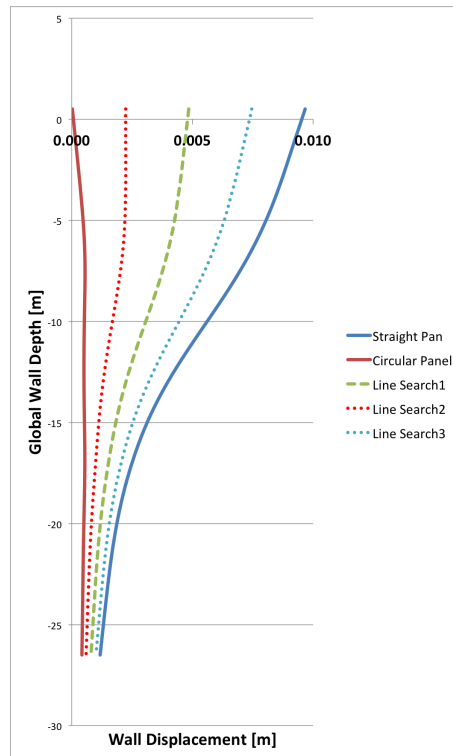


FIGURE 6.4: Line Searches For Phase 3

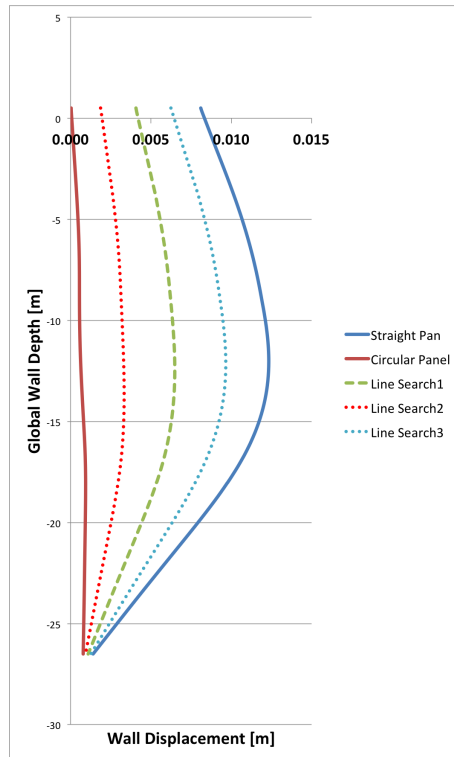
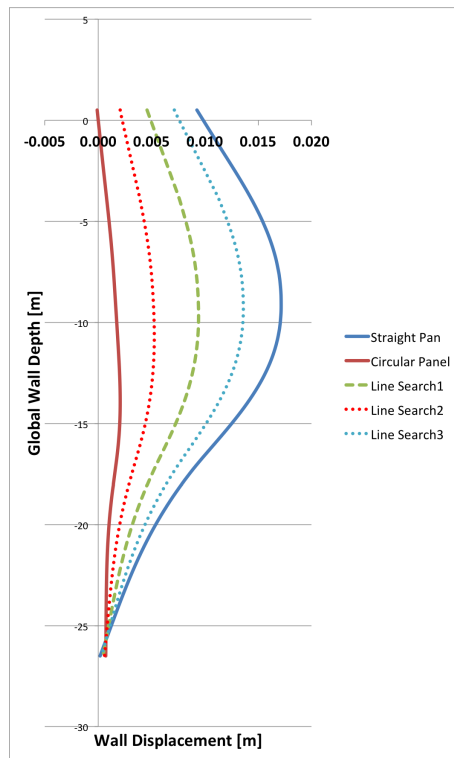


FIGURE 6.5: Line Searches For Phase 4

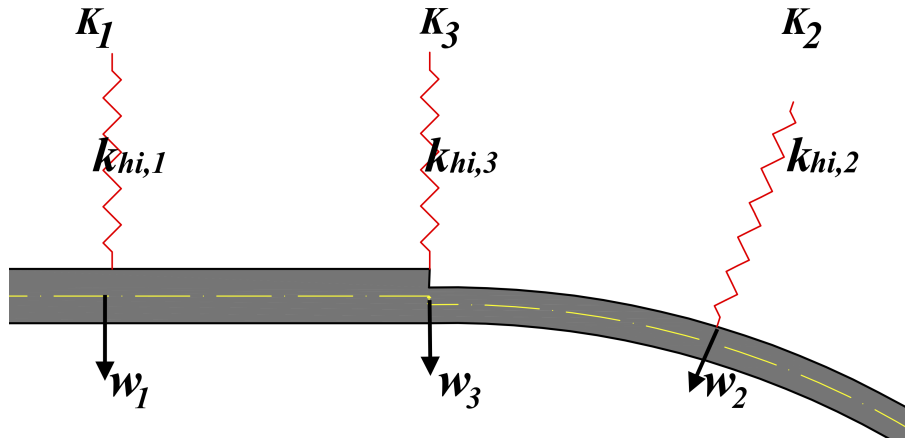


Three different line search methods when compared illustrates better the effect of the displacement distributed according to weighed average by moments of inertia. A 1.2 meter thick wall which predominantly load transfers by out of plane bending will mainly determine the resulting deformation compared to a 0.8 meter thick circular wall which predominantly load transfers by the axial force development due to the arching. That is why the displacements at construction phases are expected to develop closer to Line Search 3 (between Line Search 1 and Line Search 3 curves). Concluding from the previously mentioned reasoning Line Search 2 is not expected to be representing the site conditions, yet it is more a realistic estimation of deformation for cylindrical part of the wall compared to idealized cylindrical wall deformation.

The deformation results found by Line Search 3 must be reconfirmed with a futures study to see if the connection will behave similarly, many factors including the soil spring displacement conditions, the non complete cylindric behavior of the half arch shaped section and the eccentric connection will have an effect on the results which only can be confirmed by a full three dimensional modeling of the problem.

6.2 Estimation Of Resulting Section Forces (M, V)

FIGURE 6.6: Top View: Deformation w , Curvature κ and Subgrade Reaction Coefficient k_{hi} and Displacement w Differences At Different Positions



The soil element right behind the critical joint will have an even stress state directly at infinitesimal distance on both sides of the construction joint. This assumption is concluded from Equation 6.4, taken into account:

$$\sigma'_{soil,resulting,i} = \sigma'_{soil,initial,i} \pm k_{hi} * w_i \quad (6.4)$$

For a given depth of soil, subgrade reaction coefficient (k_{hi}) will be accepted equal for both sides and the walls will deform continuous at the critical joint (w_3). It should be pointed out that in reality different sections of the wall can be in different parts of their tri-linear stiffness diagrams due to the differences in deformations and this might result is a jump of soil stresses on both sides of the wall. On the other hand, the deformations of the wall is really small and a big stiffness difference is not expected yet should be confirmed.

Diana performs the calculations at the following order:

1. From the inner and outer loads, the deformations w_i are calculated using the stiffness values k_{hi} input for soil springs.
2. From the previously found deformations w , curvature is calculated κ .
3. From reached curvature κ , sections stresses and forces are reached.
4. Process is repeated until the force balance is achieved.

Similarly deformed sections will have similar curvature κ_i . As known from the mechanical relation of bending moment and curvature, see Equations 6.5 and 6.6, the moments that will occur at the wall sections become relative to the inertia moment of sections, see Equation 6.7. Similarly, shear force will be distributed to sections according to their inertia of moment derived according to wall depth position, see Equation 6.8. This will also conclude to the relativity of shear forces to moments of inertia, Equation 6.9.

$$\kappa = \frac{d^2w}{dx^2} \quad (6.5)$$

$$M_i = -EI_i \frac{d^2w_i}{dx^2} = -EI_i \kappa_i \quad (6.6)$$

$$\frac{M_1}{M_2} \cong \frac{I_1}{I_2} \quad (6.7)$$

$$Q = -\frac{d}{dx} (EI_i \frac{d^2w_i}{dx^2}) \quad (6.8)$$

$$\frac{Q_1}{Q_2} \cong \frac{\frac{dI_1}{dx}}{\frac{dI_2}{dx}} \quad (6.9)$$

From these relations it can be assumed that, for a given displacement, the distribution of section forces can be derived proportional to their I (moment of inertia) value for different walls. This will allow us to estimate the distribution of section forces in different wall sections, for any given displacement. And since the displacement of the critical joint is upper bounded by the displacement of the straight wall section, checking the critical section for the upper bound will give us a reliable yet over-safe solution.

A better way of estimation of resulting forces is to use the deformation found by *Line Search* methods and apply those newly obtained deformations to a Diana models as imposed deformation loads.

The third way of estimating the resulting section forces is to distribute the section forces of idealized conditions to both sides of the construction joint relative to the weighed average according to the moments of inertia.

For this thesis it is chosen to follow the last suggestion, in a future study all the methods can be tried out and results can be deducted for a more complete study about the subject.

The method to be used can be summarized in the following annotations.:

1. Bending moment of straight wall obtained from idealized fem analysis as M_1 and of circular wall from the idealized fem analysis as M_2 are taken.
2. Bending moment difference to be taken by unarmed construction joint without taking into account the balancing of deformations as $M_{diff} = M_1 - M_2$
3. Bending moment distributed to straight wall panel derived from weighed average of differential bending moment. $M_{str,redist} = (I_1 * M_{diff}) / I_{tot}$
4. Bending moment distributed to circular panel derived from weighed average of differential bending moment. $M_{cir,redist} = (I_2 * M_{diff}) / I_{tot}$
5. Resulting bending moment to be withstood by unarmed construction joint. $M_{diff,redist} = M_{str,redist} - M_{cir,redist}$

1. Shear force of straight wall obtained from idealized fem analysis as V_1 and of circular wall from the idealized fem analysis as V_2 are taken.
2. Shear force difference to be taken by unarmed construction joint without taking into account the balancing of deformations as $V_{diff} = V_1 - V_2$
3. Shear force distributed to straight wall panel derived from weighed average of differential Shear force. $V_{str,redist} = (I_1 * V_{diff})/I_{tot}$
4. Shear force distributed to circular panel derived from weighed average of differential Shear force. $V_{cir,redist} = (I_2 * V_{diff})/I_{tot}$
5. Resulting Shear force to be withstood by unarmed construction joint.
 $V_{diff,redist} = V_{str,redist} - V_{cir,redist}$

Calculated out of plane bending moments and shear forces from above mentioned methods are respectively shared from Phase 1 to Phase 4 in Figures 6.7 to 6.10:

FIGURE 6.7: Phase 1: Out Of Plane Moments And Shear Forces Redistribution

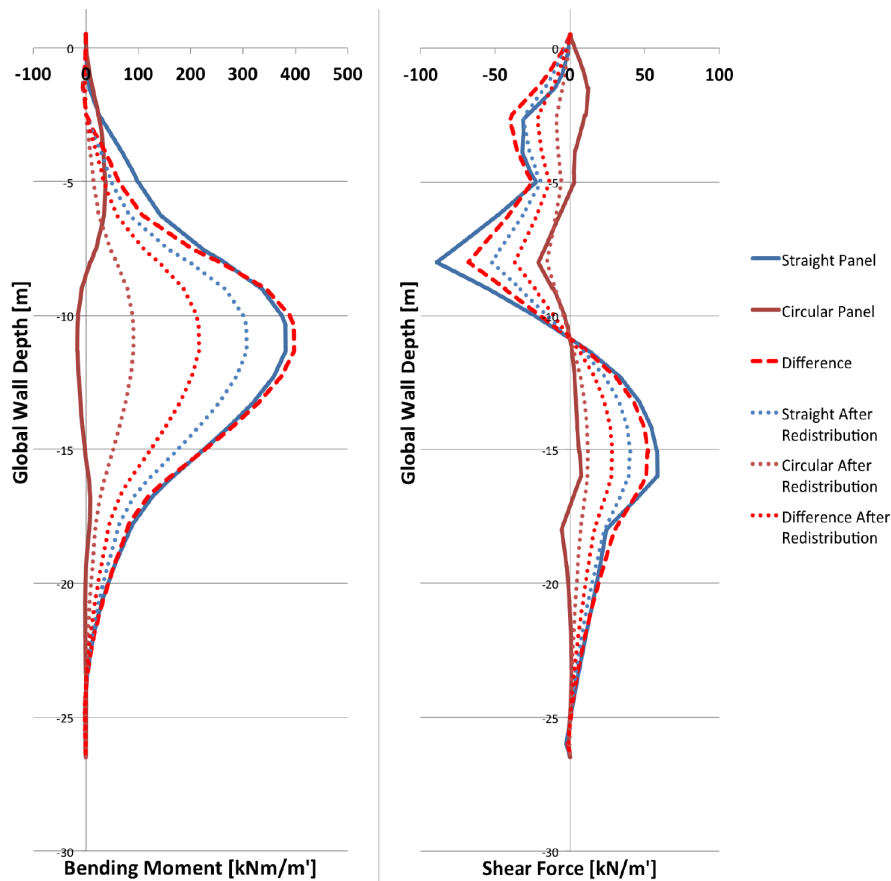


FIGURE 6.8: Phase 2: Out Of Plane Moments And Shear Forces Redistribution

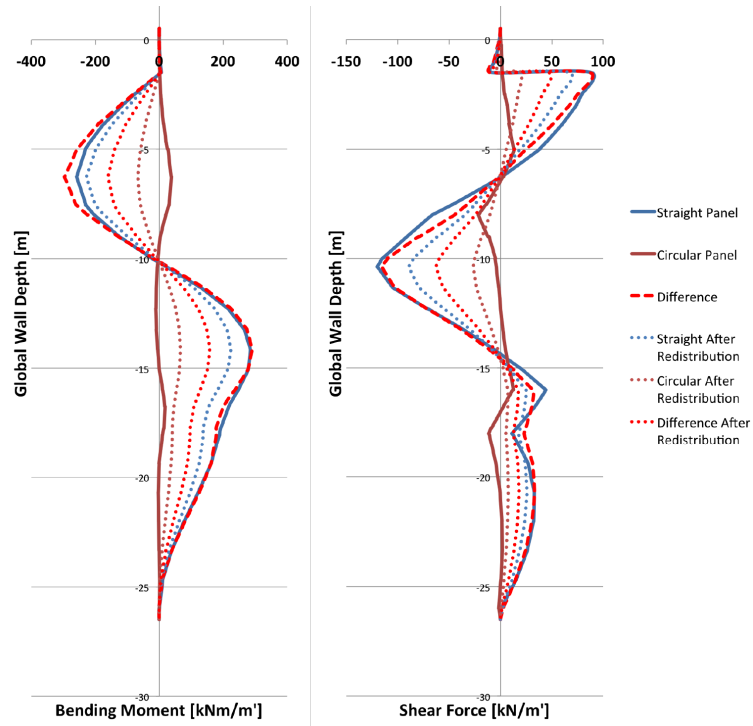


FIGURE 6.9: Phase 3: Out Of Plane Moments And Shear Forces Redistribution

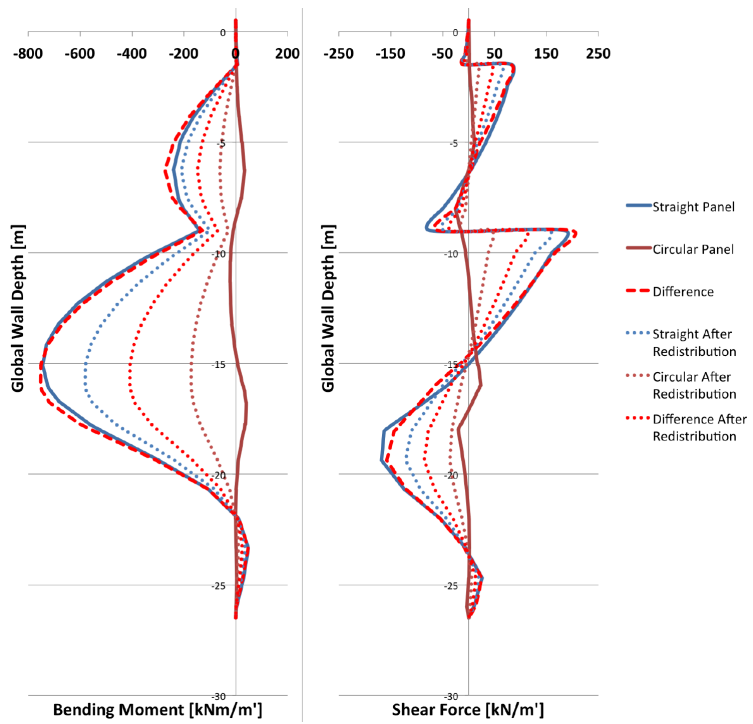
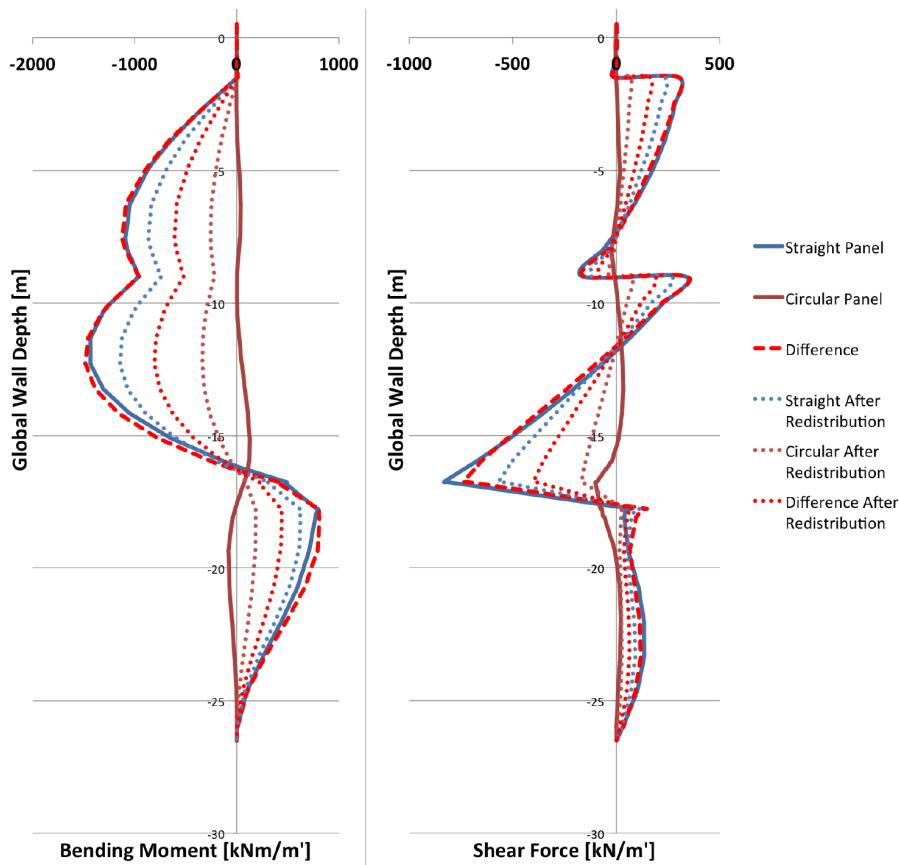


FIGURE 6.10: Phase 4: Out Of Plane Moments And Shear Forces Redistribution



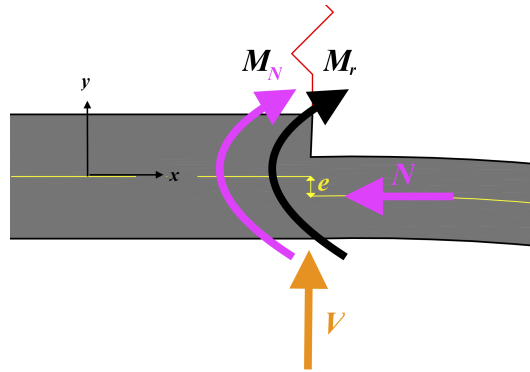
The forces acting on the unarmed critical section after redistribution of forces is as seen from figures above is less critical compared to the difference of two separate idealized analyses. This type of behavior is expected in reality, yet many factors acting on the section results is neglected while performing such analysis.

It should be reminded that all these engineering models are considered as a basis for the future research, in the long term to reduce the computational complexity and weight of building a 3-mesh. The line search method to estimate the resulting deformation at critical section should be considered while also deriving redistributed forces accordingly up to the point where all criterion are satisfied and providing proving results for each other.

On the other hand, for this study to see if the critical unarmed joint can withstand the phased construction loads, the redistributed forces acting on the critical joint and the upper limit section forces acting on the joint both can be compared by theoretical capacity of the unarmed concrete against especially shear and bending.

6.3 Determining The Effect Of Eccentricity At Critical Joint

FIGURE 6.11: Top View: Eccentric Connection And Acting Section Forces (Axes are not related to Diana Global reference system)



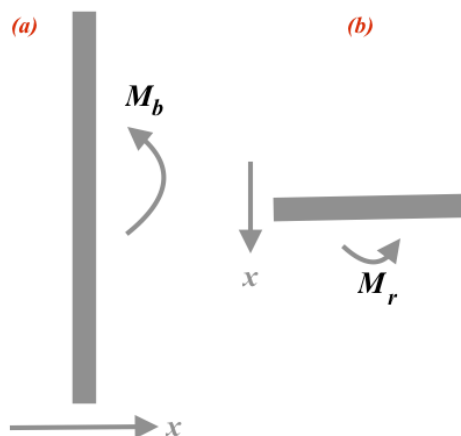
The above illustrated diagram represents a simplistic illustration of section forces acting at the critical section. The axial force (N) acting from the circular panel towards the straight panel is eccentric with the distance $e = 0.2$ m. Due to the eccentricity (e) of the axial force (N) there will be an additional in plane (rotational) bending moment:

$$M_N = N * e \quad (6.10)$$

When the force directions in the diagram 6.11 is considered positive, the total rotational moment occurring at the critical joint thus becomes:

$$M_{tot} = M_r + M_N \quad (6.11)$$

FIGURE 6.12: (a)Side View: Diaphragm Wall Subject To Out Of Plane Bending M_b (b)Top View: Diaphragm Wall Subject To In-Plane (Rotational) Bending M_r



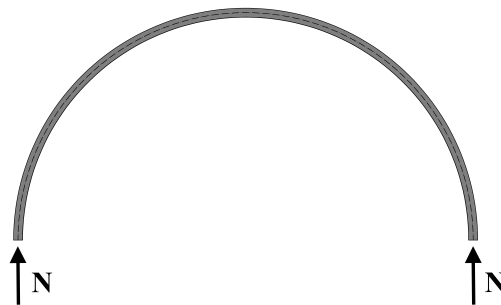
Due to the Poisson's ratio $\nu = 0.2$ input in the finite element model concrete material properties, bending moment M_b is directly five times greater than the rotational moment M_r calculated by the analysis. For a better illustration of different moments acting on the wall please see Figure 6.12. This is confirmed by the results taken from the analysis.

$$M_b = 5M_r \quad (6.12)$$

When the redistributed bending moments and shear forces and the additional bending moments due to eccentricity is defined, the only missing component of the engineering model is the determination of the axial force (N) acting on the eccentric connection.

6.4 Determination Of The Axial Hoop Forces (N) That Acts On Eccentric Connection

FIGURE 6.13: Arch with radius r Subjected to Outer Uniform Pressure P , resulting in support reaction N



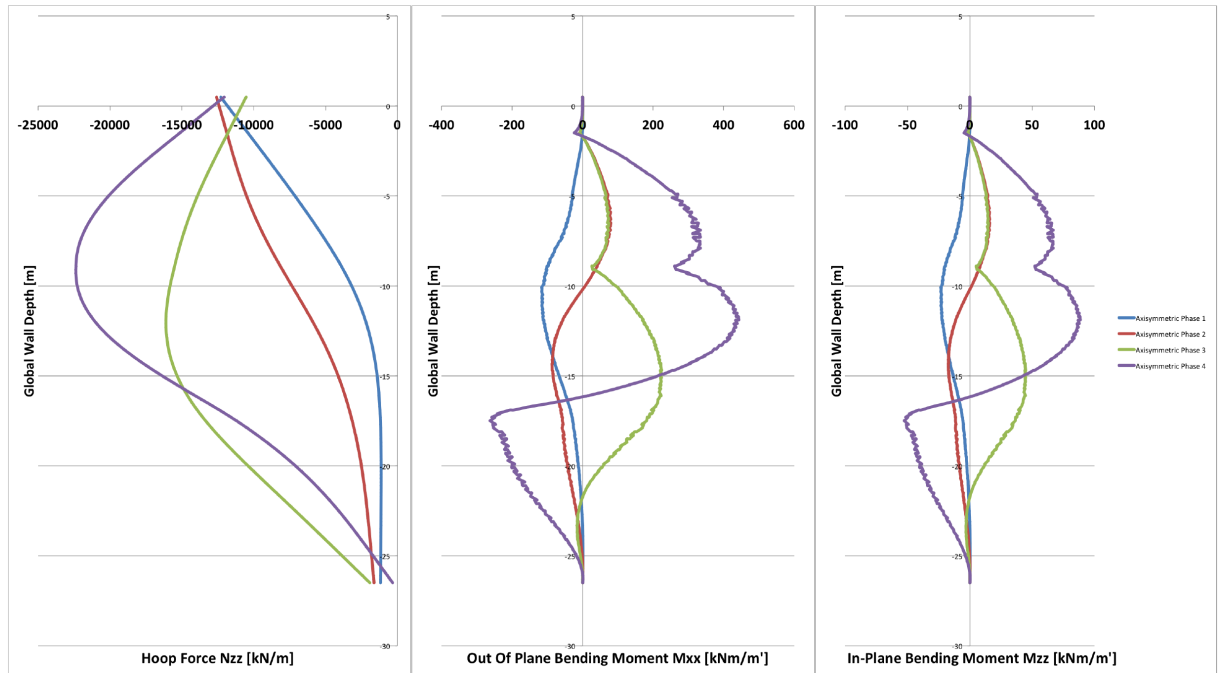
The missing sectional force is the axial force developing in the cylindrical wall section. For the engineering model two different results will be examined as follows:

- N resulting from the idealized arch subject to deformation due to soil pressure balancing, see Figure 6.13 $N = P * r$
- An upper limit N estimation by additional FEM analysis that is subjected to imposed deformation. In order to see how the upper limit axial force development might occur, the maximal wall displacements that were reached by the straight panel will be subjected to circular panel.

The 0.8 m thick cylindrical wall is modeled in axi-symmetrical design condition and the displacement that is found from the straight wall is applied on it as imposed deformation.

The comparison of section forces, for the given displacements, for the mesh subjected to imposed deformation can be seen from Figure 6.14.

FIGURE 6.14: Axi-symmetrical Mesh With Applied Imposed Deformation on 0.8 m thick cylindrical Wall



The idealized cylindrical panel analysis deforming solely due to the confining soil pressure conditions as shared by Figure 5.31, it is seen that the resulting bending moments do not go higher than $130 \text{ kNm/m}'$. When the moments are distributed according to the stiffness capacity of the different sections the resulting bending moments on the circular wall go no higher than $200 \text{ kNm/m}'$, see Figure 6.10. On the other hand, when the wall is forced to deform to a higher boundary displacement unrelated to the confining soil pressure, the bending moments occurring at the wall exceed $400 \text{ kNm/m}'$, see Figure 6.14.

In addition, the development of axial forces according to the two methods mentioned within this sub chapter (arch and the fem analysis with imposed deformation) is shared in the following Figures 6.15 and 6.16 to be able to compare the magnitude of developing axial forces. The arch method is computing the developing axial forces solely due to the soil loading conditions. Finite element analysis with imposed deformations is resulting the forces unrelated to soil pressure conditions but only by the prescribed deformations. In real site conditions, the resulting axial forces will be within the force envelope confined by these two methods because the wall will not only be subjected to soil pressures also be imposed to deform to balance the deformations between two different wall mechanisms.

FIGURE 6.15: Axial Forces Obtained From Arch Method

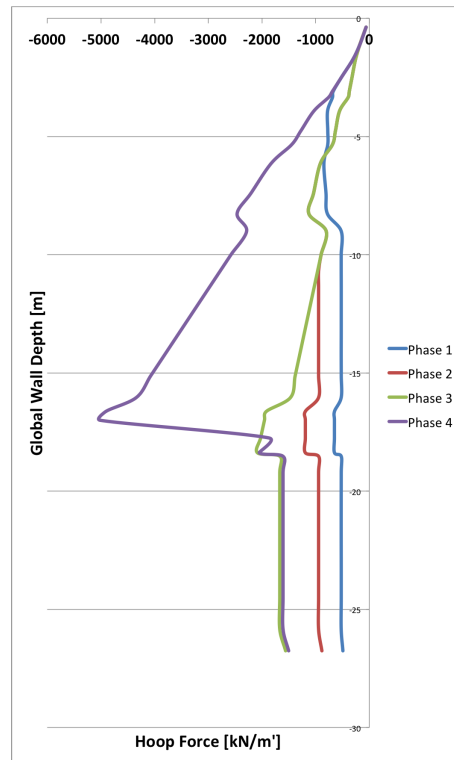
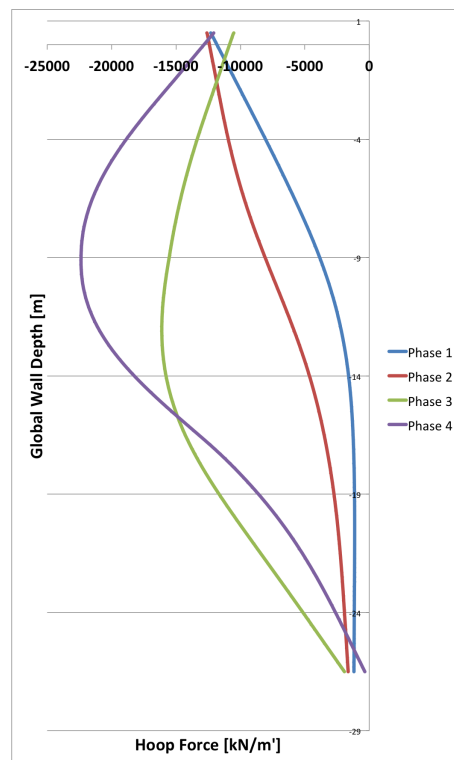


FIGURE 6.16: Axial Forces Obtained From Imposed Deformations



The importance of both analyses is to determine the region where the maximum axial forces develop unrelated to the loading and deforming conditions: Phase 4 will have the most critical axial force development and with both analyses it is clearly seen that the maximum section forces will occur between the strut leveled at -9 mNAP and the under water concrete.

The additional eccentricity moment (M_N) resulting from the the axial forces transferred to critical joint is calculated by Equation 6.10 and shared in Figures 6.17 and 6.18:

FIGURE 6.17: Resulting Eccentricity Moment M_N concluded From Arch Method

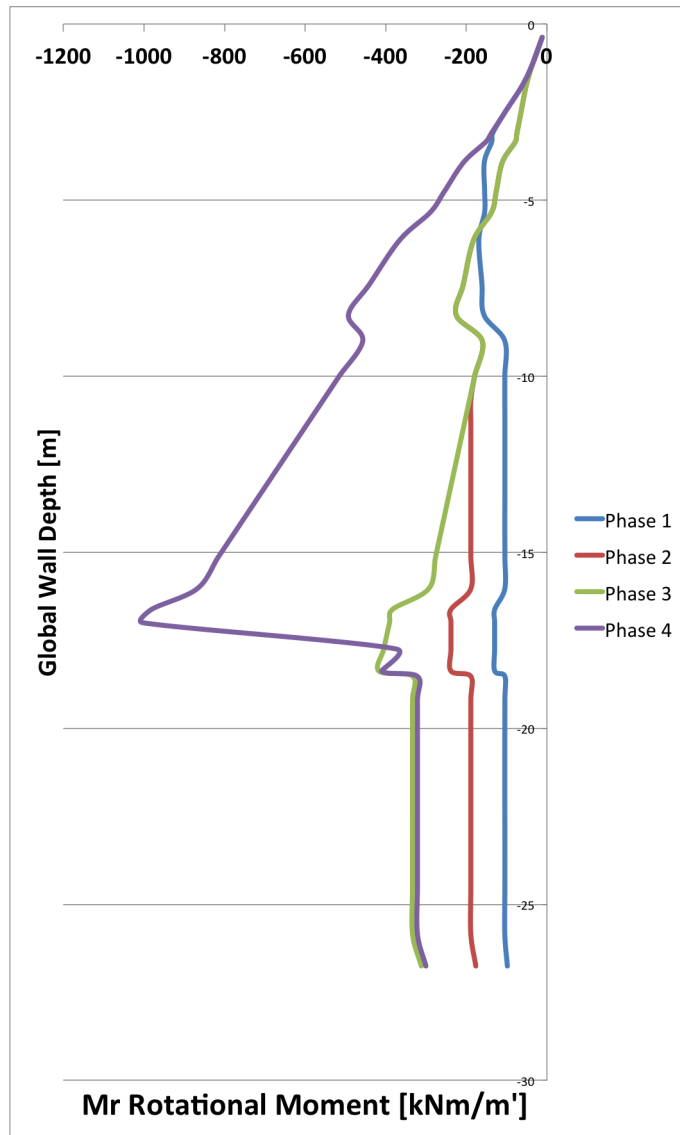
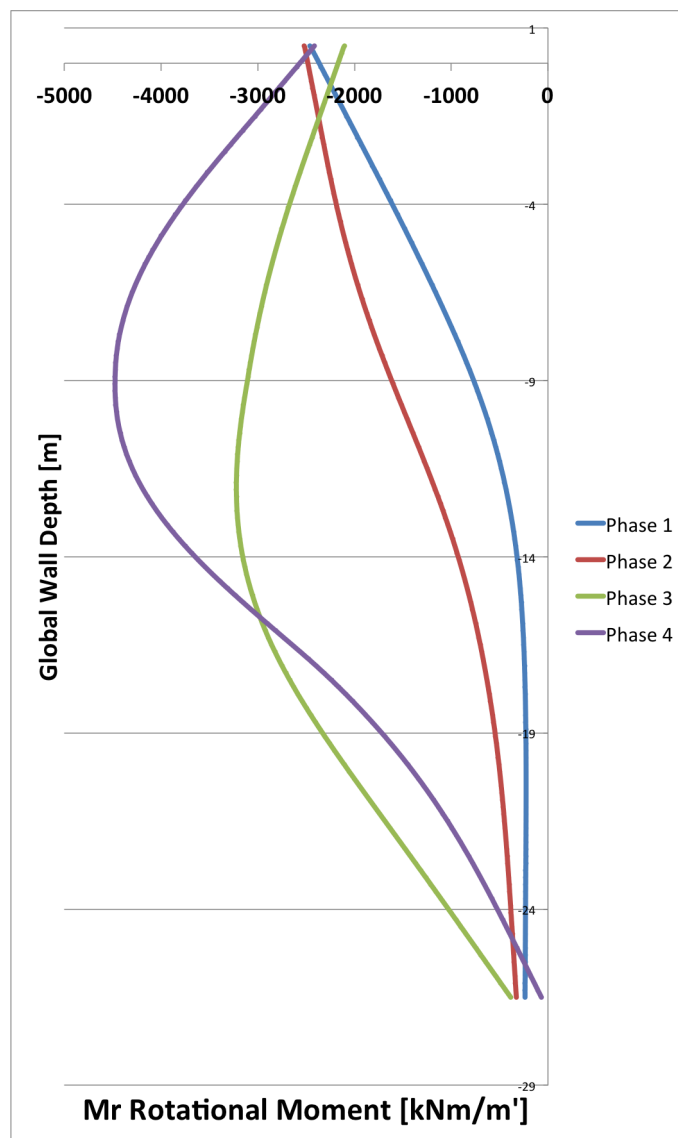


FIGURE 6.18: Resulting Eccentricity Moment M_N concluded From FEM Analysis With Imposed Deformations



6.5 Superposition Of Results

Superposition of different effects of section forces in a complex loading and load transfer mechanism condition is a challenging and complex problem. Different concepts are used in the research field. For instance, the three dimensional problem can be simplified in to two dimensional strut and tie models which demonstrates the compression and tension zones developing in the concrete and the flowing of stress vectors are examined from that starting point. The other way is to build a three dimensional finite element method of a representative solid (joint) element subject to distributed loads representing the loads acting on the section in question and reach to stress conditions at different nodes of the element. From the reached stresses in three dimensions, later the principal stresses can be computed by mechanical relations and be examined if the principal stresses are reaching to yield (in this case tensile or compressive limits) envelope.

From the practical knowledge of previously built diaphragm walls it is known that unarmed construction joints are capable of transferring flexural stresses resulting from the load transfer between two consecutive panels. That is why in order to avoid building a three dimensional finite element analysis and going further into depth, a clear determination of the critical failure mechanisms should be assessed and the results obtained from previous analyses should be implemented accordingly, to a simple model. Unarmed concrete has two obvious critical failure mechanisms:

- Tension failure
- Shear failure

Tension failure in the unarmed construction joint can be caused by bending moments resulting from the displacements. This tension failure of the critical joint is most critically can be observed in the rotational movement of critical joint along its longitudinal axis. Which means that the critical joint can be under torsion while two consecutive panels flex towards the pit and the eccentric axial force can increase this torsional moment and can cause the outer surface of the concrete exceed its tension capacity and crack open which later reduces the contact surface between the panels and lead to further instability and even risk of leakage. A good representation of this type of failure mechanism can be represented in the following Figure 6.19:

The second failure mechanism is the shear failure which is highly risky for this type of problem. First of all the straight panels are laterally supported by struts which causes the shear forces accumulate at certain height zone around the strut, in circular panels there are no struts. This type of accumulation of shear forces in one side of the panel causes a very high shear transfer zone around strut levels. These forces to be transferred are calculated in the previous sub chapter 6.2. A graphical representation of the failure mechanism is shared in Figure 6.21. Both failure mechanisms are related to two main aspects:

- Material capacity
- Loading condition

FIGURE 6.19: Uneven Displacements Resulting In Rotational Deformations, Thus Tension (t) In Unarmed Joint

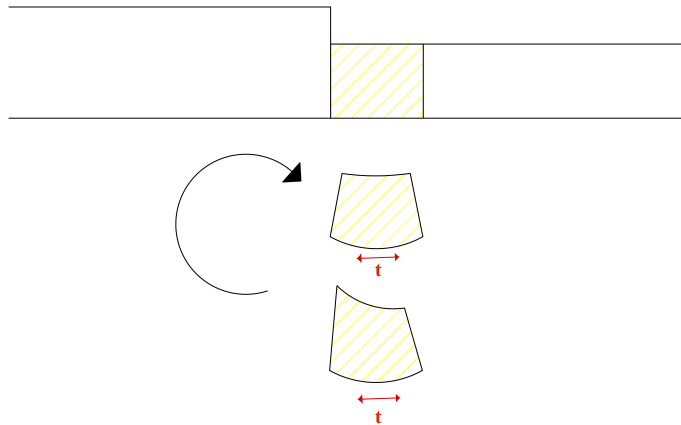


FIGURE 6.20: Eccentric Load And The Resulting Distributed Stress

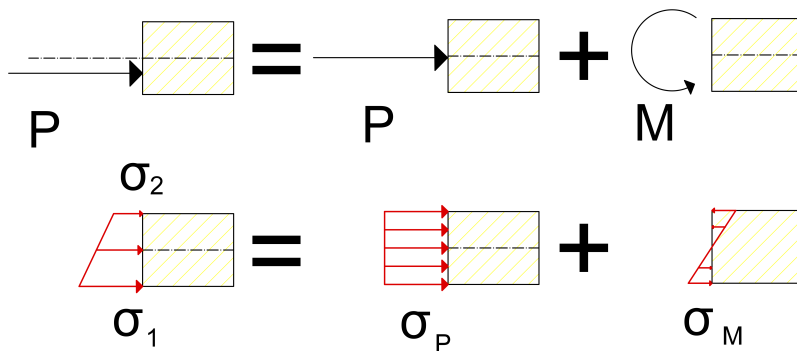
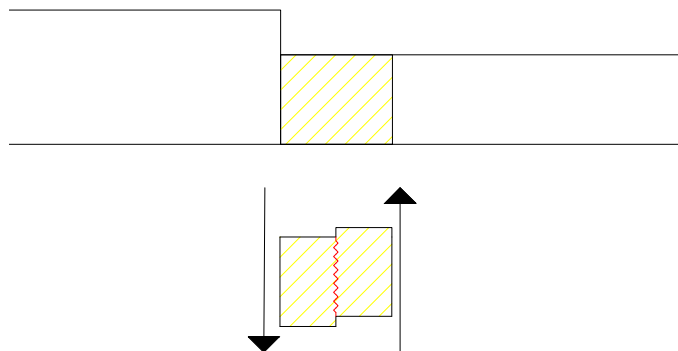


FIGURE 6.21: Shear Failure At Critical 0.8 m Thick Section



6.6 Failure Mechanisms

6.6.1 Tension Failure Mechanism

From Figure 6.20, it is seen that along the depth of wall the in-plane bending moment M_r should be derived as the one fifth of the distributed out of plane bending moment M_b . Later the axial force upper and lower limit should be transported to the axial center of the joint, later the two moment values are to be added to each other and all forces are to be transformed into stresses to check if the section reaches tensile stresses at any depth for any possible gap of different axial hoop force development possibility. All calculations will be done at the mesh levels decided at the beginning of this dissertation using D-Sheet automatic meshing. This check will only be performed for construction phase 4, the relations to be used are summarized as:

$$M_p = P * e \quad (6.13)$$

$$M_{tot} = M_r + M_p \quad (6.14)$$

$$\sigma_p = \frac{N}{t} \quad (6.15)$$

$$\sigma_m = \frac{3 * M_{tot}}{t^2} \quad (6.16)$$

$$\sigma_1 = \sigma_p + \sigma_m \quad (6.17)$$

$$\sigma_2 = \sigma_p - \sigma_m \quad (6.18)$$

Performed calculations can be observed from the following Figures 6.22 and 6.23. From the graphs it can be seen that:

- If the axial forces do not increase due to the wall movement and the circular panels develop hoop forces only due to the supported soil load: At the level of strut -1.5 mNAP, there is a low probability of cracking in the water and soil bearing side of the construction joint (Tension capacity of unreinforced concrete element is $f_{ctd} = 1600 \text{ kN/m}^2$. Yet it should not be forgotten that in this calculations surcharge loads around the wall is not included to analysis. Yet those type of loads have a really low effect on the overall behavior.
- The upper boundary calculations shows that the structure even with high eccentric loads stays in compressive zone yet most of the upper section of the structure exceeds its compressive capacity $f_{c,d} = 19000 \text{ kN/m}^2$. But if wanted the relations can be used backwards to guess the upper limit hoop forces that can be applied to structure. This type of estimations can even enable us to determine what type of uneven loading can be enabled around the circular part.

For both graphs tension is (+) and compression is (-). σ_1 is blue curve σ_2 is red curve.

FIGURE 6.22: σ_1 and σ_2 Calculated By Lower Bound N Value OF Arch Method: Construction Phase 4

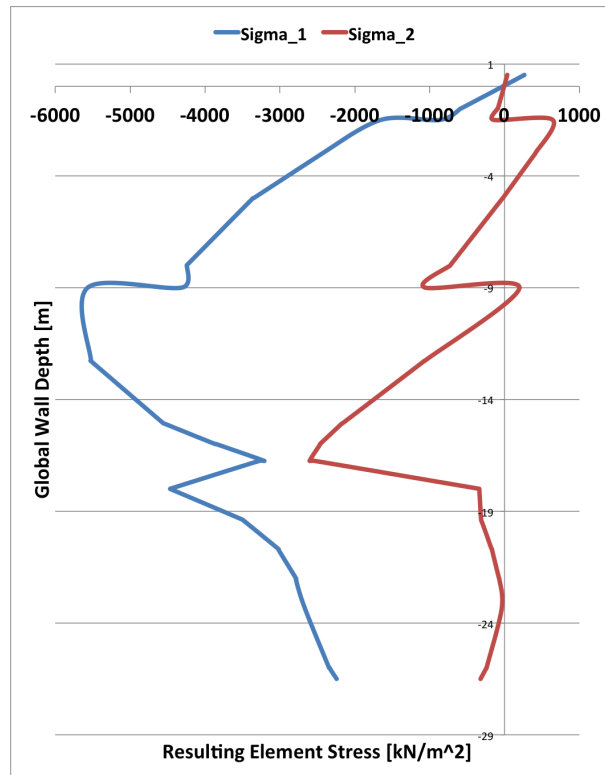
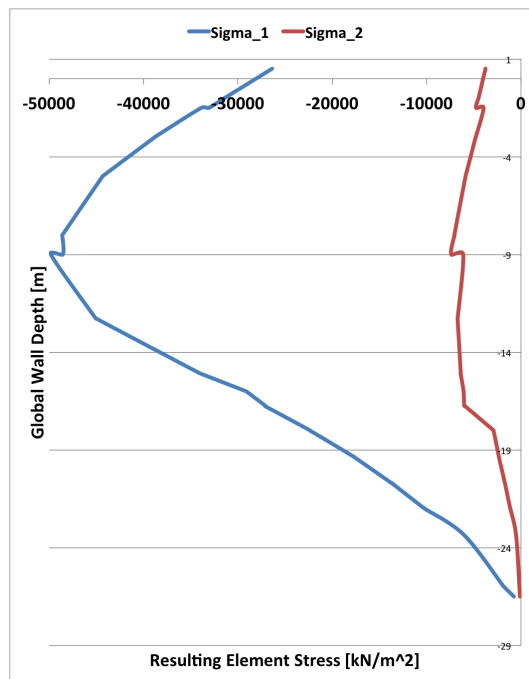


FIGURE 6.23: σ_1 and σ_2 Calculated By Upper Bound N Value OF FEM Analysis With Imposed Deformations: Construction Phase 4



6.6.2 Shear Failure Mechanism

There are many theoretical researches on the shear capacity of construction joints. Most of these researchers focus on the specific loading conditions to estimate parametrized behavior of construction joints. And most of the models are based on laboratory experiments. The shear capacity of a construction joints is related to many aspects such as:

- The friction between two concrete sections cast at different times
- Surface inclination of different sections at the connection, or cracking surface.
- Contribution of the reinforcement (if the joint is armed, which in this case not.)
- The axial forces acting on the joint, which increases the shear capacity of plain concrete.

By taking these aspects into account, the following relation is taken from Eurocode 2, clause 6.5.2:

$$v_{Rdi} = c \cdot f_{ctd} + \mu \cdot \sigma_n + \rho \cdot f_{yd} (\mu \cdot \sin\beta + \cos\beta) < 0.5 \cdot \nu \cdot f_{cd} \quad (6.19)$$

Unreinforced concrete capacity relation becomes:

$$v_{Rdi} = c \cdot f_{ctd} + \mu \cdot \sigma_n < 0.5 \cdot \nu \cdot f_{cd} \quad (6.20)$$

Where:

c is 0.25 for smooth surfaces

μ is 0.5 for smooth surfaces

ν is 0.6 for $f_{ck} < 60 \text{ MPa}$

$f_{ct,d} = 1600 \text{ kN/m}^2$

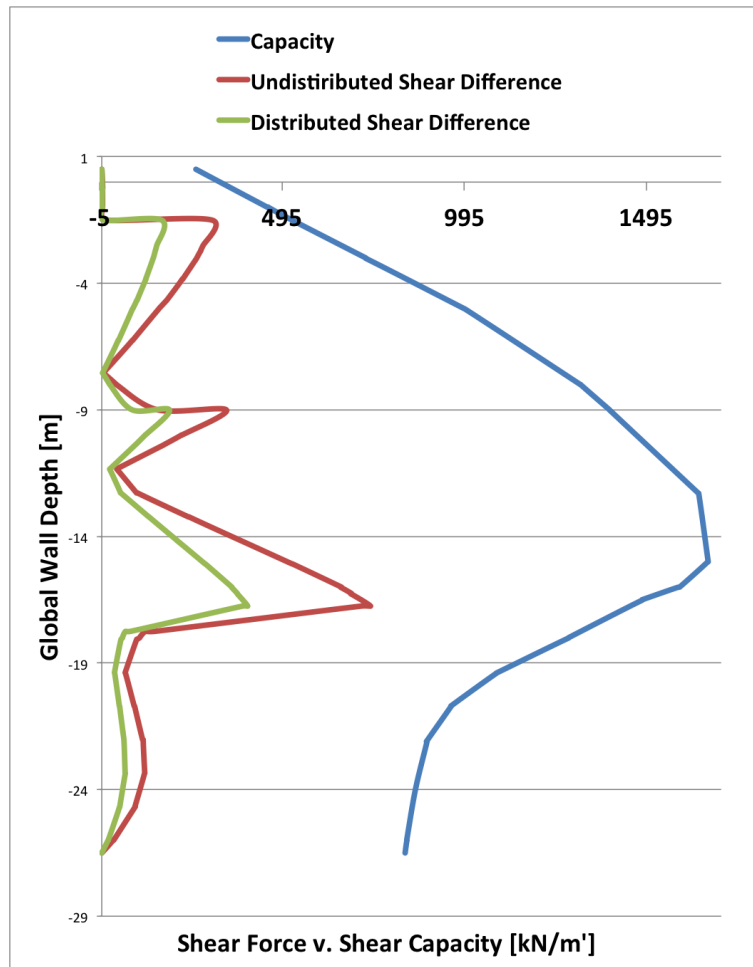
$$V_{Rd,i} = v_{Rd,i} \cdot t = (c \cdot f_{ct,d}) \cdot t + \mu \cdot (\sigma_n \cdot t) = (c \cdot f_{ct,d}) \cdot t + \mu \cdot N \quad (6.21)$$

Where:

t is the thickness of the joint 0.8 [m]

N is the hoop forces due to soil load bearing [kN]

FIGURE 6.24: Shear Capacity Compared With Absolute Shear Values: Phase 4



From Figure 6.24, it can be seen that even without doing a redistribution of shear forces and only by subtracting the shear results of idealized straight panel and idealized circular panel, the shear force to be taken by the joint is still below the shear capacity of the structure. In addition similar to the tension failure mechanism the most critical and diligence requiring location of the diaphragm wall connection is at -1.5 m NAP where laterally supported straight panel and laterally unsupported circular panel meet and go under a load transfer.

By the completion of this section also, without building a complex pit model that overestimates the structural properties of unarmed joint, a safe calculation about the load capacity of an unarmed joint is done taking into account the background information on the performance of concrete enlisted in Eurocodes. In the next chapter the resulting of the thesis will be completed along with the limitations of this research and the possible leads on the future studies.

Chapter 7

Conclusions and Recommendations

7.1 Results Taken From This Thesis

- The CUR Methodology can easily be applied with Diana Finite element using interface elements as soil springs.
- Phased construction can be modeled by Diana FEM program's phased construction property. For the correct calculation, loads should be applied as total loads at every stage.
- At the beginning of every stage the stresses of the interface elements should be recomputed. Otherwise the input should be prepared according to the incrementation for every stage by taking into account of the soil stiffness recalculated for the new phase.
- The complex layering of the soil (or cohesive non-cohesive soil) and springs do not create a stability problem for analysis.
- When similarly loaded by confining soil pressure, panels (straight vs. curved) have highly inconsistent deformation and moment patterns.
- For imposed displacements the moment distribution among the panels (straight vs. curved) will be relative to their moment of inertia.
- The axial hoop forces in the circular section reaching to the critical section is the main reason for the stability of the joint against failure conditions.
- The additional moments (M_N) due to eccentricity, at given configuration, decreases the stability of the joint at contact surface. But the effect of N axial force is heavily governs the safety.
- A normal soil-continuum model analysis that could take couple of hours by Diana FEM Package, is performed by four different analyses that takes around total 24 seconds. The effect of computational time benefit, causes a longer processing time for the results of four different analyses.
- Although the most critical section depths can be mistaken to be around -11 mNAP and -17 mNAP where section force values are the maximum. This is not the case. Because the capacity of the section is also dependent on the loading condition at the given depth.

- In the most critical shear transmission area (-1.5 mNAP), the section reaches around 80% of its shear capacity. And around 60% of its flexural capacity which is governed by the tensioning of outer fibers in unarmored concrete.
- The most critical construction stage will be at the 4th phase when the under water concrete is placed and the water in the pit is pumped out. And the main source of concern is the area at around the level of top strut closest to the circular sides of the pit.

7.2 Analysis Methodology Limitations

The limitations in this analysis is listed as:

- Both analyses takes into account perfect configured walls, which is different than reality. This limitation causes under estimated deformations for circular wall.
- The vertical soil pressure effects included to analyses is just a mere estimation of the real behavior, does not heavily effect results, but overestimates the stiffness of the overall system against displacements.
- The water loads taken into analyses are directly taken from preliminary D-Sheet analysis. Otherwise, factors like additional pore pressure under cohesive layers should be considered so that a misconception of loading is prevented. Water load is a serious load on the wall.
- This analysis does include the 3-D effects of such a construction joint by using 2-D engineering models. The real behavior is more complex and requires a 3-D Finite element model.
- Derived soil subgrade reaction constants are directly taken from CUR166 manual. The soil is not modeled realistically.
- The walls do not take into account the non-linear elastic behavior of structural concrete.
- Under estimated section forces due to limitations causes a highly conservative model. Because under estimated circular wall sections creates a bigger force gap between two different sections and overestimates the resulting forces at the construction joint.

7.3 Suggestions For Future Researches

- Same construction joint can be modeled by surface interface elements in 3-D pit configuration to check if the found critical sections are correct.
- with the three dimensional stress values taken from such analysis, primary stresses at the concrete can be computed to see if the concrete at any point is within the safe envelope.

- In addition the Relations at page 109 can be used backwards to derive the allowable axial force at given depth and from there design the dimensioning of the structure.
- If 3-dimensional stress results of the construction joint computed, these conditions can be compared with a strut-tie model and try to recreate the similar stress flow state by analogical simple models even without modeling the walls themselves.
- The geometrical nonlinear behavior of concrete can be implemented which will change the way the failure mechanisms are calculated, due to the uneven stressing of geometrically non-linear section.
- Instead of a service loads calculation, a safe ULS calculation or probabilistic approaches can be implemented by changing properties according to Table 3.9.
- The nonlinear behavior of concrete can be included to analysis.
- A certain syntax can be researched for a more inclusive behavior of different walls connected with an unarmed joint. This can be a better, more inclusive mechanical or finite element model.
- Only the half circular wall can be modeled in 3-D pit configuration with correct boundary conditions, to compare the results with perfect axi-symmetric. To grasp the behavioral difference better.
- Parameters such as cracking and softening can be included to a finite element model that is only and only focusing on deformed construction joint.

Bibliography

- Boyes, Reginald George Hector (1975). "Structural and cut-off diaphragm walls". In:
 Brinckerhoff, Parsons (2008). *Guidelines for Waterproofing of Underground Structures*.
 CUR166 (2012). In: 6.
 D-Sheet (2014). "Manual". In: 1.
 "EN1538" (2010). In: 1, pp. 1–20.
 EN1992 (2005). In: 12.
 "EN1997-1" (2005). In: 72.12.
 Jaky, J (1948). "On the bearing capacity of piles". In: *Proceedings of 2nd International Conference in Soil Mechanics and Foundation Engineering*. Éditions AA Balkema, Rotterdam. Vol. 1, pp. 100–103.
 Jones, Glyn (1997). *Analysis of beams on elastic foundations: using finite difference theory*. Thomas Telford.
 Kurian, Nainan P (2013). *An Introduction to Modern Techniques in Geotechnical and Foundation Engineering*. Alpha Science International.
 Müller-Breslau, Heinrich Franz Bernhard (1906). *Erddruck auf stuetzmauern*. A. Kröner.
 Puller, Malcolm (2003). *Deep excavations: a practical manual*. Thomas Telford.
 SEI/ASCE (2000). "Effective Analysis of Diaphragm Walls". In: 1.
 Thomas D. Richards, Jr. P.E. (2006). In: *Central PA Geotechnical Conference 12*.
 Vlachioti, Christina (2010). "Nonlinear Finite Element Modeling of Cylindrical Diaphragm Wall Sensitivity in Geometrical Imperfections and Non-symmetrical Loading Conditions". In:
 Xanthakos, Petros P (1994). *Slurry walls as structural systems*.
 Yao, Sam X, Dale E Berner, and Ben C Gerwick (1999). *Assessment of Underwater Concrete Technologies for In-the-Wet Construction of Navigation Structures*. Tech. rep. DTIC Document.